國立臺灣大學公共衛生學院環境與職業健康科學研究所

碩士論文

Institute of Environmental and Occupational Health Sciences
College of Public Health
National Taiwan University

Master's Thesis

活性碳應用於水中全氟與多氟烷基物質吸附效率之評估

Assessments on the Adsorption Efficiency of Per- and Polyfluoroalkyl Substances (PFAS) in Water with Activated Carbon

陳孝桐

Siao-Tong Chen

指導教授：王根樹 博士

Advisor: Gen-Shuh Wang, Ph.D.

中華民國 114 年 8 月

August, 2025

doi:10.6342/NTU202503155

國立臺灣大學碩士學位論文
口試委員會審定書
MASTER'S THESIS ACCEPTANCE CERTIFICATE
NATIONAL TAIWAN UNIVERSITY

活性碳應用於水中全氟與多氟烷基物質吸附效率之評估

Assessments on the Adsorption Efficiency of Per- and Polyfluoroalkyl Substances (PFAS) in Water with Activated Carbon

本論文係陳孝桐（R12852020）在國立臺灣大學環境與職業健康科學研究所完成之碩士學位論文，於民國 114 年 7 月 22 日承下列考試委員審查通過及口試及格，特此證明。

The undersigned, appointed by the Graduate Institute of Environmental and Occupational Health Science on 22nd July 2025, have examined a Master's Thesis entitled above presented by Siao-Tong Chen (R12852020) candidate and hereby certify that it is worthy of acceptance.

口試委員 Oral examination committee:

（指導教授 Advisor）

doi:10.6342/NTU202503155

誌謝

能完成這篇論文，首先要特別感謝我的指導教授王根樹特聘教授，老師不只是分享學術知識與實務經驗，同時也帶著我們全台到處採樣、讓我有機會協助 2024 IWA Micropol 研討會和參與 AOMSC 2025 研討會，讓我在這兩年的研究所生涯中，留下除了這本論文以外，更多的是深刻且珍貴的回憶，由衷地感謝老師。感謝口試委員林財富老師、童心欣老師，給予我學術觀念的指導以及論文方向上的建議，並透過論文口試的悉心指教，讓我能完成我的學術研究。

謝謝 GSW Lab 大家庭的淑婷學姊、Popo 學姊、宛玲學姊、姿蓉學姊、知頤學姊、怡婷學姊，從懵懂地跟著學習，逐漸在學姊們的引導下對做研究和實驗操作這條路上找到方向，謝謝一路上的包容與照顧；也謝謝學妹珮如和千慧，總是主動幫忙，也跟我們一起分享歡笑，等你們明年的好消息!還有玨融和佳怡，也祝福你們未來一切順利。謝謝我的同梯水寶貝珮怡，我們一起接手活性碳計畫，跟著老師出差的日子都歷歷在目，我會永遠記得寒假在澎湖被海風吹和爬窗的故事。

感謝環職所的師長們，讓我從課堂學習和擔任課程助教的機會中有所成長；以及所辦白助、佳蓉姊，總是替我們處理碩班生活中的大小事。也感謝陳家揚老師提供分析儀器的使用和則穎學長的技術支援，讓我能順利完成研究。

並肩奮鬥的碩班夥伴們，韻儒、泱孝、思圩、珈瑜、奕安、毓杰、維予、俞庭、陳忻、琦茵、巧柔，還有所有 R12 的同學們!謝謝大家堅持走完這條不容易的路。因為有你們，這一路才並不孤單，那些吵鬧的碩研室日常、續命飲料和最困難的晚餐題，都會是我最珍貴的回憶，而寫下誌謝的現在，已經開始讓我感到寂寞了。

謝謝媽媽、爸爸、哥哥這 25 年來的陪伴，謝謝你們的栽培，養成我的責任感和待人處事的種種。這兩年雖然你們只知道我早出晚歸，假日還要去學校，沒辦法跟你們分享多大的學術成就，還總是讓你們接住我的情緒，謝謝媽媽為我扛起的一切、哥哥作為讓我最沒壓力的後盾，因為是家人所以最感激也最抱歉，我愛你們。

在背後默默支持我的朋友們：惟楨、德安、紫涵、子萱、雨昕、楚君、津津、文淇、昱瑄、子晴、Jackie、蝦米，謝謝你們的關心。最後要謝謝陳孝桐，縱使求學之路充滿困惑與掙扎，但謝謝自己的勇敢堅持、每次的不放棄、為自己爭取來的每個機會，未來就算充滿未知，也希望妳享受挑戰，過不會後悔的人生吧！

doi:10.6342/NTU202503155

摘要

隨著全球對環境保護與資源永續利用的重視，聯合國永續發展目標（Sustainable Development Goals, SDGs）第 6 項：「確保所有人都能享有水與衛生及其永續管理」已成為各國水資源治理的重要方針。水資源的安全與衛生是當代關鍵議題，而新興污染物的廣泛流布，對環境與公共健康構成潛在風險。傳統自來水處理程序的目的為去除雜質以達到水質標準，但卻無法有效去除全氟與多氟烷基物質（Per- and Polyfluoroalkyl Substances, PFAS）等新興污染物，因此多種處理技術被廣泛討論以降低飲用水中 PFAS 濃度。其中活性碳吸附因其高去除效率、不產生副產物、操作簡便、成本相對較低廉等優勢，且無論粉狀或粒狀活性碳皆展現良好吸附性能，被認為是可行的 PFAS 解決方案。

本研究以實驗室規模探討活性碳對四種代表性 PFAS（PFBS、PFHxS、PFOA 與 PFOS）的吸附行為，並比較椰子殼與煤質兩種材質活性碳之處理效率。分析方法參考國家環境研究院公告之標準檢測方法「水中全氟與多氟烷基物質檢測方法－液相層析串聯式質譜儀法（NIEA W542.52B）」進行調整。另外，對於 PFAS 檢測分析前處理方式之固相萃取（Solid phase extraction, SPE）亦進行優化測試比較。實驗設計結合吸附動力學、等溫吸附模型與快速迷你管柱試驗（Rapid Small Scale Column Test, RSSCT），先於 Milli-Q 水（二次去離子水）中探討活性碳對 PFAS 吸附之模型，進一步應用 RSSCT，分別在 Milli-Q 水和實場採樣的快濾池清水進行額外添加固定濃度之 PFAS 後，使用粒狀活性碳（Granular Activated Carbon, GAC）填充之迷你管柱吸附，透過 PFAS 貫穿曲線評估 GAC 在水中吸附 PFAS 的表現。

本研究結果顯示，前處理經過初步酸化的樣本，使用 Oasis WAX 固相萃取管匣進行萃取，且管匣不再經過 0.1%甲酸潤洗，可獲得四種 PFAS 最佳 SPE 回收條件（回收率均超過 75%）。接著進行動力吸附與等溫吸附實驗，著重於討論椰子殼活性碳（TAC-C）與煙煤活性碳（F400）對 PFAS 之吸附效能。發現在 Milli-Q 水中進行吸附模型擬合下，對於所有四種 PFAS 化合物，使用 TAC-C 作為吸附劑的結果符合擬二級吸附動力學。相反，使用 F400 作為吸附劑的結果則符合擬一級吸附動力學。總結等溫吸附之模型結果，得出在 Milli-Q 水中使用 Freundlich 等溫吸附模型能更好地描述 TAC-C 和 F400 對 PFAS 的吸附，反應了異質介面相互作用。

doi:10.6342/NTU202503155

透過操作 RSSCT 兩周的實驗結果，在 Milli-Q 水中，TAC-C 較早出現貫穿，尤其是對 PFBS 和 PFOA。而 F400 表現出最佳的整體吸附能力，對大多數 PFAS 的貫穿維持在 10%以下。相比之下，在實場快濾池清水中，PFAS 吸附能力由於其他天然有機物的競爭而顯著降低 GAC 的吸附成效。以 TAC-C 而言，在 25,000 個濾床體積時除了 PFOS 以外，皆出現 90%貫穿現象；F400 在大約 15,000 個濾床體積四種 PFAS 已出現 30%貫穿現象；TAC-Q 作為與 TAC-C 來自相同品牌之煤質活性碳，其貫穿曲線在 PFBS 出現超出初始濃度之貫穿現象，然而其餘 PFAS 的貫穿程度皆低於椰子殼活性碳。

這些結果顯示水體基質效應對 PFAS 吸附行為中的重要性，並凸顯了煤質 GAC 的優異吸附性能。實際應用必須考慮到背景污染物的競爭，可能會加速 GAC 飽和並降低處理效能。以上結果確立煙煤質活性碳整體吸附效能優於椰子殼活性碳，且對長鏈 PFAS（PFOA 與 PFOS）之去除率高於短鏈 PFAS（PFBS 與 PFHxS）。本研究結果可作為未來臺灣淨水場採用活性碳處理 PFAS 之參考，並提供具體建議以協助實踐 SDGs 第 6 項永續發展目標，確保民眾飲水安全。

關鍵字：全氟與多氟烷基物質、活性碳、吸附動力學、等溫吸附模型、快速迷你管柱試驗、貫穿曲線

doi:10.6342/NTU202503155

Abstract

With growing global attention to environmental protection and sustainable resource management, the United Nations Sustainable Development Goal (SDG) 6 - "Ensure availability and sustainable management of water and sanitation for all" - has become a key policy direction for water resource management across nations. The safety of water resources remains a critical issue, particularly as the widespread presence of emerging contaminants poses potential risks to the environment and public health. Conventional drinking water treatment processes are designed to remove impurities to meet the water quality standards. However, they are ineffective in removing emerging contaminants such as Per- and Polyfluoroalkyl Substances (PFAS), and therefore, various treatment technologies have been proposed to reduce the concentration of PFAS in drinking water. Various treatment methods have been developed for different PFAS types, among which activated carbon (AC) adsorption stands out for its high removal efficiency, lack of harmful byproducts, operational simplicity, and relatively low cost. Both powdered (PAC) and granular (GAC) activated carbon have demonstrated excellent adsorption performance and are considered feasible solutions for controlling PFAS in drinking water.

In this study, the adsorption behavior of activated carbon on four representative PFAS (PFBS, PFHxS, PFOA, and PFOS) was investigated on a laboratory scale, and the treatment efficiencies of activated carbon on two materials, coconut shell and coal, were compared. The analytical method has been adjusted with the standard method "Method for Determination of Per and Polyfluoroalkyl Substances in Water by Liquid Chromatography/Tandem Mass Spectrometry (NIEA W542.52B)". In addition, the analytical pretreatment method, solid phase extraction (SPE), was optimized to compare the analytical performance of the PFAS studied. The experimental design integrated

doi:10.6342/NTU202503155

adsorption kinetics, adsorption isotherms in Milli-Q water (deionized water) to discuss the adsorption models, and further applied in the Rapid Small Scale Column Test (RSSCT) to determine the PFAS adsorption characteristics and parameters in Milli-Q water. Following this, the RSSCT assessed the breakthrough of a spiked concentration of PFAS in both Milli-Q water and rapidly filtered water collected from a drinking water treatment plant. After the addition of a fixed concentration of PFAS to Milli-Q water and field rapid filtered water, the adsorption operation was carried out using a mini column filled with granular activated carbon (GAC) to evaluate the performance of GAC in the adsorption of PFAS in water by the PFAS breakthrough curve.

The results of the study showed that the best SPE recovery conditions for all four PFAS (recovery of more than 75%) were obtained when the samples, which were initially acidified in the pre-treatment, were extracted using Oasis WAX cartridges, which were no longer lubricated with 0.1% formic acid. Kinetics and equilibrium isotherm adsorption experiments were then conducted, focusing on the adsorption efficacy of PFAS adsorption with coconut shell activated carbon (TAC-C) and bituminous activated carbon (F400). In Milli-Q water, the results using TAC-C as adsorbent were consistent with the proposed pseudo-second-order model for all four PFAS compounds. On the contrary, the results using F400 as the adsorbent were best described with the proposed pseudo-first-order model. Summarizing the results of isothermal adsorption modeling, it was concluded that in Milli-Q water, the adsorption of PFAS on both TAC-C and F400 could be better described by the Freundlich isothermal adsorption model, which reflects the heterogeneous interactions.

By manipulating the RSSCT results conducted for 2 weeks, TAC-C showed an earlier breakthrough in Milli-Q water, especially for PFBS and PFOA, whereas F400 showed the best overall adsorption capacity, maintaining breakthrough below 10% for

doi:10.6342/NTU202503155

most PFAS. In contrast, the adsorption efficacy of GAC was significantly reduced by competition from other natural organic matter (NOM) in the field rapid filtered water. In the case of TAC-C, 90% breakthrough was observed at 25,000 bed volumes except for PFOS, while F400 showed 30% breakthrough at about 15,000 bed volumes for the four types of PFAS; TAC-Q, which is the same brand of coal-based activated carbon as TAC-C, showed breakthrough curves except for breakthrough beyond the initial concentration of PFBS. However, the breakthrough degree of the other PFAS was lower than that of the coconut shell activated carbon. The findings of this study provide a reference for the future applications of activated carbon in PFAS removal at water treatment plants in Taiwan and provide specific recommendations to support the achievement of SDG 6, ensuring safe drinking water for the public.

Keywords: Per- and Polyfluoroalkyl Substances (PFAS), Granular Activated Carbon (GAC), Adsorption Kinetics, Adsorption Isotherms, Rapid Small Scale Column Test (RSSCT), Breakthrough Curves.

doi:10.6342/NTU202503155

Contents

doi:10.6342/NTU202503155

doi:10.6342/NTU202503155

doi:10.6342/NTU202503155

doi:10.6342/NTU202503155

List of figures

doi:10.6342/NTU202503155

doi:10.6342/NTU202503155

doi:10.6342/NTU202503155

List of tables

doi:10.6342/NTU202503155

doi:10.6342/NTU202503155

Chapter 1 Introduction

1.1 Background

Per- and polyfluoroalkyl substances (PFAS) are a large group of synthetic fluorinated organic compounds widely used since the 1950s in various industrial processes and consumer products. Their unique physicochemical properties, such as thermal stability, oil- and water-resistance, and resistance to chemical degradation, which are primarily attributed to the strength of the carbon–fluorine (C–F) bond, one of the strongest in organic chemistry (Wang et al., 2021; Zhanyun Wang et al., 2017). However, the properties that make PFAS industrially valuable also make them highly persistent in the environment.

PFAS resist natural degradation processes, including photolysis, hydrolysis, and biodegradation, leading to their accumulation in environmental media such as water, soil, and biota. Therefore, PFAS are also referred to as “forever chemicals”. They are classified as persistent organic pollutants (POPs). PFAS are now recognized as a major group of emerging contaminants (ECs) due to their widespread occurrence and potential health impacts (Lindstrom et al., 2011). PFAS have been detected globally, near industrial sites and in remote regions such as the Arctic, indicating their capacity for long-range transport (Young et al., 2007).

Due to increasing evidence of their toxicity and bioaccumulation, compounds like perfluorooctanoic acid (PFOA) and perfluorooctane sulfonic acid (PFOS) have been phased out in many countries. Their adverse health effects include liver damage, immune suppression, reproductive and developmental toxicity, and probable carcinogenicity (OECD Series on Risk Management of Chemicals, 2021; U.S. EPA, 2024). In 2023, the International Agency for Research on Cancer (IARC) classified PFOA as carcinogenic to

doi:10.6342/NTU202503155

humans (Group 1) and PFOS as possibly carcinogenic (Group 2B) (The International Agency for Research on Cancer (IARC), 2025; Zahm et al., 2024).

In response to regulatory restrictions, the industry has shifted toward short- and medium-chain PFAS such as perfluorobutane sulfonic acid (PFBS) and perfluorohexane sulfonic acid (PFHxS), which were initially believed to be safer alternatives due to their lower bioaccumulation potential. However, recent studies have shown that these replacements exhibit environmental persistence and potential toxicity, raising concerns over their long-term impacts (Arvaniti & Stasinakis, 2015; Cousins et al., 2020).

Notably, conventional treatments in drinking water plants are now being challenged. The strength of the C–F bond makes PFAS hard to remove through many standard technologies, such as coagulation, flocculation, sedimentation (conventional treatment), oxidation, disinfection, and biodegradation. For example, it has been shown that conventional drinking water treatment is inefficient for PFAS removal (Crone et al., 2019). According to the Drinking Water Treatability Database (TDB), several treatment technologies have been developed and tested for their ability to remove PFAS from drinking water, including biological treatment, advanced oxidation processes, fungal degradation, ion exchange resin, high- and low-pressure membranes, and activated carbon adsorption(U.S. EPA, 2025a).

Among these, activated carbon adsorption is the most widely implemented and cost-effective technology at full scale. Typically, either PAC is dosed early in the treatment train and removed through sedimentation, or GAC is used in fixed beds in combination with filtration or as a post-filtration step. GAC is particularly effective for long-chain PFAS due to their hydrophobicity and strong affinity for carbon surfaces (Appleman et al., 2014). Moreover, GAC treatment is compatible with conventional water treatment infrastructure. It is often used as a pretreatment step to reduce PFAS levels before

doi:10.6342/NTU202503155

disinfection, improving chemical safety and microbiological control in water supplies.

However, the adsorption efficiency of activated carbon can vary depending on PFAS chain length, water matrix, carbon type (e.g., coal-based vs. coconut shell), and operational parameters such as contact time. Short- and medium-chain PFAS are generally more difficult to remove with adsorption due to their higher solubility and weaker sorption interactions. These limitations highlight the need for a detailed investigation into the performance of different carbon types under controlled conditions.

1.2 Objectives

This study aims to evaluate the effectiveness of activated carbon adsorption in removing per- and polyfluoroalkyl substances (PFAS) from water, focusing on PFBS, PFHxS, PFOA, and PFOS. By conducting adsorption kinetics, isotherm studies, and rapid small-scale column tests (RSSCT), the adsorption performance of granular activated carbon (GAC) derived from coconut shell and coal-based sources is systematically compared. The specific objectives are: (1) To explore the feasibility of activated carbon adsorption as a treatment step before disinfection in conventional water treatment processes; (2) To reduce the overall PFAS concentrations in drinking water; and (3) To assess the material-dependent adsorption behavior of different types of GAC, providing a scientific basis for selecting effective adsorbents in future water treatment applications.

doi:10.6342/NTU202503155

Chapter 2 Literature Review

2.1 Occurrence and health effects of PFAS

2.1.1 Introduction of PFAS

Per- and polyfluoroalkyl substances (PFAS) are diverse synthetic compounds with varying carbon chain lengths and functional groups. According to the Interstate Technology & Regulatory Council (ITRC), PFAS can be broadly classified into nonpolymers and polymers. Nonpolymer PFAS typically contain functional groups such as carboxylic acid (-COOH) and sulfonic acid (-SO_3H), forming subcategories including perfluoroalkyl carboxylates (PFCAs) and perfluoroalkyl sulfonates (PFSAs) .

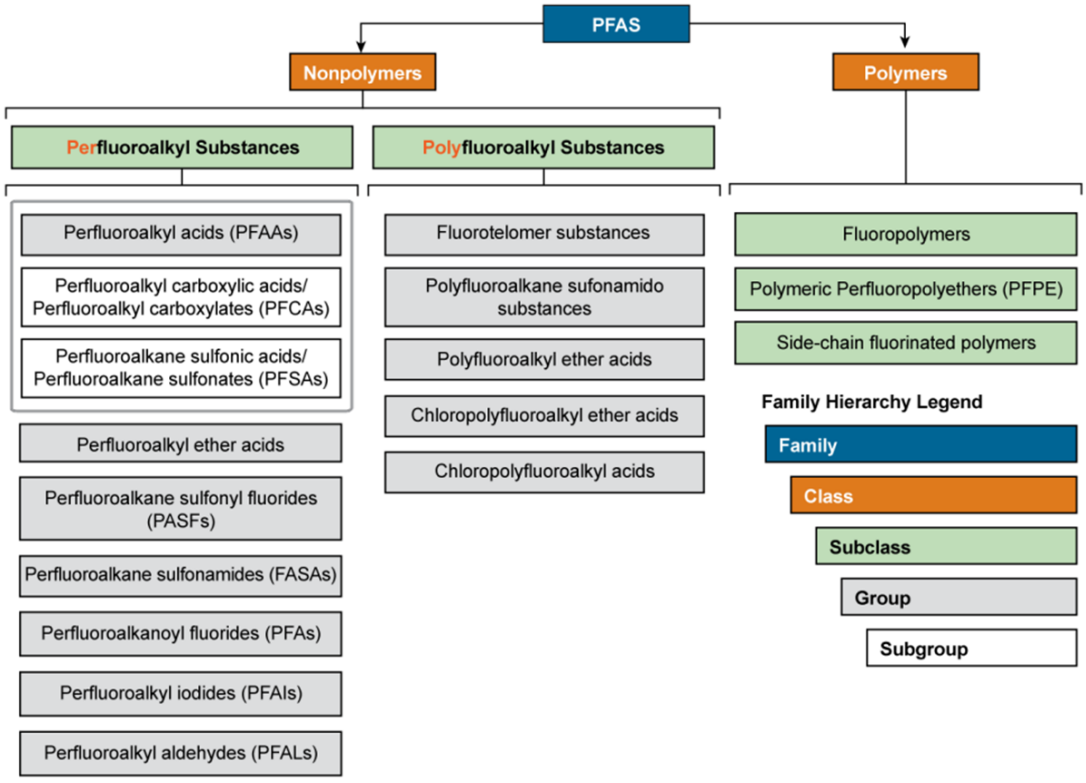

Figure 2.1 The PFAS Family (Interstate Technology & Regulatory Council, 2022).

The general chemical structure of PFAS is C_nF_{2n+1}-R, and its structural feature is that a F atom replaces at least one H atom on a C-H bond in the molecule. The substances that

doi:10.6342/NTU202503155

cause the greatest impact are usually composed of 4-9 carbon chains, and their structure is fully saturated and fluorinated, with one end connected to a sulfonate group or a carboxylic acid group. The number of identified PFAS has skyrocketed. At the end of 2021, the CompTox Chemicals Dashboard from the U.S. EPA listed over 14,000 unique PFAS structures (Carlson et al., 2022). However, this figure likely underrepresents the true scope of PFAS compounds in commercial and industrial uses.

2.1.2 Environmental Occurrence of PFAS

Since the 1950s, PFAS have been widely used in industrial processes and consumer products due to their thermal stability and resistance to water, oil, and stains. Their molecular structure, characterized by carbon-fluorine (C–F) bonds, imparts exceptional heat, water, and oil resistance. These properties have made PFAS highly desirable for uses in products such as non-stick cookware (e.g., Teflon), waterproof textiles, stain-resistant carpets, food packaging, and firefighting foams (especially aqueous film-forming foams, AFFF) (Buck et al., 2011; Zhanyun Wang et al., 2017).

Due to their widespread uses and chemical stability, PFAS have become ubiquitous environmental contaminants. Over the past 60 years, PFAS have been detected in various environmental media, including surface water, groundwater, soil, sediment, air, and even in remote areas such as the Arctic and Antarctic regions (Ahrens et al., 2010; Young et al., 2007). Their persistence is mainly due to their resistance to natural degradation processes, allowing them to remain in the environment for decades. Key sources of PFAS in the environment include industrial discharges, military training areas, airports, landfill leachate, wastewater effluent, and the application of biosolids on agricultural land (Hu et al., 2016; Post et al., 2012).

doi:10.6342/NTU202503155

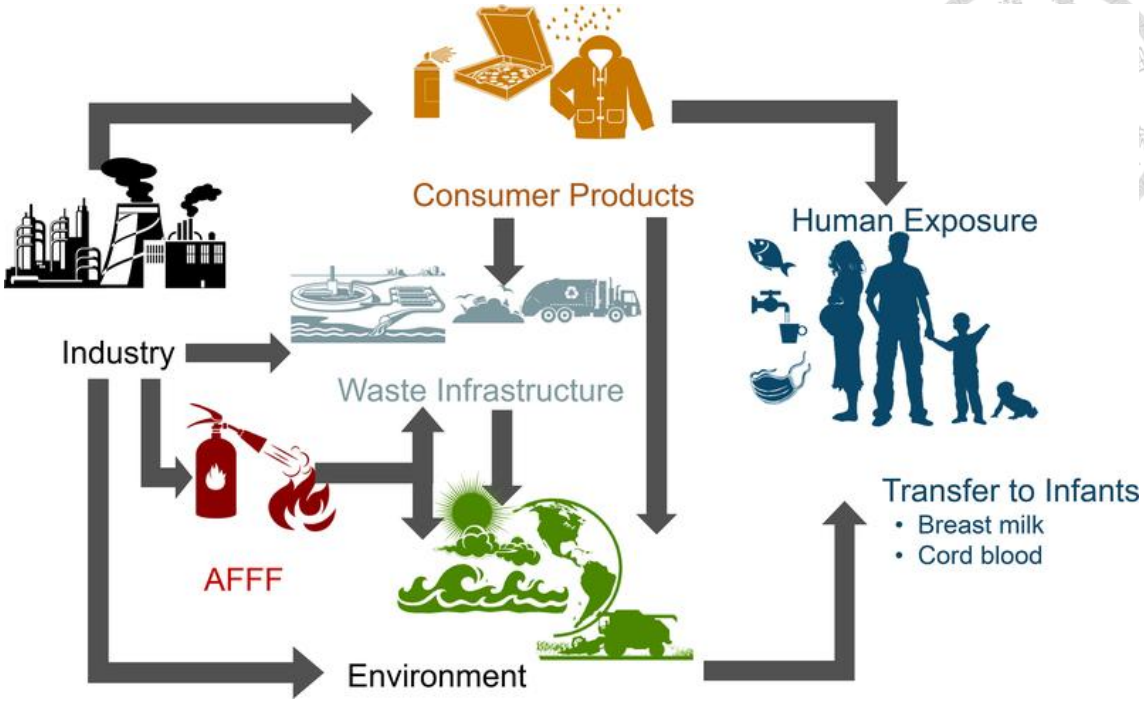

Figure 2.2 Pathways of PFAS exposure from industrial sources to humans via consumer products, waste infrastructure, and environmental compartments. (Obtained from (Sunderland et al., 2019).)

2.1.3 Health effects of PFAS

PFAS has many impacts on the ecological environment, mainly including water pollution, soil pollution, and organism accumulation. Due to their high chemical stability and hydrophobicity, PFAS are difficult to decompose in the environment and easily accumulate in water and soil. These pollutants can enter organisms through the food chain and cause long-term negative impacts on the ecosystem.

Human exposure to PFAS occurs through multiple pathways, including the ingestion of contaminated drinking water, dietary intake (particularly fish, meat, and food packaged in PFAS-treated materials), and inhalation of indoor air or dust resulting from PFAS-containing consumer products (Ericson et al., 2008; Fromme et al., 2009). Biomonitoring studies have found PFAS in most people's blood serum, with long-chain compounds such as PFOA and PFOS being most prevalent (Calafat et al., 2007).

doi:10.6342/NTU202503155

Once absorbed, PFAS are distributed primarily in the liver, kidneys, and serum, where they exhibit long biological half-lives due to their resistance to metabolic breakdown and excretion (Agency for Toxic Substances and Disease Registry (ATSDR), 2021). Epidemiological studies have associated PFAS exposure with a range of adverse health outcomes, including hepatic enzyme alterations, renal dysfunction, thyroid hormone disruption, hypercholesterolemia, immune system suppression, and reproductive or developmental toxicity (Steenland et al., 2010). Prenatal and early-life exposures are of particular concern, as PFAS can cross the placental barrier and have been detected in breast milk, contributing to postnatal exposure in infants (Fenton et al., 2021).

Regarding carcinogenicity, the International Agency for Research on Cancer (IARC) has classified PFOA as Group 1 (carcinogenic to humans), based on sufficient evidence linking it to kidney and testicular cancers. PFOS is classified as Group 2B (possibly carcinogenic to humans), based on limited evidence (The International Agency for Research on Cancer (IARC), 2025). Immunotoxic effects have also been observed, including reduced vaccine efficacy and increased susceptibility to infections in children, possibly due to suppressed antibody responses (Grandjean et al., 2012).

Given these widespread health concerns, the regulation of PFAS levels in drinking water, food, and consumer products has become a public health priority in many countries. Continued biomonitoring and the development of health-based exposure guidelines remain essential for managing risks associated with both legacy and emerging PFAS compounds.

doi:10.6342/NTU202503155

2.2 Overview of PFAS in the aquatic environment

2.2.1 Occurrence of PFAS in the aquatic environment worldwide

The presence of PFAS in the aquatic environment demonstrates a close link between the anthroposphere and the hydrologic cycle. Concentrations of PFAS reported in surface water and groundwater typically range from nanograms per liter (ng/L) to micrograms per liter (μg/L). Due to their high water solubility and environmental persistence, certain PFAS compounds tend to accumulate in major aquatic systems, making oceans, groundwater, and surface waters significant global sinks. Their presence in waste streams poses a significant risk to surface and groundwater, two of the primary drinking water sources worldwide (Kurwadkar et al., 2022).

Previous studies have expanded our understanding of PFAS distribution across various marine environments. For example, the spatial distribution of C4, C6, and C8 perfluoroalkyl sulfonates, C6–C14 perfluoroalkyl carboxylates, and perfluorooctanesulfonamide has been reported in the Atlantic and Arctic Oceans, including previously unstudied coastal waters of North and South America and the Canadian Arctic Archipelago (Benskin et al., 2012).

PFAS contamination in Asia is most prominent in surface waters, with concentrations generally higher than those found in groundwater. Notably, countries such as China, Japan, and South Korea reported PFAS levels exceeding recommended thresholds, comparable to levels observed in the United States. In contrast, South and Southeast Asia levels were generally lower but still concerning (Baluyot et al., 2021). The elevated PFAS concentration in high-income Asian countries may be attributed to the increasing number of PFAS-related manufacturing industries and consumer products in these regions. China and Japan, for instance, follow closely behind the U.S. and EU in

doi:10.6342/NTU202503155

global e-waste generation, contributing to PFAS releases through surface runoff and industrial discharge (Cai et al., 2018; Garg et al., 2020). As these nations continue to expand their industrial activities, their role as major contributors to regional PFAS pollution is expected to grow.

2.2.2 Occurrence of PFAS in the aquatic environment in Taiwan

PFAS have been widely detected in environmental matrices worldwide; however, only limited research on PFAS has been conducted in Taiwan regarding their occurrence, source apportionment, and potential health risks in drinking water sources.

In 2009, Lin et al. reported elevated levels of PFAS in the wastewater of the Hsinchu Science Park. (Lin et al., 2009). In 2014, the team found that the concentration of PFAS in fish in the Keya River, which was affected by the Hsinchu Science Park's wastewater, was 200 times that of fish in the Keelung River, indicating that the park's wastewater caused severe pollution to the surrounding water bodies and ecosystems (Lin et al., 2014). The results of these studies showed that wastewater discharged from the industrial areas is an important source of PFAS pollution, which significantly impacts local water bodies and ecosystems.

According to a study by Jiang et al. (2021) conducted on surface water from Taiwan’s Baoshan Reservoir. Positive Matrix Factorization (PMF) was applied to identify potential sources of PFAS contamination. Health risk was assessed using the Health Index (HI) and compared against various international guideline values. PFOA and PFOS were the dominant compounds, with average concentrations of 20.2 ng/L and 16.7 ng/L, respectively. While the calculated HI based on the U.S. EPA reference dose indicated no immediate health concern (HI < 1.0), the combined concentration of PFOA and PFOS (130 ng/L) exceeded the U.S. EPA Lifetime Health Advisory level of 70 ng/L, suggesting

doi:10.6342/NTU202503155

potential long-term human health risks. Additionally, the Baoshan Reservoir in Taiwan identified domestic and commercial wastewater as the primary source (61.2%) of PFAS contamination, with urban activities as the secondary source (38.8%). Among the ten PFAS compounds analyzed, PFOA and PFOS were the most prevalent. At one sampling point near a lodging facility, their combined concentration exceeded the U.S. EPA Health Advisory level (70 ng/L), highlighting localized contamination. While short-term health risks were low, long-term exposure may pose potential concerns due to bioaccumulation. (Jiang et al., 2021).

On the other hand, the Ministry of Environment of Taiwan continuously monitors and detects the concentration of different emerging compounds through the "Investigation of Compounds of Emerging Concern in Drinking Water and Management of Water Quality" every year. The results found that at the sampling points near some of the airports, PFOA, PFOS, and PFHxS have records exceeding the current guideline values in Taiwan. Therefore, PFAS in drinking water should be continuously monitored (環境部, 2023).

2.2.3 The selected PFAS

A comprehensive meta-analysis compiled groundwater PFAS concentration data from 96 published studies between 1999 and 2021, spanning 20 countries worldwide (Kurwadkar et al., 2022). After filtering out time-series data, duplicates, and non-detects, the final dataset included approximately 21,000 data points covering over 35 PFAS compounds. Concentration levels varied greatly, ranging from nanograms per liter (ng/L) to milligrams per liter (mg/L). Notably, sites near direct contamination sources exhibited significantly higher PFAS levels than background locations. Among the compounds

doi:10.6342/NTU202503155

reported, PFOA and PFOS were the most frequently detected, with concentration ranges of <0.03 ng/L to 7 mg/L for PFOA and 0.01 ng/L to 5 mg/L for PFOS (Johnson et al., 2022).

In 2023, the U.S. Geological Survey (USGS) sampled tap water from more than 700 homes, businesses, and water suppliers across the country and found that 45% of the samples contained PFAS. 1 to 9 PFAS were detected in contaminated water samples, with total concentrations ranging from 0.348 to 346 ng/L. 17 PFAS were detected at least once in the detected samples, of which PFBS, PFHxS, and PFOA were the most common in about 15% of the samples. The study used the Benchmark risk assessment method to evaluate the results. When the PFAS chemicals were detected, the potential human exposure risk mainly came from the chemicals. The potential human exposure risk mainly came from PFOA and PFOS (Smalling et al., 2023).

Past research indicates that PFOA and PFOS are the most widely used and studied PFAS (Domingo & Nadal, 2019). These chemicals are commonly found in drinking water, surface water, sediments, and various living organisms worldwide (Xu et al., 2021). Due to their persistence in the environment and associated toxicity, they have been subject to global regulatory measures. Shorter-chain analogs, such as PFHxS and PFBS, have been used as substitutes for PFOS and PFOA following regulatory restrictions. However, concerns regarding the safety of these replacements are growing. PFHxS has since been listed in the Stockholm Convention (Li et al., 2023) and exhibits a long biological half-life in humans comparable to PFOS. U.S. EPA has finalized the IRIS Toxicological Review of PFHxS and Related Salts. This assessment addresses the potential cancer and noncancer human health effects from exposure to PFHxS and related salts. PFHxS is likely to affect the human thyroid and cause developmental immune issues negatively. A key evidence supporting immune effects is decreased antibody responses to common

doi:10.6342/NTU202503155

childhood vaccinations (Integrated Risk Information System (IRIS), 2025). Meanwhile, PFBS is also recognized for its potential health concerns, especially in complex mixtures. In recent research on cancer cases attributable to PFAS in drinking water, the strongest association was observed between PFBS and oral cavity cancers (Li et al., 2025).

The selection of PFBS, PFHxS, PFOS, and PFOA in this study reflects a strategic focus on legacy PFAS and their replacement compounds, enabling the study of changing contamination trends, potential risks, and the effectiveness of treatment technologies.

2.3 The challenges of conventional water treatments

2.3.1 The conventional water treatment processes

Conventional water treatment processes employed in drinking water treatment plants typically follow a series of physical and chemical operations to remove suspended solids, a portion of organic matter, and pathogenic microorganisms. As illustrated in Figure 2.3, raw water is first introduced through an intake structure and temporarily stored in a raw water regulation basin, where initial hydraulic and water quality adjustments are performed. The water is then transferred to a distribution well, where coagulants and prechlorination agents are dosed to initiate particle destabilization.

Subsequently, the water passes through a flash mixer, where rapid mixing promotes the dispersion of coagulants, followed by slow mixing in the flocculation basin to facilitate the aggregation of destabilized particles into larger flocs. These flocs are settled in the sedimentation basin, significantly reducing turbidity and particulate load.

The clarified water then undergoes filtration via a rapid sand filter, which removes remaining suspended solids and microbial contaminants. After filtration, a postchlorination step is applied to ensure adequate disinfection before distribution. The

doi:10.6342/NTU202503155

treated water is stored in a finished reservoir and distributed to the public through a distribution system.

In addition to the primary treatment stream, the plant manages sludge and wastewater produced during treatment. Settled sludge is collected in sludge wells and further processed through a sludge thickener, conditioning pool, and dewatering unit. Recycled water from sludge processing is returned to the system, while excess wastewater is directed to a wastewater regulation basin and discharged after appropriate handling.

doi:10.6342/NTU202503155

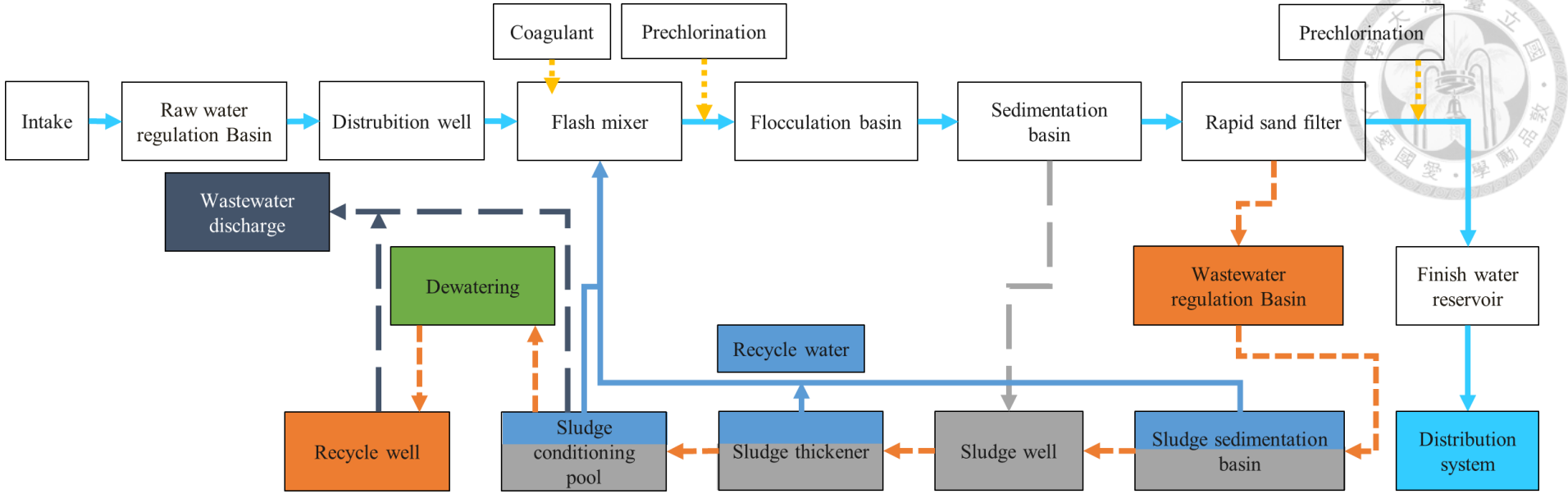

Figure 2.3 Conventional water treatment processes in the drinking water treatment plant. (Reference from (台灣自來水股份有限公司).)

doi:10.6342/NTU202503155

2.3.2 The challenges of conventional water treatments

Conventional water treatment processes were primarily designed and constructed several decades ago. They were engineered to address the prevalent concerns of that time, focusing on removing suspended solids, turbidity, and pathogenic microorganisms. However, these legacy systems were developed without foresight into the widespread and persistent nature of emerging contaminants, such as PFAS.

Numerous studies have highlighted the limitations of conventional methods, such as coagulation, flocculation, sedimentation, and basic filtration, ineffectively eliminating PFAS from water sources, including PFAS-contaminated groundwater and wastewater (Appleman et al., 2014). For instance, Previous research demonstrated that while some traditional processes can reduce certain PFAS levels, they are generally insufficient for comprehensive removal (Dauchy, 2019; Pan et al., 2016).

Compounding this inherent limitation is the escalating impact of climate change on water quality. Extreme weather events, including intense rainfall and typhoons, which are becoming more frequent and severe in regions like Taiwan, significantly exacerbate water quality challenges. Such events lead to sharp increases in turbidity, enhance the runoff of various contaminants, and place immense stress on existing treatment infrastructure (Delpla et al., 2009; Whitehead et al., 2009). These climatic disturbances can mobilize and introduce PFAS and other contaminants from contaminated soils and industrial areas into surface water and groundwater sources, overwhelming the already limited capabilities of conventional treatment processes. For example, heavy rainfall can transport PFAS-laden materials directly into drinking water reservoirs. At the same time, the high turbidity accompanying storm events can drastically reduce the effectiveness of conventional filtration, compromising the safety of the treated water.

These dual pressures, the persistent issue of emerging contaminants and the

doi:10.6342/NTU202503155

increasing variability in water quality driven by climate change, pose a significant and evolving threat to public health. Current infrastructure limitations necessitate a proactive approach to safeguarding drinking water supplies. Therefore, there is an urgent need to enhance public awareness of these evolving drinking water safety risks and to upgrade treatment technologies to address these challenges.

2.4 Regulations of PFAS in water

2.4.1 International PFAS regulations in drinking water

In recent years, there has been a significant increase in global awareness of the potential health risks associated with PFAS in drinking water. Many countries have implemented monitoring programs and developed regulatory frameworks to address these concerns. While regulatory approaches differ by region, they share common trends, including group-based thresholds and stricter health-based limits, as shown in Table 2.1.

The Environmental Protection Agency (EPA) finalized its first enforceable National Primary Drinking Water Regulation (NPDWR) for PFAS in the United States in April 2024. This regulation sets the Maximum Contaminant Level (MCL) at 4 ng/L for both PFOA and PFOS. In addition, the Maximum Contaminant Level Goal (MCLG) and MCL are both set at 10 ng/L for PFHxS, PFNA, and HFPO-DA (GenX chemicals) (U.S. EPA, 2025d).

In addition to individual limits, the regulation introduced a cumulative Hazard Index (HI) of 1.0 for mixtures including PFHxS, PFNA, HFPO-DA (GenX chemicals), and PFBS, triggering remedial action even if individual PFAS concentrations remain below their respective limits. This highlights their widespread occurrence. Comprehensive monitoring under the fifth Unregulated Contaminant Monitoring Rule

doi:10.6342/NTU202503155

(UCMR 5) is being conducted between 2023 and 2025, with full compliance with MCLs required by April 26, 2029. However, in May 2025, the EPA signaled a possible extension of the compliance deadline to 2031 and announced a reassessment of some MCLs (U.S. EPA, 2025b).

In the European Union (EU), the Drinking Water Directive (EU 2020/2184) established binding concentration limits for PFAS in drinking water. Member States were required to transpose the directive into national legislation by January 12, 2023, and ensure compliance by January 13, 2026. The directive specifies a maximum concentration of 0.10 μg/L for the sum of the 20 specific PFAS compounds (PFAS 20), and 0.50 μg/L for total PFAS. Furthermore, several Member States, such as France, have proposed more stringent national standards. For example, France recommended a limit of 20 ng/L for the combined concentration of PFOA, PFHxS, PFOS, and PFNA (European Union, 2020).

Denmark was the first country to ban PFAS in food packaging materials by 2020. PFAS is commonly used as a water and grease repellent in food packaging paper and cartons, and is highly transferable to food and humans. The Danish Environmental Protection Agency has implemented strict limits for PFAS in drinking water. These regulations are among the most stringent globally: A Total of 22 PFAS compounds were regulated, and the sum of the 22 specific PFAS substances must not exceed 100 ng/L. In addition, the sum of the four specific PFAS (PFOA, PFOS, PFHxS, PFNA) must not exceed 2 ng/L (Danish Environmental Protection Agency, 2024; Miljøstyrelsen, 2024).

The national drinking water regulator in New Zealand, Taumata Arowai, and the government set these current standards in 2022. According to the Drinking Water Standards for New Zealand 2022, the following Maximum Allowable Values (MAVs) are set for PFAS substances. MAV of PFOA is 560 ng/L, and the combined PFHxS and PFOS is 70 ng/L (Rt Hon Dame Helen Winkelmann, 2022).

doi:10.6342/NTU202503155

In Australia, the National Health and Medical Research Council (NHMRC) updated its health-based guideline values for PFAS in the Australian Drinking Water Guidelines (ADWG) in June 2025. The revised values are: 200 ng/L for PFOA, 8 ng/L for PFOS, 30 ng/L for PFHxS, and 1000 ng/L for PFBS. These values trigger further investigation rather than strict regulatory limits (NHMRC, 2025).

Canada adopted a precautionary, group-based regulatory approach in August 2024. Health Canada revised its drinking water quality objective to a total concentration of 30 ng/L for the 25 specific PFAS compounds, replacing earlier compound-specific guidelines. The objective is based on the "As Low As Reasonably Achievable" (ALARA) principle, given the limited toxicological data available for many PFAS. Although not legally binding at the federal level, this objective guides provincial and territorial jurisdictions in setting enforceable regulations (Government of Canada, 2024).

Japan has recently advanced its regulatory framework for PFAS, particularly focusing on PFOS and PFOA in drinking water. In December 2024, expert panels proposed the existing provisional target value of 50 ng/L (combined PFOS and PFOA) as an official drinking water standard, with enforcement scheduled for April 1, 2026 (Ministry of the Environment (Japan), 2024). Routine monitoring is proposed every three months. On 30 June 2025, the Consumer Affairs Agency (CAA) released the promulgated order for new PFOS and PFOA standards (combined value = 50 ng/L) for mineral water on the e-GOV Public Comment Portal. The newly established standards are expected to be enforced from 1 April 2026 (e-GOV Public Comment Portal (Japan), 2025).

The guideline values for PFOA and PFOS are included for the first time in the new version of the Standards for Drinking Water Quality (GB 5749-2022) to be published in China in 2022, which is advisory but has been used as a basis for monitoring and risk management (Standardization Administration of China (SAC), 2022).

doi:10.6342/NTU202503155

Table 2.1 International PFAS regulations in drinking water

Country / Region	Regulation / Guideline	Covered Substances	Limit Value (Drinking Water)
USA	EPA National Primary Drinking Water Regulation	PFOA, PFOS, PFNA, PFHxS, HFPO-DA (GenX), PFBS	PFOA/PFOS: 4 ppt (individual MCL) PFBS, PFNA, PFHxS, GenX: ・ 10 ppt (individual MCL) ・ hazard index < 1
European Union (EU)	Drinking Water Directive (EU 2020/2184)	Total PFAS Sum of 20 PFAS	Total PFAS: 0.5 µg/L Sum of 20 PFAS: 0.1 µg/L
Denmark	Agreement on a National Action Plan for PFAS	22 PFAS	Total 22 PFAS: 100 ng/L PFOA+PFOS+ PFHxS+PFNA
New Zealand	Drinking Water Standards for New Zealand 2022	PFOA, PFOS, PFHxS,	PFOA: 560 ng/L PFHxS & PFOS: 70 ng/L
Australia	Australian Drinking Water Guidelines (ADWG)	PFOS, PFOA, PFHxS, PFBS	PFOS: 8 ng/L PFOA: 200 ng/L PFHxS: 30 ng/L PFBS: 1000 ng/L
Canada	Health Canada's Drinking Water Objective	25 specific PFAS	Sum of 25 PFAS: 30 ng/L

doi:10.6342/NTU202503155

Japan	For tap water: Revised Policy on Handling of PFOS and PFOA Levels in Tap Water (Draft) For mineral water, water quality standards under the Food Sanitation Act	PFOA, PFOS	Combined: 50 ng/L
China	Standards for drinking water quality (GB 5749-2022)	PFOA, PFOS	PFOS: 40 ng/L PFOA: 80 ng/L

doi:10.6342/NTU202503155

2.4.2 Evolution of PFAS regulations in Taiwan

Taiwan has been increasingly active in addressing PFAS contamination, reflecting growing global awareness and scientific understanding of these "forever chemicals." The evolution of its regulations demonstrates a progressive shift from initial awareness to establishing concrete limits, particularly in drinking water. Complying with the Stockholm Convention, Taiwan has actively aligned its chemical management policies with international norms. Initial regulatory attention was directed toward PFOS and PFOA. In September 2020, the Environmental Protection Administration (now the Ministry of Environment, MOENV) reclassified PFOA and related precursors, such as perfluorooctane sulfonyl fluoride, as Class 1 Toxic Chemical Substances, thereby imposing strict limitations on their production and use, which was restricted primarily to research, analysis, and education (行政院, 2024).

In addition to the previously listed substances, the following substances are also listed: Perfluorooctane sulfonic acid lithium salt (PFOS-Li) (Class I and Class II toxic substances) and Perfluorooctane sulfonyl fluoride (PFOSF) (Class I toxic substance). Besides, PFHxS and its salts (Class I toxic substance) were officially announced in the list published in April 2024. All of them were listed in the announcement and are now banned or restricted in use. However, due to the widespread use and distribution in the past few decades, some of them are still in use, coupled with the mobility and persistence of PFAS substances, PFAS pollution is still ubiquitous in the environment. Through the bioaccumulation and biomagnification effects of the food chain, the impact on organisms and the ecosystem cannot be ignored (Chemicals Administration Ministry of Environment (CAME), 2025).

Since 2007, the Ministry of Environment of Taiwan has conducted a program titled

doi:10.6342/NTU202503155

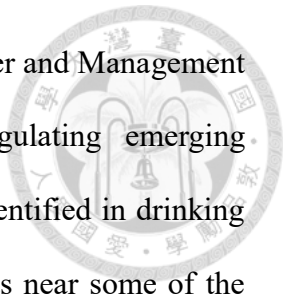

"Investigation of Compounds of Emerging Concern in Drinking Water and Management of Water Quality" every year, focusing on detecting and regulating emerging contaminants. Between 2020 and 2023, PFAS contamination was identified in drinking water sources, particularly near industrial zones and sampling points near some of the airports. In 2023, 37 water treatment plants reported PFAS levels exceeding international reference values, with PFOA and PFOS being the most frequently detected. (環境部, 2023).

Concurrently, Taiwan developed legally binding PFAS standards for drinking water. In August 2024, the MOENV announced proposed amendments to the Drinking Water Quality Standards, aiming to establish maximum permissible levels for specific PFAS. The proposed limits include a combined concentration of PFOA and PFOS not exceeding 50 ng/L, and a combined concentration of PFOS and PFHxS limited to below 70 ng/L. After public consultation, these standards are expected to take legal effect on July 1, 2027. Under the new regulations, non-compliance would trigger mandatory mitigation actions, including detailed risk assessments, remediation planning, and fines ranging from NT$60,000 to NT$600,000 (環境部水質保護司, 2024).

Taiwan has established standard analytical procedures for PFAS detection to support enforcement and data reliability. National Environmental Research Agency (NERA) employs liquid chromatography-tandem mass spectrometry (LC-MS/MS) as the principal analytical platform. Specifically, the NIEA W542.51B (was started in April 2021, and was ended up in April 2025) and NIEA W542.52B (was started in April 2025) - entitled "Method for Determination of Per- and Polyfluoroalkyl Substances in Water by Liquid Chromatography/Tandem Mass Spectrometry" - are the nationally recognized protocols for the quantification of PFAS in environmental water samples. These methods provide robust sensitivity and specificity, supporting accurate detection of trace levels of PFAS

doi:10.6342/NTU202503155

compounds across various water matrices (National Environmental Research Agency (NERA), 2024).

To further enhance analytical capacity, Taiwan plans to adopt the U.S. EPA Method 1633, which enables broader PFAS coverage, including up to 40 targeted compounds. This initiative aligns with international standards and supports Taiwan's intention to harmonize its monitoring framework with global efforts such as the U.S. Unregulated Contaminant Monitoring Rule 5 (UCMR5).

Despite these efforts, Taiwan faces several ongoing challenges, including data gaps on exposure pathways (e.g., dietary intake, dust), limited availability of advanced analytical instruments, and stronger interdepartmental coordination. Long-term concerns remain due to PFAS bioaccumulation and environmental persistence. Strengthening surveillance systems, refining risk assessments, and enhancing regulatory enforcement remain critical to ensuring long-term public health protection.

2.5 Overview of emerging and experimental PFAS treatment methods

2.5.1 Comparison of different PFAS treatment technologies

As previously mentioned, conventional water treatment processes are mainly used to remove suspended solids and control pathogens in water, but cannot effectively remove emerging pollutants such as PFAS. Advanced treatment technologies listed in Table 2.2 offer the robust removal capabilities necessary to mitigate the risks posed by both legacy and emerging water quality challenges, and should be considered essential components of future water infrastructure planning and investment (Saeidi et al., 2024; Sanzana et al., 2025; Z. Wang et al., 2017; Yadav et al., 2022).

doi:10.6342/NTU202503155

Table 2.2 Summary of PFAS Treatment Technologies

Technology	Advantages	Limitations / Challenges	References
Granular Activated Carbon (GAC)	Proven, cost-effective for long-chain PFAS	Less effective on short-chain PFAS; media replacement needed	(Appleman et al., 2014); (U.S. EPA, 2017) (Sanzana et al., 2025)
Ion Exchange (IX) Ion Exchange Resins (IER)	Anionic exchange resins (AER); high removal efficiency, fast kinetics	Disposal of spent resin; less effective on some compounds	(Ross et al., 2018); (U.S. EPA, 2025a) (Sanzana et al., 2025)
Reverse Osmosis (RO)	Very high removal rate (broad-spectrum PFAS)	High cost, produces concentrate that needs disposal	(Rahman et al., 2014)
Advanced Oxidation Processes (AOP)	Capable of degrading some PFAS; suitable for post-treatment destruction	Less effective on highly stable PFAS (e.g., PFOA, PFOS); energy intensive; may form byproducts	(Lutze et al., 2018); (Ersan et al., 2024)
Electrochemical Oxidation	Destroys PFAS instead of capturing	High energy input; still under development	(Smith et al., 2023)
Foam Fractionation	Effective pre-treatment for destruction processes	Works best on long-chain PFAS with surfactant-like behavior	(Smith et al., 2022); (We et al., 2024)
Thermal Destruction (incineration)	Permanent destruction possible	High cost, regulatory scrutiny over emissions	(Winchell et al., 2021)

doi:10.6342/NTU202503155

2.5.2 The removal of PFAS by activated carbon adsorption

1. The mechanism of activated carbon adsorption

Granular activated carbon (GAC) is a porous adsorption medium known for its extremely high internal surface area. GAC is produced from various raw materials with porous structures, including bituminous coal, lignite coal, peat, wood, and coconut shells. Physical and chemical manufacturing processes are applied to these raw materials to create or enhance the pore structure. This results in a material with a high surface area for each unit of mass. GAC effectively removes taste- and odor-causing compounds, natural organic matter, volatile organic compounds (VOCs), synthetic organic compounds, and precursors to disinfection byproducts. Organic compounds with high molecular weights are particularly amenable to adsorption. The treatment capacities for different contaminants depend on the properties of the specific GAC used, which can vary significantly based on the raw materials and manufacturing processes employed (U.S. EPA, 2025c).

Activated carbon removes PFAS primarily through a combination of physical adsorption and chemical adsorption mechanisms. Physical adsorption is governed by weak intermolecular forces such as van der Waals interactions and is typically reversible. It enables monolayer or multilayer adsorption and dominates the interaction between activated carbon and most PFAS compounds under typical water treatment conditions (Rossner et al., 2009).

2. Removal of PFAS by activated carbon adsorption

Activated carbon adsorption is widely recognized as one of the most effective technologies for removing PFAS from water. The primary mechanism involves interactions between PFAS molecules and the large specific surface area and porous structure of activated carbon. These interactions particularly favor the removal of

doi:10.6342/NTU202503155

long-chain PFAS, such as PFOA and PFOS, due to their greater hydrophobicity (Cantoni et al., 2021).

Activated carbon is commercially available in two main forms: powdered activated carbon (PAC) and granular activated carbon (GAC), and can be produced from various raw materials such as coal, coconut shell, and wood. PAC, characterized by its small particle size, offers a rapid adsorption rate and is commonly applied in short-term or emergency water treatment scenarios. However, its fine nature necessitates the use of additional coagulation or sedimentation processes to facilitate removal. In contrast, GAC is generally used in fixed-bed filter systems due to its structural stability and longer operational lifespan, making it more suitable for continuous and long-term applications (Gidstedt et al., 2022).

The performance of activated carbon can also vary significantly depending on its origin and manufacturing process. McNamara et al. (2018) reported that bituminous coal-based re-agglomerated carbons exhibited superior removal efficiency for targeted PFAS compounds compared to coconut-based activated carbon. Their study also highlighted the potential benefits of carbon reactivation for improving economic feasibility (McNamara et al., 2018).

The adsorption mechanisms of PFAS onto activated carbon involve both physical and chemical interactions. According to a review by Sanzana et al. (2025), the dominant mechanism for PFAS adsorption onto GAC is hydrophobic interaction with the carbon's pore surfaces. This is often supported by secondary electrostatic interactions, which may either enhance or hinder adsorption depending on the net surface charge of the GAC. Wu et al. (2020) further emphasized that smaller carbon particle sizes enhance adsorption performance due to an increased external surface area (Chow et al., 2022; Sanzana et al., 2025; Wu et al., 2020).

doi:10.6342/NTU202503155

In contrast, chemisorption involves stronger and often irreversible interactions, such as covalent bonding, electrostatic attraction, or hydrogen bonding. These are associated with higher adsorption enthalpies and typically result in monolayer adsorption. The contribution of chemisorption depends on the surface chemistry of the activated carbon, including the presence of functional groups, as well as the specific PFAS compound involved (Babel & Kurniawan, 2003).

Several physical and chemical properties of activated carbon, such as specific surface area, porosity, iodine value, phenol value, and methylene blue adsorption capacity, affect its adsorption performance. The hydrophobicity of PFAS compounds is a key factor, with longer-chain PFAS generally showing higher adsorption affinity (Kempisty et al., 2022; Park et al., 2020). Moreover, carbon materials with higher micropore surface area and a positive surface charge are more effective at adsorbing hydrophilic and moderately hydrophobic PFAS, whereas mesoporous carbons perform better for more hydrophobic species (Cantoni et al., 2021; Park et al., 2020). Additionally, the pore structure influences the adsorption behavior; for example, mesoporous sorbents may facilitate the assembly of PFAS molecules within the pores (Robertson et al., 2025).

Finally, water matrix characteristics also play an important role. The presence of background organic matter can compete with PFAS for adsorption sites, often reducing GAC performance. Consequently, GAC generally shows lower carbon usage rates in groundwater compared to surface water (Kempisty et al., 2022). These insights underscore the importance of considering both adsorbent properties and water quality when designing treatment systems for PFAS removal.

doi:10.6342/NTU202503155

Table 2.3 PFAS removal efficiency in water matrices through different types of activated carbon

Adsorbent Description	Doses of adsorbent	Target PFAS	Operational condition (Initial concentration, time)	Removal Efficiency (%)	Reference
PAC	10 mg/L	The total $PFAS_{76}$ Long-chain PFAS	10 min	40 20	(Alameddine et al., 2025)
GAC	10 mg/L	The total $PFAS_{76}$ Long-chain PFAS	27,000 BV	43 80	(Alameddine et al., 2025)
PAC (coconut husk), PAC (coal), PAC (wood)	1ppm 10ppm	PFOS and PFOA	100 ng/L, 72 h (25°C)	> 90	(Eun et al., 2022)
GAC (coconut husk)	1ppm 10ppm	PFOS PFOA	100 ng/L, 72 h (25°C)	- 12	(Eun et al., 2022)
Filtrasorb 400 GAC	-	PFBA, 4:2 FTS, 8:2 FTS PFBS, PFOA, PFOS	428.08-1054.26 μg/L, 336 h	30-50	(Zhang et al., 2023)[a]
GAC PAC	-	PFBA, PFBS, PFHxA, PFHxS, PFHpA, PFOA, PFOS, PFDA, GenX, 6:2 FTSA	200 μg/L, 24 h	> 90	(Tan et al., 2023)[a]
GAC	-	PFBA, PFOA, PFHxA, PFPrS, PFBS, PFGxS, PFPeS, PFPeA, PFECHS	0.001-0.36 μg/L, 4.22-22 min	23-99	(Tisler et al., 2025)[a]

[a] Obtained from (Sanzana et al., 2025).

doi:10.6342/NTU202503155

2.5.3 Laboratory experiments for assessing adsorption efficiency

1. Adsorption kinetics

Adsorption kinetics refer to the rates of adsorption and desorption processes and how they are influenced by various operational conditions such as temperature, pressure, adsorbate concentration, and adsorbent characteristics. Understanding these mechanisms offers insights into adsorption efficiency and the controlling factors involved in pollutant removal (Ho & McKay, 1999; Yu et al., 2009).

(1) Pseudo-first-order model

The pseudo-first-order kinetic model assumes that the occupation rate of adsorption sites is proportional to the number of unoccupied sites. This model is primarily applicable when the adsorbate-adsorbent interaction is relatively weak and the surface coverage is low, making it suitable for systems dominated by physical adsorption. The differential form of the model is expressed:

$$\frac{dq_t}{dt} = k_1(q_e - q_t) \qquad (2\text{-}1)$$

Integrating this equation with boundary conditions $q_t = 0$ at $t = 0$, and $q_t = q_t$ at $t = t$, yields the linearized form:

$$\ln(q_e - q_t) = \ln q_e - k_1 t \qquad (2\text{-}2)$$

Where:

q_t (mg/g) is the amount of PFAS adsorbed per unit mass of activated carbon at time, q_e (mg/g) is the equilibrium adsorption capacity, k_1 (1/min) is the pseudo-first-order rate constant, and t (min) is the adsorption time.

This model is commonly applied to systems where physisorption dominates and is particularly effective under low concentration conditions.

doi:10.6342/NTU202503155

(2) Pseudo-second-order model

The pseudo-second-order kinetic model assumes that the adsorption process is chemisorption-controlled, involving valence forces through sharing or exchange of electrons between adsorbent and adsorbate. The rate-limiting step is assumed to be related to the square of the available adsorption sites, often making this model more suitable for systems with high surface coverage and stronger adsorbate-adsorbent interactions. The differential equation is given as:

$$\frac{dq_t}{dt} = k_2(q_e - q_t)^2 \quad (2\text{-}3)$$

Integrating with the same boundary conditions, the equation becomes:

$$\frac{t}{q_t} = \frac{1}{k_2 {q_e}^2} + \frac{t}{q_e} \quad (2\text{-}4)$$

Where:

q_t (mg/g) is the amount of PFAS adsorbed per unit mass of activated carbon at time, q_e (mg/g) is the equilibrium adsorption capacity, k_2 (g/(mg·min)) is the pseudo-second-order rate constant, and t (min) is the adsorption time.

This model has been widely applied to water and air treatment processes with dominant chemical interactions. Comparing the experimental data with both models allows us to assess the dominant adsorption mechanism under various conditions.

2. Adsorption isotherms

To evaluate the adsorption behavior of PFAS onto activated carbon, equilibrium data were fitted to two widely accepted isotherm models: the Langmuir Isotherm Model and the Freundlich Isotherm Model (Allen et al., 2004; Kalam et al., 2021).

(1) Langmuir Isotherm Model

The Langmuir model assumes monolayer adsorption onto a surface with a finite number of identical binding sites. It is particularly suitable for describing

doi:10.6342/NTU202503155

adsorption processes with limited and uniform surface coverage.

The nonlinear form of the Langmuir equation is expressed as:

$$q_e = \frac{q_{max} K_L C_e}{1 + K_L C_e} \quad (2\text{-}5)$$

which can also transfer into linearized form:

$$\frac{C_e}{q_e} = \frac{1}{q_{max}} C_e + \frac{1}{q_{max} K_L} \quad (2\text{-}6)$$

Where:

q_e (ng/mg) is the amount of PFAS adsorbed per unit mass of activated carbon at equilibrium, C_e (ng/L) is the equilibrium concentration of PFAS in solution, q_{max} (ng/mg) is the maximum adsorption capacity, and K_L (L/ng) is the Langmuir constant related to the affinity between adsorbate and adsorbent.

This model helps determine the theoretical saturation capacity of the adsorbent and assess its suitability for PFAS removal from aqueous systems.

(2) Freundlich Isotherm Model

The Freundlich isotherm is an empirical model that describes adsorption on heterogeneous surfaces and multilayer interactions. It is particularly relevant to real-world water treatment scenarios with common surface heterogeneity and varied binding site energies.

The Freundlich equation is given by:

$$q_e = K_F {C_e}^{1/n} \quad (2\text{-}7)$$

or its linearized logarithmic form:

$$\log q_e = \log K_F + \frac{1}{n} \log C_e \quad (2\text{-}8)$$

Where:

q_e (ng/mg) is the amount of PFAS adsorbed per unit mass of activated carbon at equilibrium. K_F [(ng/mg)(L/ng)$^{1/n}$] is the Freundlich constant indicative of

doi:10.6342/NTU202503155

adsorption capacity, $1/n$ is a dimensionless heterogeneity factor, with values between 0 and 1 indicating favorable adsorption.

A plot of $\log q_e$ versus $\log C_e$ should yield a straight line. The slope of this line gives $1/n$, and the intercept gives $\log K_F$. The value of $1/n$ typically lies between 0 and 1 for favorable adsorption. If $1/n$ is close to 0, the adsorption is highly favorable, while values closer to 1 suggest weaker adsorption.

Comparison of the two models provides insight into the adsorption mechanisms and surface interactions between PFAS molecules and activated carbon.

3. Rapid Small Scale Column Test (RSSCT)

The Rapid Small-Scale Column Test (RSSCT) is an established laboratory-scale method used to simulate the breakthrough behavior of full-scale GAC systems (Crittenden et al., 1991). This approach is particularly valuable in evaluating trace contaminant removal, such as PFAS, under realistic water treatment conditions. By appropriately scaling down system parameters, which include GAC particle size, bed dimensions, and flow rate, the results of RSSCT tests can be used to forecast the performance of full-scale GAC columns. RSSCT allows for simulation of long-term adsorption processes, which typically span one to three months in full-scale operations, to be modeled within a significantly shorter duration, usually three days to three weeks. The underlying principle of RSSCT is to preserve similarity between the laboratory-scale and full-scale systems by maintaining geometric and kinetic relationships, most notably the ratio between empty bed contact time (EBCT) and GAC particle diameter. Critical mass transfer processes, such as film diffusion and intraparticle diffusion, can be reasonably approximated through this proportional scaling.

doi:10.6342/NTU202503155

In practice, the design of an RSSCT requires careful selection and adjustment of several operational parameters (Poddar, 2013). These include the EBCT, flow velocity, hydraulic loading rate, total bed volume treated, and properties of the activated carbon such as particle size and pore structure. Together, these factors determine the contact time and the accessibility of adsorption sites within the media, thereby influencing the shape and position of the resulting breakthrough curve. The small internal diameter of the RSSCT column and the choice of adsorbent layer thickness must also be calibrated to ensure sufficient resolution of breakthrough behavior while minimizing wall effects or flow channeling. Because of the reduced scale and time, RSSCTs allow researchers to perform parallel comparisons of activated carbons under identical water matrices, facilitating media selection and design optimization for full-scale implementation.

One of the main advantages of the RSSCT method lies in its efficiency. Compared to pilot-scale column studies, RSSCTs consume significantly less water and require fewer operational resources, making them particularly useful for testing under low contaminant concentrations. Furthermore, they provide a practical and scalable means to estimate carbon bed life, assess the relative adsorption performance of various media, and simulate long-term operation within a reasonable experimental window.

However, the method is not without limitations. While theoretical scaling principles suggest that RSSCT breakthrough curves should match those of full-scale systems, discrepancies may arise due to real-world complexities. For instance, the presence of natural organic matter (NOM), variability in background water quality, biological activity, and operational disturbances such as pore clogging or channeling may cause the actual performance of full-scale systems to deviate from laboratory

doi:10.6342/NTU202503155

projections (Corwin & Summers, 2010). Moreover, the assumptions inherent to RSSCT design, such as homogeneity of flow and uniform particle geometry, may not fully capture the hydrodynamic diversity of large-scale systems. These factors, as described by Crittenden et al. (1991), can lead to differences in adsorption kinetics and breakthrough time, particularly when NOM or other background constituents compete for adsorption sites (Crittenden et al., 1991). Nevertheless, despite these challenges, RSSCT remains a highly useful tool for predicting PFAS removal efficiency, providing cost-effective and timely insights that can support the design and operation of full-scale activated carbon systems.

doi:10.6342/NTU202503155

Chapter 3 Materials and Methods

3.1 Research Frameworks

This study aims to evaluate the effectiveness of activated carbon adsorption in removing PFAS from drinking water, specifically focusing on PFBS, PFHxS, PFOA, and PFOS. To achieve this goal, a multi-stage experimental framework was developed. This framework includes laboratory-scale batch experiments and dynamic column simulations, supported by advanced analytical techniques.

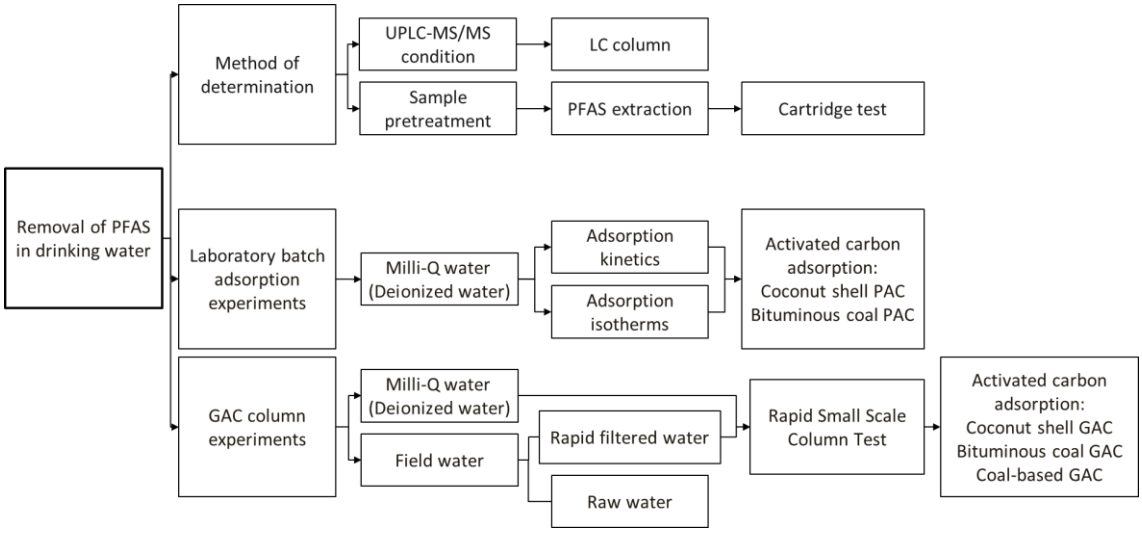

Figure 3.1 Research framework of the present study

First of all, the analytical determination of PFAS standard was conducted using Ultraperformance Liquid Chromatography-Tandem Quadrupole Mass Spectrometer (UPLC-MS/MS). This followed appropriate sample pretreatment procedures and PFAS extraction utilizing solid-phase cartridges. A suitable liquid chromatography (LC) column was chosen to ensure reliable separation and quantification of the target analytes.

The experimental framework comprised two main components: laboratory batch adsorption experiments and granular activated carbon (GAC) column experiments. In the batch experiments, both Milli-Q water and rapid filtered water were utilized to examine

doi:10.6342/NTU202503155

adsorption behavior under controlled conditions. These tests focused on adsorption kinetics and isotherms to understand the rate and capacity of PFAS uptake by two types of activated carbon - coconut shell-based and bituminous coal GAC.

Rapid small-scale column tests (RSSCT) were performed to simulate real-world scenarios and assess the adsorbents' long-term performance. These column experiments employed various water matrices, including Milli-Q water and field rapid filtered water taken from the treatment plant, to evaluate the PFAS breakthrough behavior and effectiveness of activated carbon under dynamic flow conditions.

Through this integrated experimental and analytical approach, this study aims to provide actionable insights into the application of activated carbon for PFAS removal and to inform decision-making in water treatment practices.

3.2 Sample collection and preparation

Raw water and unchlorinated rapid filtered water samples were collected from the Drinking Water Treatment Plant (DWTP) in northern Taiwan in December 2024 and April 2025. The daily water output from the DWTP is approximately 350,000 metric tons. The coagulation unit at the DWTP carries out the coagulation process by adding polyaluminum chloride (PAC).

To assess the concentration of specific PFAS in raw water and to evaluate the adsorption performance of GAC in removing PFAS from rapid filtered water, the samples were collected directly from the effluent of the rapid filter. After collection, the samples were sealed in 20 L pre-cleaned plastic water storage buckets and stored at 4 °C until analysis.

doi:10.6342/NTU202503155

3.3 Chemicals and Materials

3.3.1 PFAS analyzed

The common PFAS structures are shown in Table 3.1. The difference between PFCAs and PFSAs is that they separately contain functional groups such as carboxylic acid (-COOH) and sulfonic acid (-SO_3H).

Table 3.1 The common PFAS structures

Perfluoroalkyl carboxylic acids							**Perfluoroalkyl sulfonic acids**		
n=5	n=6	n=7	n=8	n=9	n=10	n=12	n=4	n=6	n=8
PFPeA	PFHxA	PFHpA	PFOA	PFNA	PFDA	PFDoA	PFBS	PFHxS	PFOS
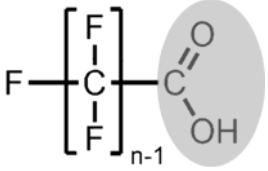							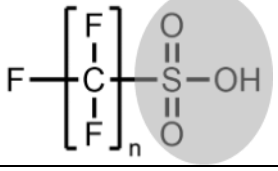		

Several PFAS had been mentioned and should be of concern; they were selected as the target compounds in this study, including Perfluorobutane sulfonic acid (PFBS), Perfluorohexane sulfonic acid (PFHxS), Perfluorooctanoic acid (PFOA), and Perfluorooctane sulfonic acid (PFOS). The Physicochemical properties of the target PFAS are shown in Table 3.2.

1. Equipment and reagents:
   (1) Perfluobutane-1-sulfonic acid (PFBS), 100 μg/mL(100 ppm) in Methanol, 1 mL, AccStandard®, New Haven, CT, USA
   (2) Perfluorohexane-1-sulfonic acid (PFHxS), 100 μg/mL(100 ppm) in Methanol, 1 mL, AccStandard®, New Haven, CT, USA
   (3) Perfluorooctanoic acid (PFOA), 100 μg/mL(100 ppm) in Methanol, 1 mL, AccStandard®, New Haven, CT, USA

doi:10.6342/NTU202503155

(4) Perfluorooctane sulfonic acid (PFOS), 100 μg/mL(100 ppm) in Methanol, 1 mL, AccStandard®, New Haven, CT, USA

(5) Perfluoro-n-(1,2,3,4-$^{13}C_4$)octanoic acid, 1.2 mL × 50 μg/mL, Wellington Laboratories Inc., CANADA

(6) Sodium perfluoro-1-(1,2,3,4-$^{13}C_4$)octanesulfonate, 1.2 mL × 50 μg/mL, Wellington Laboratories Inc., CANADA

(7) Methanol, LC-MS grade, LC-MS CHROMASOLV™, Honeywell, Muskegon, MI, USA

2. Chemical preparation

(1) Pre-dilution of Individual Standards:

Dilute each of the four high-concentration raw standards to an intermediate concentration of 5000 μg/L for subsequent quantitative mixing. The solvent used for dilution is LC-MS grade methanol. The internal standards were also diluted into low-concentration solutions.

(2) Mixing operation:

Each of the 5000 μg/L standard solutions listed above was mixed to make a mixed standard. The concentration of each PFAS in the mixed standard is 1000 ng/mL. The initial concentration of each experiment situation is 100 ng/L. The internal standards were also mixed into 100 μg/L.

(3) Sample collecting

Each of the samples was collected in a 50 mL glass sampling bottle, and then spiked with 20 μL of the mixed internal standards.

doi:10.6342/NTU202503155

Table 3.2 Physicochemical properties of the target PFAS.

Compounds	Acronym	Chain length	Molecular structure	Structural formula[a]	Mw (g/mol)	$LogK_{ow}$ [b]	pK_a [b]
Perfluorobutane sulfonic acid	PFBS	4	$C_4HF_9SO_3$	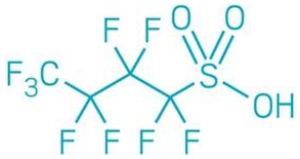	299	1.82	−3.31
Perfluorohexane sulfonic acid	PFHxS	6	$C_6HF_{13}SO_3$	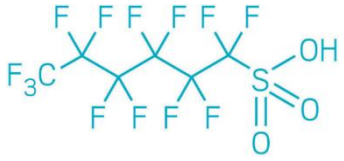	399	3.16	0.14
Perfluorooctane sulfonic acid	PFOS	8	$C_8HF_{17}SO_3$	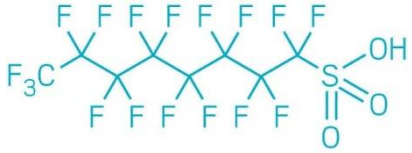	499	4.49	< 0.1
Perfluorooctanoic acid	PFOA	8	$C_8HF_{15}O_2$	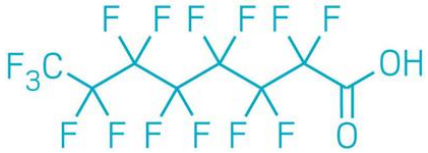	414	4.81	< 4.2

[a] Obtained from (CHEMICAL & ENGINEERING NEWS)

[b] Obtained from (Erica Gagliano et al., 2020)

doi:10.6342/NTU202503155

3.3.2 Activated carbon adsorption

The factors that make activated carbon adsorption a widely used treatment technology include the different applications of activated carbon particle size, the functional activity of activated carbon surface, specific surface area, activated carbon pore size and area, factors affecting adsorption capacity, etc. Among them, factors such as specific surface area and surface porosity affect activated carbon adsorption(Bansal, 2005; National Research Council (US) Safe Drinking Water Committee, 1980).

The activated carbons used in the experiment included FILTRASORB® 400 (F400, granular activated carbon) produced by Calgon Carbon Corporation (USA); TAC-Q (granular coal-based activated carbon) and TAC-C (granular coconut shell activated carbon) produced by TAIWAN ACTIVATE CARBON (Taipei, Taiwan).

Before experiments, the activated carbon was sieved to control the particle size distribution. After shaking through the sieves of different particle sizes for more than 30 minutes, the samples on the last sieve were taken. Since the activated carbon itself easily adsorbs some impurities, in order to achieve the best adsorption effect, the granular and powdered activated carbon used in this study refers to the method published by Newcombe et al. in 1997. A large amount of deionized water is used to clean the activated carbon for a few hours, then it is placed in a 105ºC oven for about 48 hours to dry it. Finally, it is placed in a drying oven to cool down to prevent the activated carbon from getting damp again due to contact with the outside air (Newcombe et al., 1997).

Due to the difference in activated carbon sizes, the size between 30-50 mesh would be collected for granular activated carbon (GAC) in this study, and the size between 100-200 mesh would be collected as the powder activated carbon (PAC) in this study.

doi:10.6342/NTU202503155

Table 3.3 Comparison of activated carbon adsorption characteristics

Material	Product name/ Code	Mesh	BET surface area (m^2/g)	Mesopore volume (m^3/g)	t-Plot micropore area (m^2/g)	t-Plot micropore volume (m^3/g)	Supplier
Bituminous coal	FILTRASORB® 400 (F400)	8 × 30	969.6	0.1941	758.1	0.298	Calgon carbon
Coal	TAC-Q	8 × 30	1040.5	0.3169	648.7	0.2579	TAIWAN ACTIVATE CARBON (台灣炭素)
Coconut shell	TAC-C	8 × 30	1139.2	0.1298	932.8	0.3716	TAIWAN ACTIVATE CARBON (台灣炭素)

doi:10.6342/NTU202503155

3.4 Experiment processes

3.4.1 Adsorption kinetics

1. Equipment for adsorption kinetics

The adsorption kinetics system, shown in Figure 3.2, consists of a 5 L glass serum bottle holding 4 L of Milli-Q water. A stirring bar is placed inside the bottle, and the bottle is placed on a magnetic stirrer for mixing.

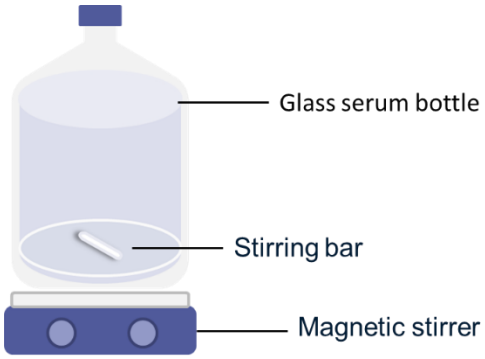

Figure 3.2 Adsorption kinetics processes system

2. Procedures of adsorption kinetics

To compare the performances of two types of activated carbon (AC), experiments were conducted using 15 mg/L of each type of activated carbon in Milli-Q water. The initial concentration of each specific PFAS added to the water matrix was 100 ng/L. For sampling, each sample was collected in a volume of 50 mL. The sampling times for this experiment were as follows: 0 hours (before adding AC), and then at 0.5, 1, 1.5, 2, 4, 6, 12, and 24 hours after adding the AC. The results of the adsorption kinetics were used to study the adsorption rate of contaminants as they transfer into the pores of the adsorbent over time.

doi:10.6342/NTU202503155

3.4.2 Adsorption isotherms

1. Equipment for adsorption isotherms

The adsorption isotherm system, illustrated in Figure 3.3, consists of a flocculator capable of setting six different doses of powdered activated carbon (PAC) in Milli-Q water, using six 1 L beakers. The flocculator is designed to maintain a constant mixing rate to ensure uniformity of the samples. In each 3-hour session during the day, a mercury thermometer is used to monitor the temperature of the water samples, ensuring it remains at room temperature. The result may be similar to that obtained in the stirring water bath.

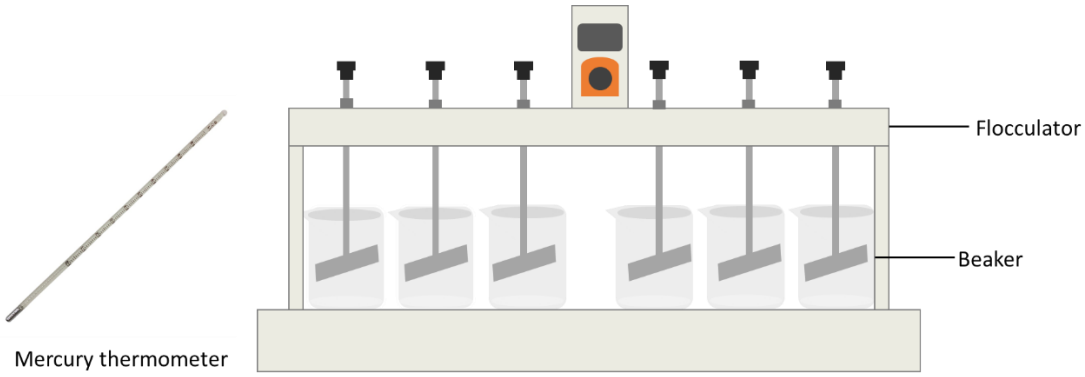

Figure 3.3 Adsorption isotherms process system

2. Procedures of adsorption isotherms

Experiments were conducted using concentrations of 0, 10, 20, 30, 40, and 50 mg/L for each type of AC in Milli-Q water. The initial concentration of each specific PFAS in the water matrices was set at 100 ng/L within a 6 L water sample, which was then divided into six 1 L beakers. A flocculator was set up with a stirring rate of 50 rpm.

For sampling, each sample was collected in a volume of 50 mL, with sampling times occurring at 0 hours (prior to adding AC) and at 72 hours after AC addition.

doi:10.6342/NTU202503155

The results of the adsorption isotherms were used to investigate the maximum adsorption capacity of the adsorbent at equilibrium under constant temperature conditions.

3.4.3 Rapid Small Scale Column Test (RSSCT)

1. Equipment of Rapid Small Scale Column Test

   (1) Glass column, outer diameter 6 mm, thickness 1 mm, length 130 mm.

   (2) Quartz sand

   (3) Glass fiber

   (4) Granular activated carbon, 30-50 mesh

   (5) Isocratic pump

   (6) 1/4” teflon pipe

   (7) 1/16” teflon pipe

   (8) Stainless steel bulkhead female connector

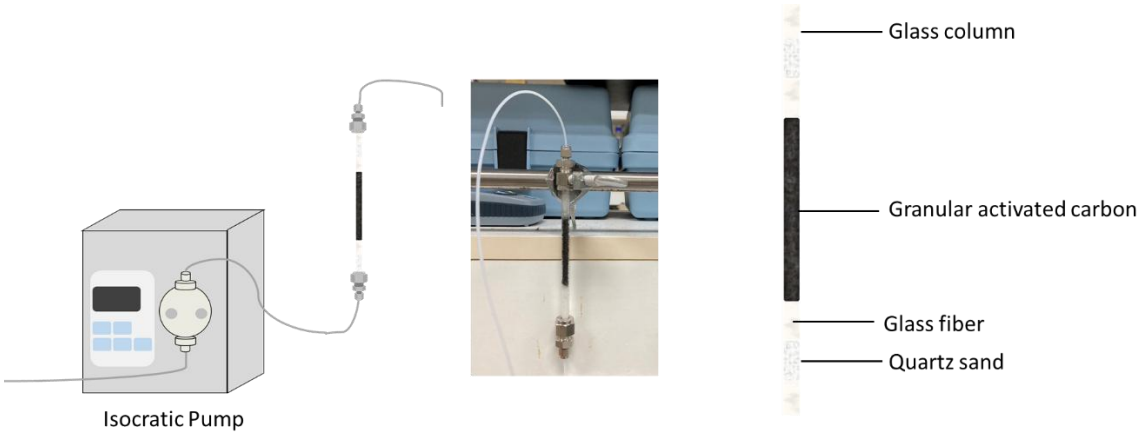

Figure 3.4 Rapid Small Scale Column Test (RSSCT) processes system

2. Procedures of Rapid Small Scale Column Test

   (1) Filling the GAC column

doi:10.6342/NTU202503155

I. An experimental platform in the fume hood is required to fill the activated carbon column.

II. Use a forcep to fill about 1 cm of glass fiber and poke it inward to 3 cm. Operate in the fume hood to prevent the glass fiber from floating.

III. Use spatulas to fill about 1 cm of quartz sand, and vibrate while filling to reduce the gaps.

IV. Use a forcep to fill about 1.3 cm of glass fiber.

V. Use a fine medicine spoon to fill 5.1~5.2 cm of granular activated carbon, and vibrate while filling.

VI. Use a forcep to fill about 1 cm of glass fiber on the other side.

VII. Use spatulas to fill about 1 cm of quartz sand on the other side, and vibrate while filling to reduce the gaps.

VIII. Use a forcep to fill about 1.3 cm of glass fiber on the other side.

(2) Set up the RSSCT system

I. Connect the pump to the power supply.

II. Set up the flow rate, which is close to 1 mL/min.

III. Tighten the top and bottom connecting pipes of the pump and tighten them manually with the bulkhead female connector on the pipes.

i. Top: 1/16” teflon pipe

ii. Bottom: 1/4” teflon pipe

IV. Tighten the 1/16” teflon pipe (pump outlet; column inlet) to the top and bottom of the glass column.

V. Tighten the lower 1/4” teflon pipe in a beaker containing 150 mL Milli-Q water. Make sure that the pipe is submerged below the water surface.

VI. Turn on the pump switch and press the RUN/STOP button to start rinsing

doi:10.6342/NTU202503155

the pipe with Milli-Q water. (The rinsing time is about 1~2 hours.)

VII. Place the 1/16" teflon pipe (water outlet) in a beaker, pay attention to the outflow volume and time, and adjust the flow rate.

VIII. After the rinsing is completed, put the 1/4” teflon pipe in the 20 L pre-cleaned plastic water storage buckets, and the other side is put in the sampling glass bottle, and press the RUN/STOP button to pause.

(3) Collect the sample

The initial concentration of each specific PFAS in the water matrices was set at 100 ng/L within a 20 L water sample, which was mixed for 30 minutes before experimentation.

For sampling, each sample was collected in a volume of 50 mL. In two weeks, the short-term water sample flowing out of the mini activated carbon column is collected at a fixed time every day, waiting about 60 minutes. The average initial concentration of influent was collected on days 1, 5, 10, and 14 from a 20 L sampling bucket. The experiment will continue for two weeks or until the pipeline is about to rise above the liquid level.

doi:10.6342/NTU202503155

Table 3.4 The parameters of RSSCT

Activated carbon type	Coconut shell	Bituminous coal	Coal-based
Empty Bed Contact Time (min)	1.6		
Bed diameter (cm)	0.4		
Bed height (cm)	5		
Bed volume (cm^3)*	0.62832		
Flow rate (mL/min)	1		
Particle size (mesh)	30-50		

* Bed volume = $(\frac{1}{2}\ \text{diameter})^2 \times$ height

3.5 Sample analysis

3.5.1 Pretreatments of the analysis

A robust pretreatment protocol is essential to ensure the accurate and reliable quantification of PFAS in environmental water samples. Solid Phase Extraction (SPE) is adopted in this study for pre-concentration and purification of PFAS prior to instrumental analysis. This section details the equipment and reagents, chemical preparations, extraction methods, and SPE procedures.

1. Equipment and reagents for SPE

The experimental setup for SPE is illustrated in Figure 3.5, and the required instruments and chemicals are listed as follows:

(1) Solid Phase Extraction (SPE) tank with valve to adjust flow rate, ChromTech

(2) Solid Phase Extraction (SPE) cartridges

I. Oasis HLB 6 cc Vac Cartridge, 200 mg Sorbent per Cartridge, 30 μm Particle Size, Waters Corporation, Milford, MA, USA

II. Oasis WAX for PFAS Analysis 6 cc Vac Cartridge, 150mg Sorbent per

doi:10.6342/NTU202503155

Cartridge, 30μm Particle Size, Waters Corporation, Milford, MA, USA

(3) Vacuum pump

(4) Thermo Scientific™ Savant™ SPD1010, SpeedVac Concentrator System, Thermo Fisher Scientific Inc., Waltham, MA, USA

(5) Methyl Alcohol (methanol), LC-MS grade, DUKSAN PURE CHEMICALS, Gyeonggi-do, Korea

(6) Ammonium Hydroxide, 28.0-30.0% BAKER ANALYZED® A.C.S. Reagent, J.T. Baker™, Phillipsburg, NJ, USA

(7) Formic Acid, 88% BAKER ANALYZED® A.C.S. Reagent, J.T. Baker™, Phillipsburg, NJ, USA

(8) Milli-Q water.

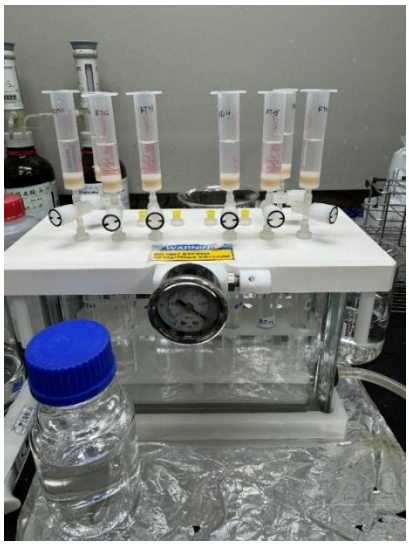

Figure 3.5 Solid Phase Extraction (SPE) process system

2. Chemical preparation

(1) 2% ammonium hydroxide in methanol: take 7 mL of approximately 28% to 30% ammonium hydroxide and add methanol to 100 mL. The methanol solution contains approximately 1.96% to 2.1% ammonia hydroxide. Prepare

doi:10.6342/NTU202503155

before use.

(2) 0.1% formic acid in Milli-Q water: take 1 mL of formic acid and add Milli-Q water to 1 L

3. Methods of SPE

Solid Phase Extraction (SPE) is a widely used sample preparation technique for isolating and concentrating target analytes from complex matrices. The process consists of two main steps: (1) adsorption, where the sample passes through a cartridge filled with a sorbent material that selectively retains the analytes of interest while allowing other substances to be washed away; and (2) elution, during which the retained analytes are recovered using appropriate solvents that disrupt the interactions between the analytes and the sorbent.

SPE effectively reduces matrix effects such as ion suppression or enhancement in LC-MS/MS, simplifies the sample composition, and enables compound-specific fractionation. This is especially important in PFAS analysis, as these contaminants often exist at ultra-trace levels in the presence of salts, organic matter, and particulates.

Selecting the right cartridges and elution solvents for SPE helps separate PFAS species based on their functional groups and carbon chain lengths, improving analytical clarity and reliability. The choice between hydrophilic-lipophilic balanced (HLB) cartridges and weak anion exchange (WAX) cartridges depends on the target analytes and the sample matrix. The comparison of the two types of cartridges is shown in Table 3.5.

HLB and WAX are two common types of SPE cartridges used for extracting PFAS. Oasis HLB cartridges contain a balanced polymeric sorbent that utilizes both hydrophilic and hydrophobic retention mechanisms, enabling the extraction of a

doi:10.6342/NTU202503155

broad range of PFAS compounds with varying polarities and functional groups. Due to this versatility, HLB cartridges have been applied to various sample types and are suitable for neutral and short-chain PFAS. They also demonstrated high extraction recovery in environmental samples (Lee et al., 2018).

In contrast, Oasis WAX cartridges employ a mixed-mode mechanism combining reversed-phase and weak anion exchange interactions. This design allows for selective retention of anionic PFAS, especially long-chain and ionic species, offering high sensitivity and reproducibility in complex matrices such as groundwater, drinking water, soil, and food. Studies have shown WAX to be more effective than HLB for certain acidic PFAS, including short-chain perfluorocarboxylic acids (Fontanals et al., 2008; Lee et al., 2018).

doi:10.6342/NTU202503155

Table 3.5 The comparison of the two types of cartridges (Compiled from (Margot Lee, 2024; Waters, 2025))

Feature	Oasis HLB	Oasis WAX
Full Name	Hydrophilic-Lipophilic Balanced sorbent	Weak Anion eXchange sorbent
Base Material	DVB–NVP copolymer (divinylbenzene–N-vinylpyrrolidone)	DVB–NVP copolymer with weak anion exchange functional groups
Sorbent Type	Reversed-phase only	Mixed-mode: reversed-phase + weak anion exchange
Surface Properties	Balanced hydrophilic and lipophilic	Primarily lipophilic with anion exchange selectivity
Retention Mechanism	Hydrophobic interactions, hydrogen bonding, π–π interactions	Hydrophobic + ionic interaction with negatively charged analytes
Target Compounds	Wide range: neutral, polar, and non-polar compounds	Strong acids, sulfonates, organic acids, PFAS
Typical Applications	Pharmaceuticals, metabolites, and environmental pollutants	PFAS extraction, strong acid drugs, acidic metabolites
Selectivity	Broad, non-selective	High selectivity for anionic compounds

doi:10.6342/NTU202503155

4. Procedures of SPE

Samples collected for PFAS quantification, with a volume of 50 mL at each designated sampling time, will be extracted for further analysis. The SPE conditions have rarely been optimized, and the analytical conditions must be adapted for accurate PFAS quantification in low-concentration water samples. Therefore, before extracting the experimental samples, the pretreatment conditions for SPE will be tested to improve the recovery of results in Milli-Q water samples. The following factors may influence the recovery: (1) whether to adjust the pH of the water sample, (2) deciding whether to rinse the cartridges with 0.1% formic acid, and (3) testing different cartridges. This optimization aims to enhance the sample pretreatment process and improve the recovery of target PFAS compounds.

The details of SPE, including condition, sample loading, washing, and elution steps, are summarized in Table 3.6. After finishing the SPE procedures, the samples were placed into the concentrator system. Each sample would be concentrated to 0.5 mL.

doi:10.6342/NTU202503155

Table 3.6 The pretreatment conditions for the procedure of Solid Phase Extraction

Cartridges		**Oasis HLB cartridges (6cc x 200 mg)**		**Oasis WAX cartridges (6cc x 150 mg)**	
		Soak (min:sec)	Air drying (min:sec)	Soak (min:sec)	Air drying (min:sec)
Flow washing	5 mL 2% ammonium hydroxide in methanol	02:00	-	02:00	-
	5 mL methanol	02:00	-	02:00	-
	5 mL Milli-Q water	02:00	-	02:00	-
	2 mL 0.1% formic acid in Milli-Q water	02:00	-	02:00	-
Sample loading (with or without pH adjustment)		The sample was loaded at a flow rate of approximately 3 mL/min to 5 mL/min.			
Cartridge rinsing (with or without using Milli-Q water and 0.1% formic acid in Milli-Q water)		3 mL 0.1% formic acid in Milli-Q water			
		2 mL Milli-Q water			
Air drying		-	15:00	-	15:00
Elution	3 mL methanol	04:00	-	04:00	-
	3 mL methanol	04:00	02:00	04:00	02:00
	3 mL 2% ammonium hydroxide in methanol	04:00	-	04:00	-
	3 mL 2% ammonium hydroxide in methanol	04:00	05:00	04:00	05:00

doi:10.6342/NTU202503155

3.5.2 PFAS determination by UPLC-MS/MS

UPLC-MS/MS was used to quantify PFAS in this study. Prior to analysis, the concentrated sample was filtered into a 0.5 mL screw neck vial using a 0.22 μm nylon filter, preparing it for the subsequent UPLC-MS/MS quantification process.

1. Equipment and reagents
   (1) Ultraperformance Liquid Chromatography-Tandem Quadrupole Mass Spectrometer
      I. Liquid chromatography: Waters Acquity UPLC I-Class PLUS, Waters Corporation, Milford, MA, USA.
      II. Mass spectrometer: Waters Xevo® TQ-XS, Waters Corporation, Milford, MA, USA.
   (2) HPLC column: ACQUITY UPLC HSS T3 (100 x 2.1 mm, 1.8 μm), Waters Corporation, Milford, MA, USA.
   (3) Methyl Alcohol (methanol), LC-MS grade, DUKSAN PURE CHEMICALS, Gyeonggido, Korea.
   (4) Acetonitrile, HPLC grade, J.T. Baker™, Phillipsburg, NJ, USA.
   (5) Ammonium acetate, ≥99.0%, Sigma-Aldrich, St. Louis, MO, USA.
   (6) Milli-Q water.
   (7) LCGC Certified Clear Glass 12 x 32 mm Screw Neck Vial, with Cap and PTFE/Silicone Septum, 2 mL Volume, Waters Corporation, Milford, MA, USA.
   (8) Disposable syringe, 2.5 mL, TOP, Kaohsiung, Taiwan.
   (9) Syringe Filter, Nylon, 0.2 μm, 13 mm, E-ChromTech, Taipei, Taiwan
2. Chemical preparation
   (1) Mobile phase solutions

doi:10.6342/NTU202503155

I. 100%(v/v) methanol containing 5-mM ammonium acetate: dissolve 0.1927 g of ammonium acetate into 500 mL of LC-MS grade methanol (Methyl Alcohol).

II. 5 mM ammonium acetate solution: dissolve 0.1927 g of ammonium acetate into 500 mL of Milli-Q water.

III. Acetonitrile.

IV. Milli-Q water

(2) Wash solutions

I. 10 %(v/v) Methanol: dilute 100 mL LC-MS grade methanol to 1 L with Milli-Q water

II. 100 %(v/v) Methanol

3. Methods and procedures

(1) Preparation of samples, HPLC column, mobile phase solutions, and wash solutions.

(2) Tune the mass spectrometer parameters and configure the UPLC system conditions.

(3) Inlet 5 μL of each sample for PFAS quantification.

doi:10.6342/NTU202503155

4. Analytical conditions of UPLC-MS/MS

Table 3.7 MS parameters of target PFAS

Compounds	Cone voltage (V)	Ion transition (collision voltage, eV)
Perfluorobutane sulfonic acid (PFBS)	10	(-) 299→80 (15)
	10	(-) 299→99 (15)
Perfluorohexane sulfonic acid (PFHxS)	10	(-) 399→80 (45)
	10	(-) 399→99 (45)
Perfluorooctane sulfonic acid (PFOS)	10	(-) 499→80 (45)
	10	(-) 499→80 (40)
Sodium perfluoro-1-(1, 2, 3, 4-$^{13}C_4$)octanesulfonate (MPFOS)	10	(-) 503→80 (42)
Perfluorooctanoic acid (PFOA)	10	(-) 412→169 (15)
	10	(-) 412→369 (15)
Perfluoro-n-(1, 2, 3, 4-$^{13}C_4$) octanoic acid (MPFOA)	12	(-) 417→372 (8)

Table 3.8 Ion source parameters of MS

Ion mode	ESI-
Source temperature (℃)	120
Desolvation temperature (℃)	500
Cone gas flow (L/hr)	300
Desolvation gas flow (L/hr)	1000

doi:10.6342/NTU202503155

Table 3.9 UPLC-MS/MS analytical conditions

Instruments	Liquid Chromatograph: Waters Acquity UPLC I-Class PLUS Mass Spectrometer: Waters Xevo TQ-XS		
Column	ACQUITY UPLC HSS T3 (100 x 2.1 mm, 1.8 μm)		
Ionization mode	ESI-		
Column temperature (℃)	40		
Flow rate (mL/min)	0.4		
Injection volume (μL)	5		
Mobile phase	A: 5 mM ammonium acetate (aq) B: 100%(v/v) Methanol containing 5-mM ammonium acetate		
Gradient (min)	**Time**	**A (%)**	**B (%)**
	Initial (0)	80	20
	1	60	40
	2	20	80
	5	5	95
	6	80	20
	8	80	20

5. Data Processing

The experimental data were initially processed using the instrument-specific software, MassLynx V4.2, for chromatographic and mass spectrometric analysis. Subsequently, the data were organized, calculated, and visualized using Microsoft Excel 2019 for further interpretation and statistical evaluation.

doi:10.6342/NTU202503155

Chapter 4 Results and Discussions

4.1 Water quality characteristics of the water samples

Before further treatments, water samples obtained from the DWTP in northern Taiwan in December 2024 and April 2025 were first measured for water quality parameters, including pH and non-purgeable dissolved organic carbon (NPDOC). Table 4.1 displays the water quality characteristics of each water matrix used for adsorption tests. The pH of raw water ranged from 7.42 to 7.50, and the pH value in rapid filtered water ranged from 7.43 to 7.45. Besides, non-purgeable dissolved organic carbon (NPDOC) in raw water ranged from 0.69 to 0.77 mg/L, and NPDOC in rapid filtered water ranged from 0.40 to 0.53 mg/L.

Table 4.1 Parameters of raw water and rapid filtered water

Sapling date	Water type	pH value[a]	Absorbance (Abs) 254 nm[b]	NPDOC (mg/L)[c]
26th Dec., 2024	Raw water	7.42	0.061	0.69
	Rapid filtered water	7.45	0.012	0.53
18th Apr., 2025	Raw water	7.50	0.052	0.77
	Rapid filtered water	7.43	0.009	0.40

[a] The analysis instrument: Laboratory pH Meter Lab 850, SI Analytics, Germany
[b] The analysis instrument: UV-1800 UV-Vis spectrophotometer, SHIMADZU, Japan
[c] The analysis instrument: OIA_1030W TOC Analyzer, Xylem

doi:10.6342/NTU202503155

4.2 PFAS determination

4.2.1 Solid Phase Extraction (SPE) method verification

To optimize the recovery efficiency of PFAS in water samples, this study examined three variables in the SPE pretreatment process: (1) whether to acidify water samples to pH ≤ 3, (2) whether to rinse cartridges with 0.1% formic acid before elution, and (3) the choice of SPE cartridge material (Oasis HLB vs. Oasis WAX). The results of different pretreatments are shown in Figure 4.1 and Figure 4.2.

A comparative evaluation was conducted to investigate the influence of pretreatment conditions on the recovery efficiency of four selected PFAS compounds (PFBS, PFHxS, PFOS, and PFOA) from Milli-Q water spiked at an initial concentration of 100 ng/L. The variables included sample acidification to pH ≤ 3 and the application of a 0.1% formic acid rinse before elution. Both SPE cartridges, Oasis HLB and Oasis WAX, were examined under identical experimental conditions.

For Oasis HLB cartridges, the results showed that sample acidification had limited or even adverse effects on recovery. Under the most basic condition (no acidification and no rinsing), HLB cartridges achieved the highest recoveries for PFOS (72.3%) and PFOA (80.1%). In contrast, when samples were acidified and rinsed, the recoveries dropped to 51.1% and 78.3%, respectively. A similar trend was observed for the short-chain compounds PFBS and PFHxS: the best recoveries were observed under non-acidified, non-rinsed conditions (68.0% and 61.5%), whereas acidification with rinsing yielded lower recoveries (62.3% and 58.1%).

By contrast, Oasis WAX cartridges exhibited a markedly different behavior. The application of sample acidification significantly improved recovery across all PFAS. The highest recoveries were observed under acidified and non-rinsed conditions: PFOA

doi:10.6342/NTU202503155

reached 97.9%, PFOS 81.8%, PFHxS 78.2%, and PFBS 78.2%. These values were substantially higher than those obtained under non-acidified and non-rinsed conditions, which yielded only 78.4% for PFOA, and dropped to 53.3% and 55.1% for PFOS and PFHxS, respectively. The formic acid rinse step showed only marginal effects on recovery and, in some cases, even slightly reduced performance, suggesting that acidification is the dominant factor influencing PFAS retention in WAX cartridges.

Regarding cartridge performance, WAX cartridges consistently outperformed HLB cartridges for all analytes, particularly for long-chain and ionic PFAS such as PFOS and PFOA. This can be attributed to the mixed-mode retention mechanism of WAX sorbents, which combine reversed-phase and weak anion exchange interactions, thereby enhancing selectivity and retention for negatively charged PFAS molecules. In contrast, HLB cartridges, which operate primarily through hydrophilic-lipophilic balance, appear less suited for strong ionic retention, particularly without matrix optimization.

In conclusion, the optimal SPE condition for PFAS recovery was achieved using Oasis WAX cartridges under acidified conditions without a formic acid rinse, yielding recoveries exceeding 75% for all tested PFAS. For applications using Oasis HLB cartridges, neutral pH and no rinsing offered the best compromise, although overall recoveries remained lower than those from WAX. These results highlight the critical role of sorbent selection and sample pH adjustment in optimizing low-concentration PFAS extraction from aqueous matrices.

doi:10.6342/NTU202503155

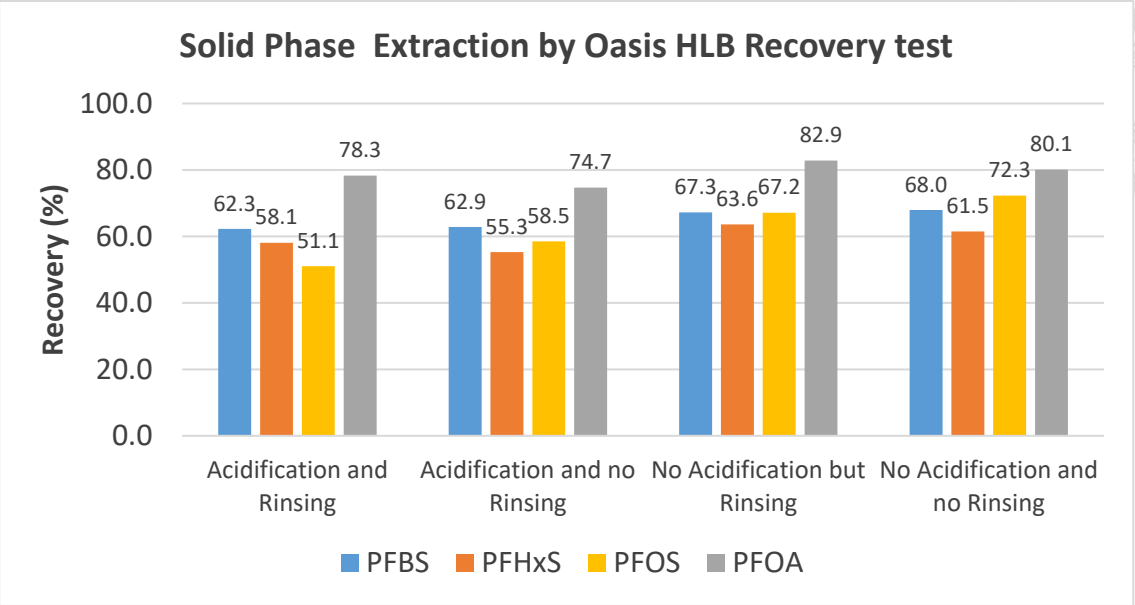

Figure 4.1 Influence of pH adjustment ($pH \leq 3$ versus no pH adjustment) and rinsing with 0.1% formic acid on the recovery obtained using Oasis HLB cartridges in Milli-Q water.

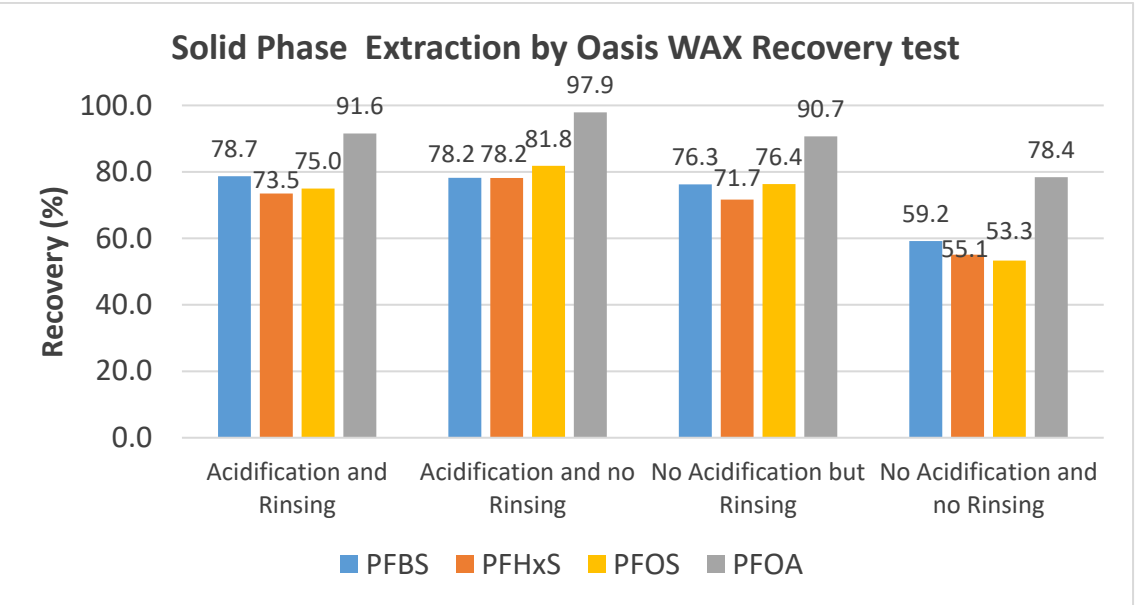

Figure 4.2 Influence of pH adjustment ($pH \leq 3$ versus no pH adjustment) and rinsing with 0.1% formic acid on the recovery obtained using Oasis WAX cartridges in Milli-Q water.

doi:10.6342/NTU202503155

4.2.2 Evaluation of recoveries and analytical accuracy in SPE pretreatment

In this study, the test of cartridges for the PFAS recovery rate is calculated using the external standard method. While internal standards - especially isotopically labeled analogs - are commonly utilized to account for matrix effects and variability in low concentration quantification, the result showed that external calibration was appropriate for the specific conditions of this study.

The primary objective of the recovery tests was to compare various SPE pretreatment conditions rather than to achieve absolute quantification. Additionally, the matrix used throughout the experiment was Milli-Q water, which is relatively free from organic and inorganic interferences. This reduced the potential for matrix-induced ion suppression or enhancement, making external calibration an appropriate approach for assessing relative recovery.

Acknowledge that an internal standard method is crucial for complex environmental matrices or regulatory-level quantification to ensure analytical accuracy and reproducibility.

4.2.3 Method validation

After confirming the best method for SPE pretreatment, the recoveries of real samples were calculated based on the internal standard calibrations, and measurements with different matrices (including Milli-Q water and field rapid filtered water) were tested.

Table 4.2 shows the respective recoveries for each PFAS. In the recovery tests, each water sample was spiked with 100 ng/L of selected PFAS to estimate the percentage recovery; and each analytical processes were conducted in triplicate.

doi:10.6342/NTU202503155

In this study, the instrument detection limit (IDL) and instrument quantitation limit (IQL) were evaluated based on the signal-to-noise ratio (S/N) approach. The IDL is defined as the lowest analyte concentration at which the signal-to-noise ratio is at least 3:1 ($S/N \geq 3$), signifying the minimum concentration detectable by the instrument. Conversely, IQL is defined as the concentration corresponding to an S/N ratio of 10:1 ($S/N = 10$), at which the analyte can be reliably and precisely quantified. Table 4.3 shows the results of quantitative parameters. It is important to note that since the calculated IDL and IQL typically fall below the lowest calibrated concentration point, these results are derived through linear extrapolation.

doi:10.6342/NTU202503155

Table 4.2 Recoveries of selected PFAS in Milli-Q water and field rapid filtered water sample (with the concentration = 100 ng/L).

	Recoveries±RSD, % (n=3)	
	Milli-Q water	Field rapid filtered water
PFBS	112 ± 12	78 ± 17
PFHxS	104 ± 12	84 ± 6
PFOS	100 ± 10	85 ± 6
PFOA	100 ± 8	89 ± 12

Table 4.3 The retention time, IDL, IQL, calibration curve range, and coefficient of determination (R^2) of selected PFAS.

Compounds	**Retention Time (RT) (min)**	**IQL (ng/L)**	**IDL (ng/L)**	**Linear range (ng/L)**	**R^2**
PFBS	2.36	0.109	0.047	1-250	0.999
PFHxS	2.68	0.32	0.26	1-250	0.994
PFOS	2.91	0.71	0.66	1-250	0.990
PFOA	2.80	1.01	0.95	1-250	0.985

doi:10.6342/NTU202503155

4.3 Adsorption kinetics

The adsorption kinetics of PFBS, PFHxS, PFOS, and PFOA on two types of PAC were investigated using a batch adsorption system. The experimental setup, depicted in Figure 3.2, utilized a 5 L glass serum bottle containing 4 L of Milli-Q water with a stirring bar for continuous mixing, placed on a magnetic stirrer. Activated carbon was dosed at 15 mg/L, resulting in a total adsorbent mass ($m_{adsorbent}$) of 0.06 g. The initial concentrations (C_0) of each specific PFAS added to the water matrices were measured at the start time. Sampling was collected at various time points up to 24 hours.

The amount of PFAS adsorbed per unit mass of activated carbon at time t (q_t) was calculated using the following mass balance equation for batch systems:

$$q_t = \frac{(C_0 - C_t) \times V}{m_{adsorbent}} \quad (4\text{-}1)$$

Where:

C_t (mg/L) is the concentration of PFAS in the solution at time t, V (4 L) is the initial volume of the solution, and $m_{adsorbent}$ (0.06 g) is the mass of the activated carbon. The measured concentrations (C_t) and the calculated q_t values are transferred from the normalized concentration (C/C_0) curves, which visually represent the percentage removal over time.

4.3.1 The results of adsorption kinetics in Milli-Q water with coconut shell PAC

Initially, the curves represent the ratio of the concentrations at sampling time to the initial concentration (Ct/C_0), which illustrates the percentage residual over time. As shown in Figure 4.3, a distinct difference in adsorption kinetics was observed between PFBS and other PFAS compounds. Specifically, PFOA and PFOS demonstrated

doi:10.6342/NTU202503155

extremely rapid adsorption rates. Their C_t/C_0 values, which indicate the remaining concentration in solution, dropped sharply to below 5% within the first hour of contact time (at 0.5 hours, PFOA was measured at 22 ng/L and PFOS at 10.5 ng/L). The concentrations continued to decline for both PFOA and PFOS, reaching 1.5 ng/L by 6 hours and achieving complete removal (0 ng/L) by 24 hours. These results highlight the high affinity and fast adsorption rate of TAC-C for PFOA and PFOS. In contrast, the change in C_t/C_0 value for PFHxS followed a trajectory similar to that of PFOA.

According to Figure 4.3, the rate of concentration decline for PFHxS, PFOS, and PFOA significantly slowed down after 2 hours. At later time points, such as 4, 6, and 8 hours, the concentrations were already very low or had even dropped to zero, indicating that equilibrium was either reached or very close to reaching after 2 hours of adsorption. The concentration of PFBS continued to decrease significantly after 2 hours and did not reach a lower steady state of 8.5 ng/L until 24 hours. However, the equilibrium time of PFBS discussed in this study is 2 hours, as faster adsorption rates are typically described.

Table 4.4 The initial concentration, equilibrium concentration, and equilibrium time of selected PFAS. (The adsorbent is TAC-C.)

Compounds	**C_0 (mg/L)**	**C_e (mg/L)**	**t_e (hr)**
PFBS	6.65×10^{-5}	3.85×10^{-5}	2
PFHxS	6.45×10^{-5}	6.00×10^{-6}	2
PFOS	7.10×10^{-5}	7.00×10^{-6}	2
PFOA	5.95×10^{-5}	3.50×10^{-6}	2

doi:10.6342/NTU202503155

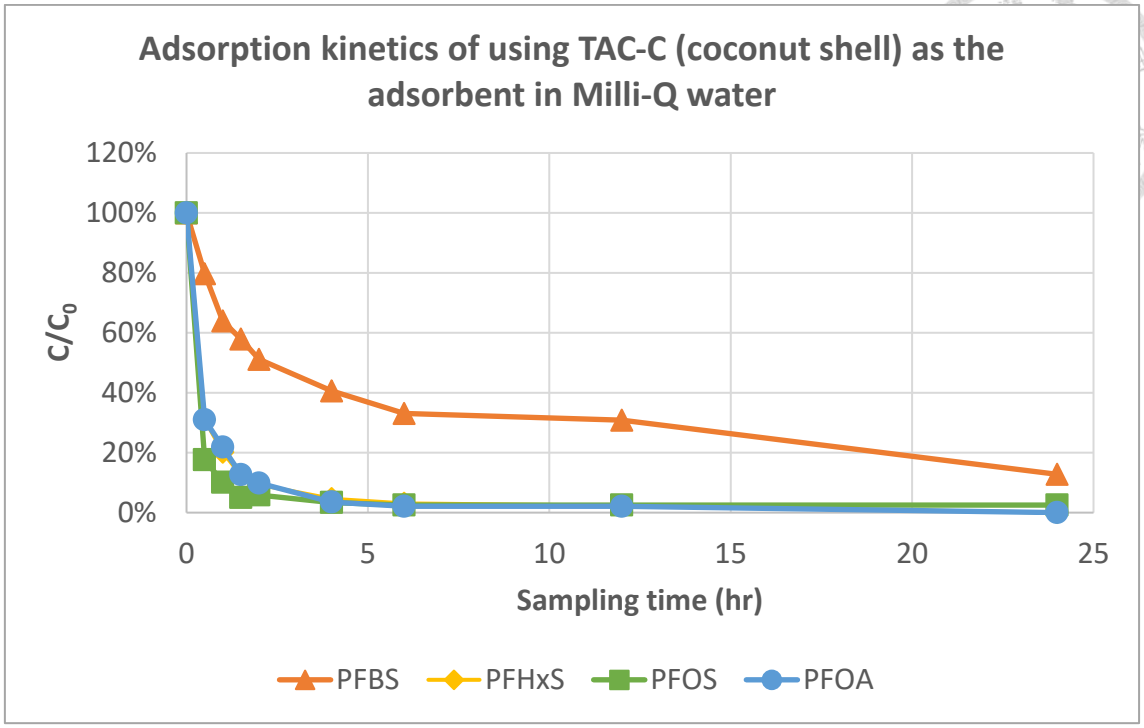

Figure 4.3 Adsorption kinetics of using TAC-C (coconut shell) as the adsorbent in Milli-Q water for 24 hours.

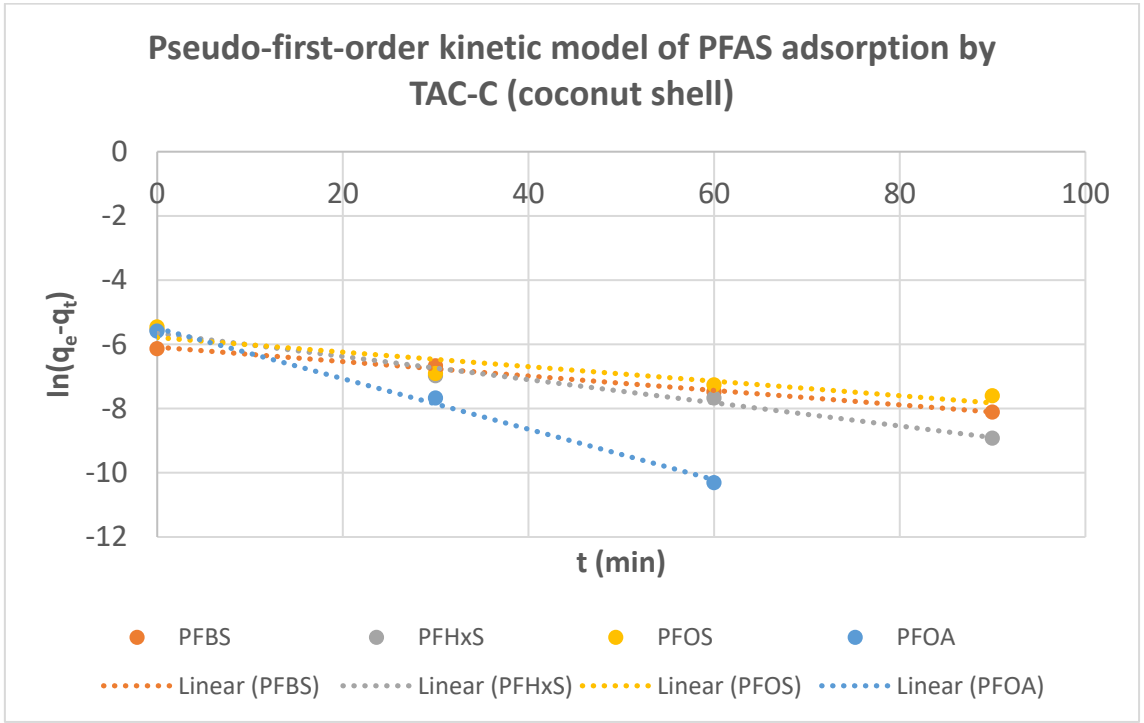

Figure 4.4 The pseudo-first-order kinetic model of PFAS adsorption in Milli-Q water by TAC-C (coconut shell).

doi:10.6342/NTU202503155

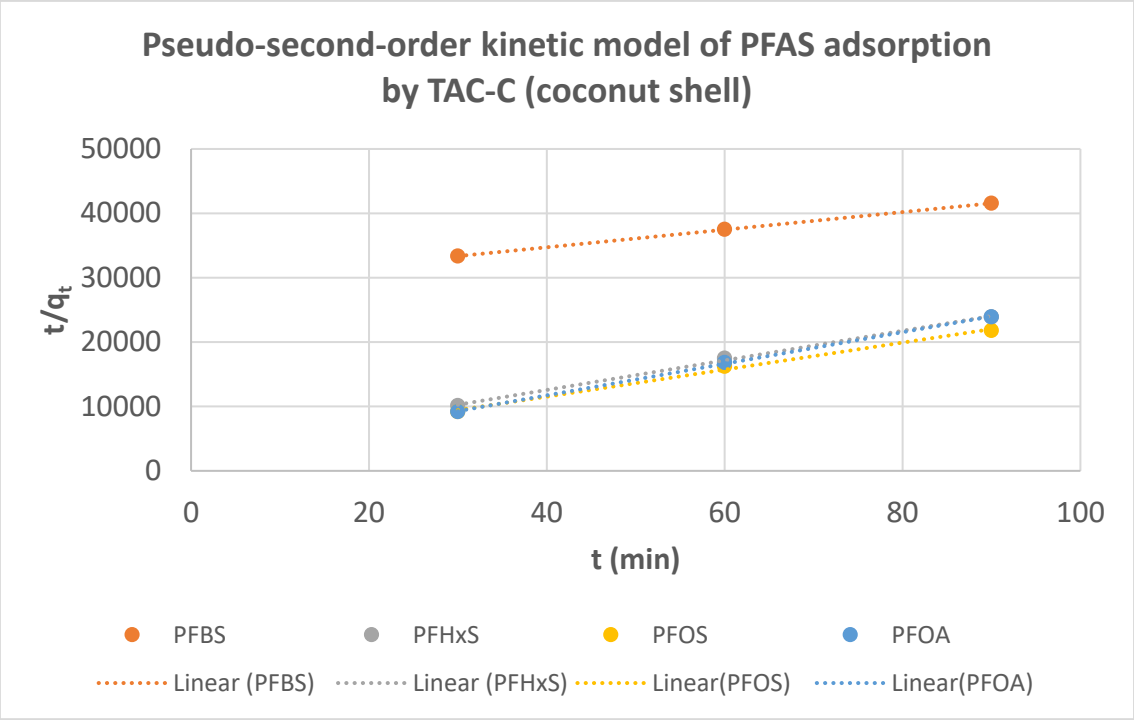

Figure 4.5 The pseudo-second-order kinetic model of PFAS adsorption in Milli-Q water by TAC-C (coconut shell).

The parameters of the equations (2-2) and (2-4) are calculated and presented in Table 4.5. Following this, Figure 4.4 and Figure 4.5 are plotted. The pseudo-first-order kinetics plot is a plot of time (t) versus $\ln(q_e - q_t)$. From the slope k_1 and intercept $\ln q_e$ of the linear equation in the graph, k_1 and q_e are calculated, and the relative error between the actual equilibrium adsorption amount and the theoretical adsorption amount are also calculated.

The pseudo-second-order adsorption kinetics plot represents a plot of time (t) versus the natural logarithm of the difference between the equilibrium adsorption amount (q_e) and the adsorption amount at time t (q_t). The values of k_2 and q_e can be calculated from the intercept $(\frac{1}{k_2 {q_e}^2})$ and slop $\left(\frac{1}{q_e}\right)$ of the linear equation displayed in the graph, and the relative error between the actual and theoretical adsorption amounts can be calculated.

doi:10.6342/NTU202503155

The model with the smallest relative error is chosen for fitting by analyzing the relative errors. Therefore, for all the four PFAS tested in this study, utilizing TAC-C as the adsorbent aligns with the pseudo-second-order adsorption kinetics.

doi:10.6342/NTU202503155

Table 4.5 The parameters of the pseudo-first-order model and the pseudo-second-order model. (The adsorbent is TAC-C.)

Pseudo-first-order model					
Compounds	**k_1 (1/min)**	**q_{e_model} (mg/g)**	**q_{e_exp} (mg/g)**	**relative error (%)**	**R^2**
PFBS	0.023	0.0026	0.0022	4.55	0.8994
PFHxS	0.036	0.0035	0.0039	11.53	0.9845
PFOS	0.023	0.0031	0.0042	39.41	0.8623
PFOA	0.079	0.0033	0.0037	8.90	0.9953
Pseudo-second-order model					
Compounds	**k_2 (g/(mg·min))**	**q_{e_model} (mg/g)**	**q_{e_exp} (mg/g)**	**relative error (%)**	**R^2**
PFBS	0.639	0.0073	0.0022	70.37	0.9999
PFHxS	15.612	0.0044	0.0039	10.42	0.9984
PFOS	14.049	0.0048	0.0042	10.46	0.9954
PFOA	31.254	0.0041	0.0037	8.47	0.9999

doi:10.6342/NTU202503155

4.3.2 The results of adsorption kinetics in Milli-Q water with bituminous coal PAC

Figure 4.6 illustrates the adsorption kinetics of PFBS, PFHxS, PFOS, and PFOA using F400 (bituminous coal) as the adsorbent with Milli-Q water. The vertical axis represents the concentration ratio (C_t/C_0), indicating the residual concentration of each PFAS compound over time, while the horizontal axis shows the sampling time in hours. The concentration of all the four PFAS compounds showed a rapid decrease in the values of C_t/C_0 within the first 1 to 3 hours of contact time, indicating efficient initial adsorption by F400. Among them, PFOA, PFOS, and PFHxS exhibited nearly identical adsorption profiles, with their concentrations dropping sharply to below 20% of the initial concentration within 1 hour of reaction and approaching 0% by around 4 to 6 hours. Therefore, the equilibrium time of the four PFAS is approximately 4 hours. In contrast, PFBS demonstrated relatively slower adsorption. Although the values of C_t/C_0 also declined rapidly, the values were consistently higher than those of the other compounds during the early phase of adsorption (0 to 2 hours). This indicates that PFBS had a slower adsorption rate and potentially lower affinity for F400 than the longer-chain PFAS. These results highlight the superior adsorption performance of F400 for longer-chain PFAS, particularly PFOA, PFOS, and PFHxS, under the tested conditions.

The parameters of the equations (2-2) and (2-4) are calculated and presented in Table 4.7. Following this, Figure 4.7 and Figure 4.8 are plotted. The model with the smallest relative error is chosen for fitting by analyzing the relative errors. Therefore, for all four PFAS, utilizing F400 as the adsorbent aligns with the pseudo-first-order adsorption kinetics.

doi:10.6342/NTU202503155

Table 4.6 The initial concentration, equilibrium concentration, and equilibrium time of selected PFAS. (The adsorbent is F400.)

PFAS	**C_0 (mg/L)**	**C_e (mg/L)**	**t_e (hr)**
PFBS	6.7×10^{-5}	4.0×10^{-6}	4
PFHxS	6.7×10^{-5}	1.0×10^{-6}	4
PFOS	5.7×10^{-5}	5.0×10^{-7}	4
PFOA	7.2×10^{-5}	1.5×10^{-6}	4

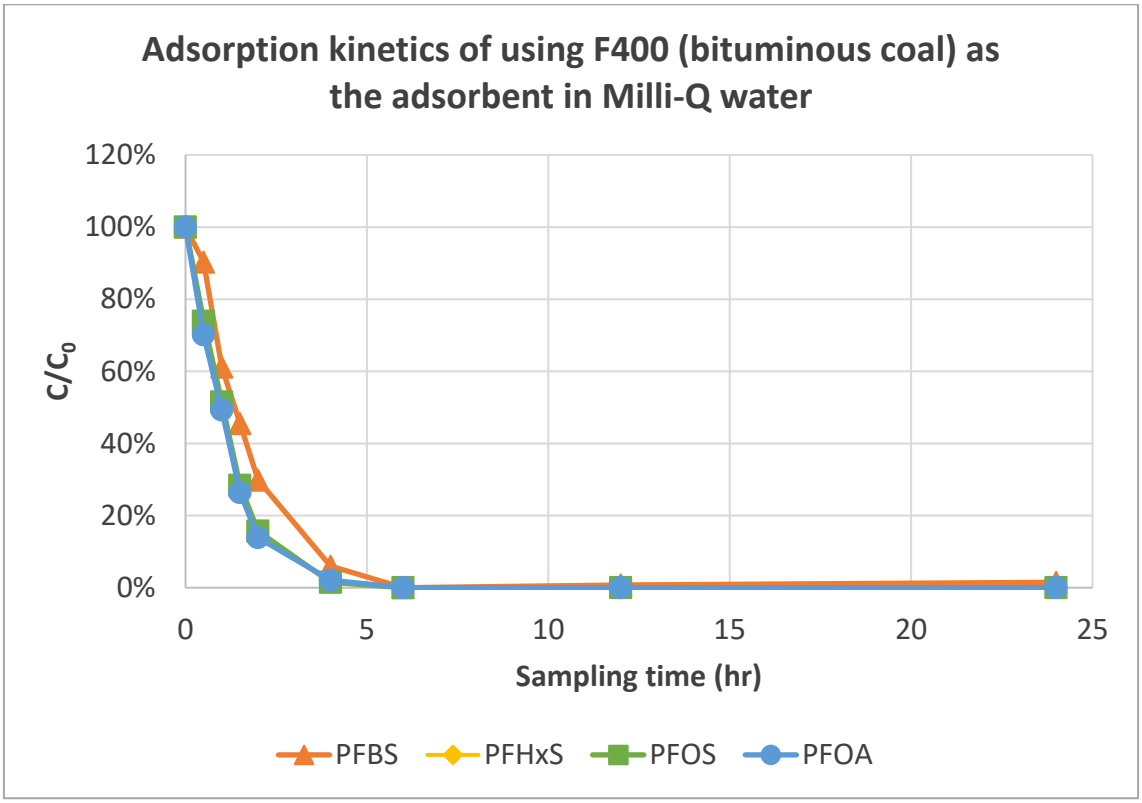

Figure 4.6 Adsorption kinetics of using F400 (bituminous coal) as the adsorbent in Milli-Q water for 24 hours.

doi:10.6342/NTU202503155

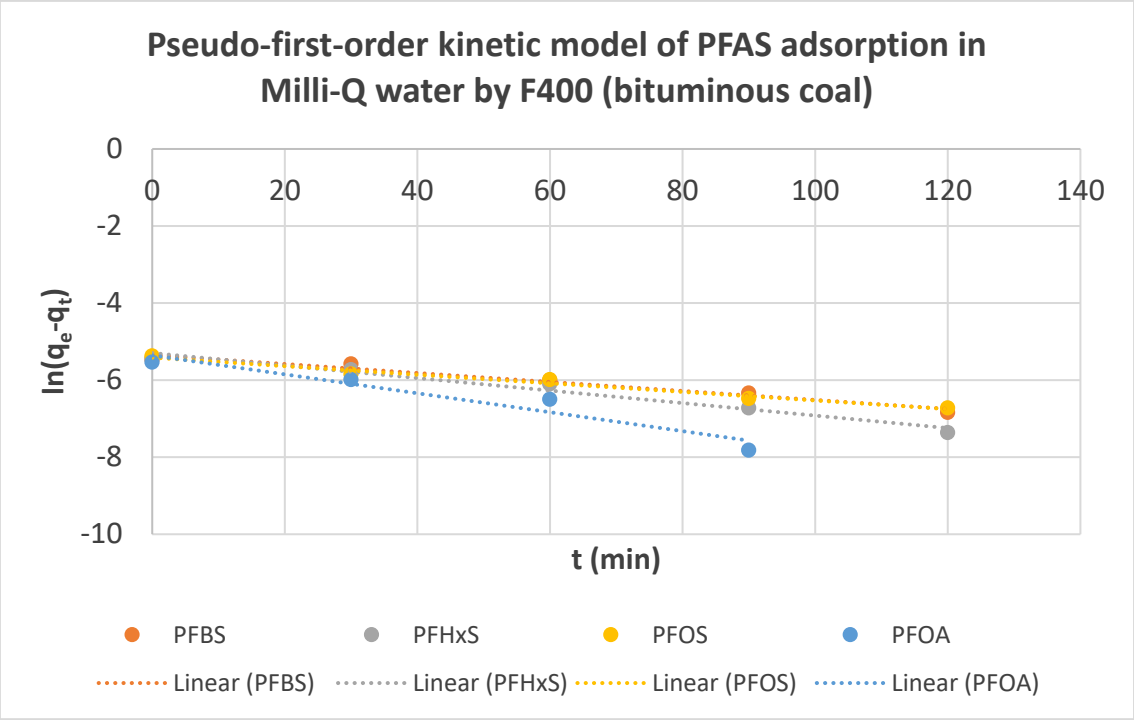

Figure 4.7 The pseudo-first-order kinetic model of PFAS adsorption in Milli-Q water by F400 (bituminous coal).

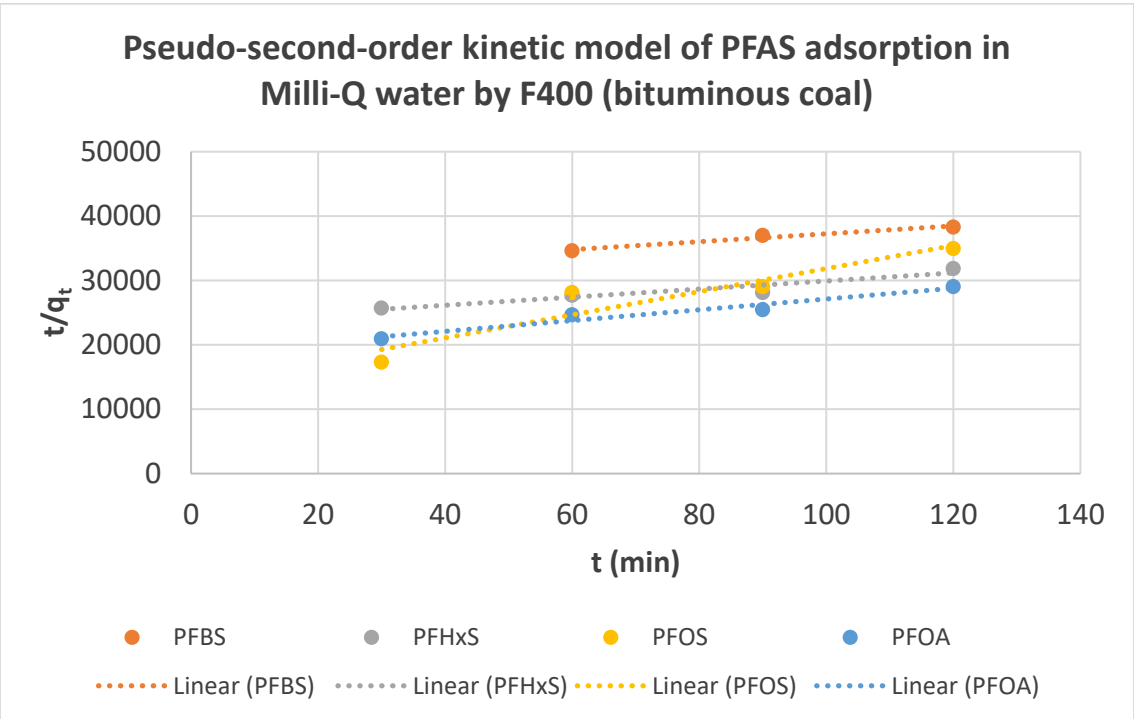

Figure 4.8 The pseudo-second-order kinetic model of PFAS adsorption in Milli-Q water by F400 (bituminous coal).

doi:10.6342/NTU202503155

Table 4.7 The parameters of the pseudo-first-order model and the pseudo-second-order model. (The adsorbent is F400.)

Pseudo-first-order model					
Compounds	**k_1 (1/min)**	**q_{e_model} (mg/g)**	**q_{e_exp} (mg/g)**	**relative error (%)**	**R^2**
PFBS	0.012	0.0048	0.0042	11.67	0.9656
PFHxS	0.016	0.0050	0.0044	12.09	0.9744
PFOS	0.011	0.0044	0.0046	4.15	0.9793
PFOA	0.025	0.0047	0.0039	16.43	0.9260
Pseudo-second-order model					
Compounds	**k_2 (g/(mg·min))**	**q_{e_model} (mg/g)**	**q_{e_exp} (mg/g)**	**relative error (%)**	**R^2**
PFBS	0.121	0.0163	0.0042	74.22	0.9732
PFHxS	0.167	0.0159	0.0044	72.33	0.9015
PFOS	2.318	0.0056	0.0046	16.85	0.8943
PFOA	0.374	0.0119	0.0039	67.06	0.9515

doi:10.6342/NTU202503155

4.4 Adsorption isotherms

The experimental data were fitted to the Langmuir and the Freundlich isotherm models to evaluate the adsorption equilibrium of selected PFAS onto TAC-C (coconut shell) and F400 (bituminous coal) GAC.

Following equation (2-6), Langmuir isotherm models can be graphed as a plot of $\frac{C_e}{q_e}$ versus C_e and yield a straight line with slope $\frac{1}{q_{max}}$ and intercept $\frac{1}{q_{max}K_L}$. Additionally, following equation (2-8), Freundlich isotherm models can be graphed as a plot of $\log q_e$ versus $\log C_e$ and yield a straight line with slope $\frac{1}{n}$ and intercept $\log K_F$.

As shown in Figure 3.3. The adsorption isotherm experiments utilized six beakers, each containing 1 L of Milli-Q water, placed on a flocculator. Activated carbon was dosed at 0, 10, 20, 30, 40, and 50 mg/L for each beaker. For the other water matrix – rapid filtered water, activated carbon was dosed at 0, 5, 10, 15, 20, 25, 30 mg/L. The initial concentrations (C_0) of each specific PFAS added to the water matrices were measured at the start time. The PFAS concentrations were analyzed for water samples collected at 0 hour (prior to adding AC) and 72 hours after AC addition.

4.4.1 The results of adsorption isotherms in Milli-Q water with coconut shell PAC

The results of isotherm experiments with TAC-C are shown in Figure 4.9 and Figure 4.10. The isotherm parameters of equations (2-6) and (2-8), as well as correlation coefficients (R^2) for the four PFAS, are calculated and presented in Table 4.8.

According to the Langmuir isotherm model, which assumes monolayer adsorption on a homogeneous surface, PFOS exhibited q_{max} = 5.27 ng/mg at the highest equilibrium aqueous concentration, followed by PFBS (3.98 ng/mg), PFHxS (3.37 ng/mg), and PFOA

doi:10.6342/NTU202503155

(2.78 ng/mg). This suggests that PFOS has a stronger interaction with the TAC-C surface, potentially due to its longer carbon chain and higher hydrophobicity. However, the adsorption affinity constant (K_L) was highest for PFOA (0.499 L/ng) and PFHxS (0.470 L/ng), indicating their relatively high adsorption efficiencies at low concentrations. The Langmuir R^2 values ranged from 0.6526 to 0.6671, suggesting a moderate fit to the experimental data.

In contrast, the Freundlich isotherm model, which describes heterogeneous multilayer adsorption, demonstrated a better fit for PFOS, with a correlation coefficient (R^2) of 0.9058, significantly higher than those for the other PFAS (R^2 = 0.6412–0.6698). The Freundlich constant (K_F), indicative of adsorption capacity, followed the order PFBS (1.159) > PFHxS (1.060) > PFOS (0.835) > PFOA (0.625). Additionally, all 1/n values were below 1, confirming favorable adsorption for all compounds. Notably, PFOS had the highest 1/n value (0.586), suggesting stronger adsorption intensity than the other PFAS.

These results imply that the adsorption of PFOS onto TAC-C is best described by the Freundlich isotherm model, likely due to the heterogeneity of the TAC-C surface. For PFOA and PFHxS, the higher K_L values in the Langmuir model suggest a higher affinity under dilute conditions. In contrast, PFBS and PFHxS showed relatively strong adsorption capacities under both models. Overall, both models provide useful insights, but the Freundlich isotherm model offers a better representation of PFAS adsorption behavior onto TAC-C.

doi:10.6342/NTU202503155

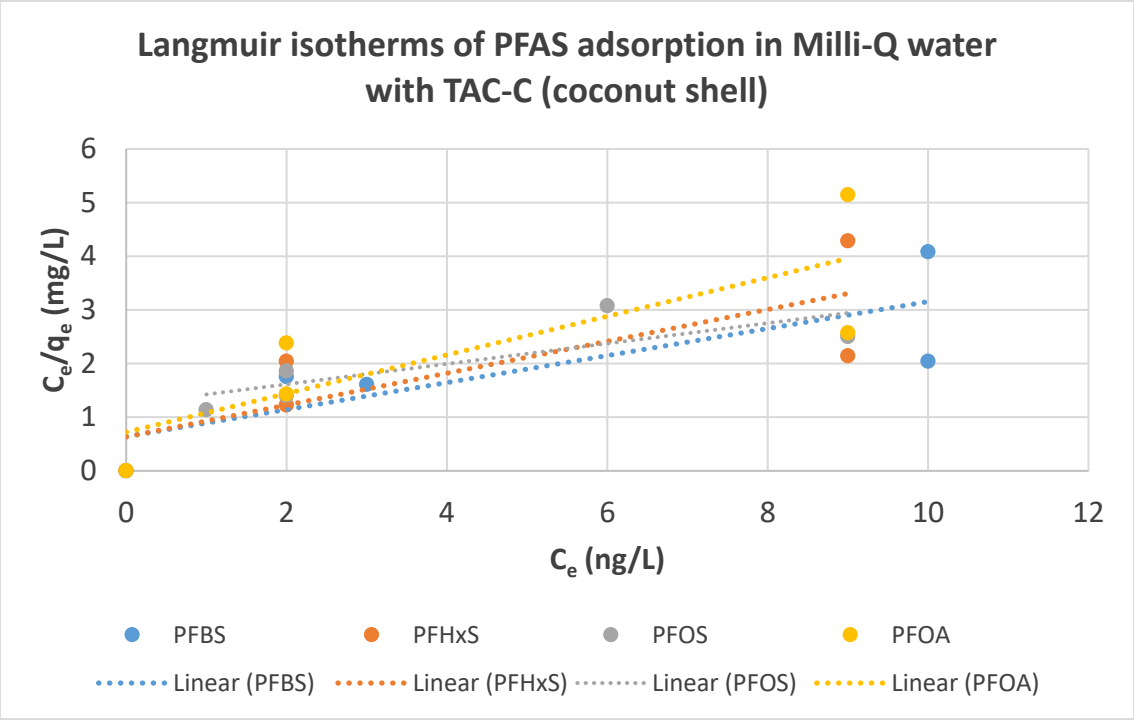

Figure 4.9 Langmuir isotherms of PFAS adsorption in Milli-Q water with TAC-C (coconut shell).

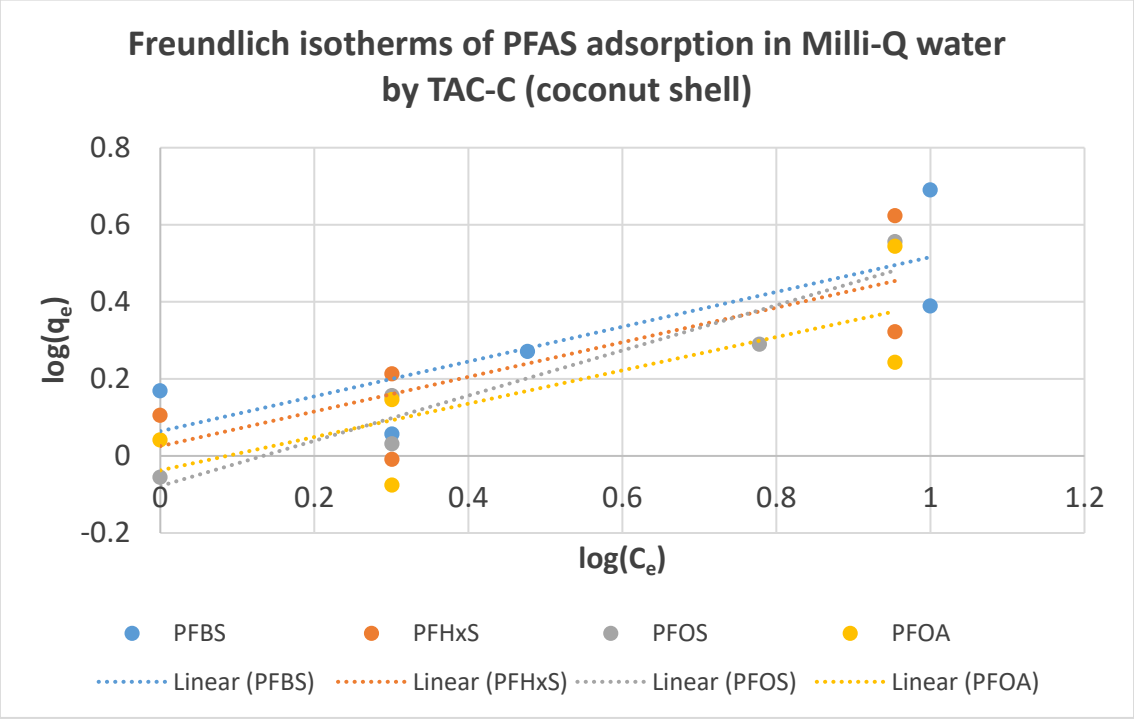

Figure 4.10 Freundlich isotherms of PFAS adsorption in Milli-Q water with TAC-C (coconut shell).

doi:10.6342/NTU202503155

Table 4.8 The parameters of the Langmuir isotherm model and the Freundlich isotherm model. (The adsorbent is TAC-C.)

Langmuir isotherm model			
	q_{max} (ng/mg)	**K_L (L/ng)**	**R^2**
PFBS	3.976	0.063	0.6650
PFHxS	3.368	0.470	0.6566
PFOS	5.266	0.154	0.6526
PFOA	2.779	0.499	0.6671
Freundlich isotherm model			
	1/n	**K_F [(ng/mg)(L/ng)$^{1/n}$]**	**R^2**
PFBS	0.4519	1.159	0.6698
PFHxS	0.4495	1.060	0.6412
PFOS	0.5864	0.835	0.9058
PFOA	0.4326	0.625	0.6247

doi:10.6342/NTU202503155

4.4.2 The results of Adsorption isotherms in Milli-Q water with bituminous coal PAC

The results of isotherm experiments with F400 are shown in Figure 4.11 and Figure 4.12. The parameters of equations (2-6) and (2-8) for the four PFAS are calculated and presented in Table 4.9.

According to the Langmuir isotherm model, PFBS exhibited qmax = 3.96 ng/mg at the highest equilibrium aqueous concentration, followed by PFHxS (3.44 ng/mg), PFOS (3.05 ng/mg), and PFOA (2.84 ng/mg). This trend suggests that PFBS interacts most strongly with the F400 surface regarding capacity, although the differences among the PFAS are relatively small. The adsorption affinity constant (K_L) was highest for PFOS (0.715 L/ng), followed by PFOA (0.373 L/ng), PFHxS (0.359 L/ng), and PFBS (0.261 L/ng), indicating that PFOS has both a strong adsorption affinity and a reasonably high capacity. The correlation coefficient (R^2) of Langmuir isotherm model ranged from 0.5231 to 0.7085, suggesting a moderate fit to the experimental data, with PFOS demonstrating the best agreement.

In contrast, the Freundlich isotherm model provided a better fit for different PFAS, particularly PFOS, with an R^2 value of 0.7886. The adsorption capacity, as represented by the Freundlich constant (K_F), followed the order PFOS (1.020) > PFHxS (0.905) > PFBS (0.881) > PFOA (0.758). All 1/n values were below 1, ranging from 0.5118 to 0.5304, indicating favorable adsorption conditions for all four PFAS compounds with F400. Notably, the smallest 1/n value was observed for PFOS (0.5118), suggesting higher adsorption intensity than the others.

doi:10.6342/NTU202503155

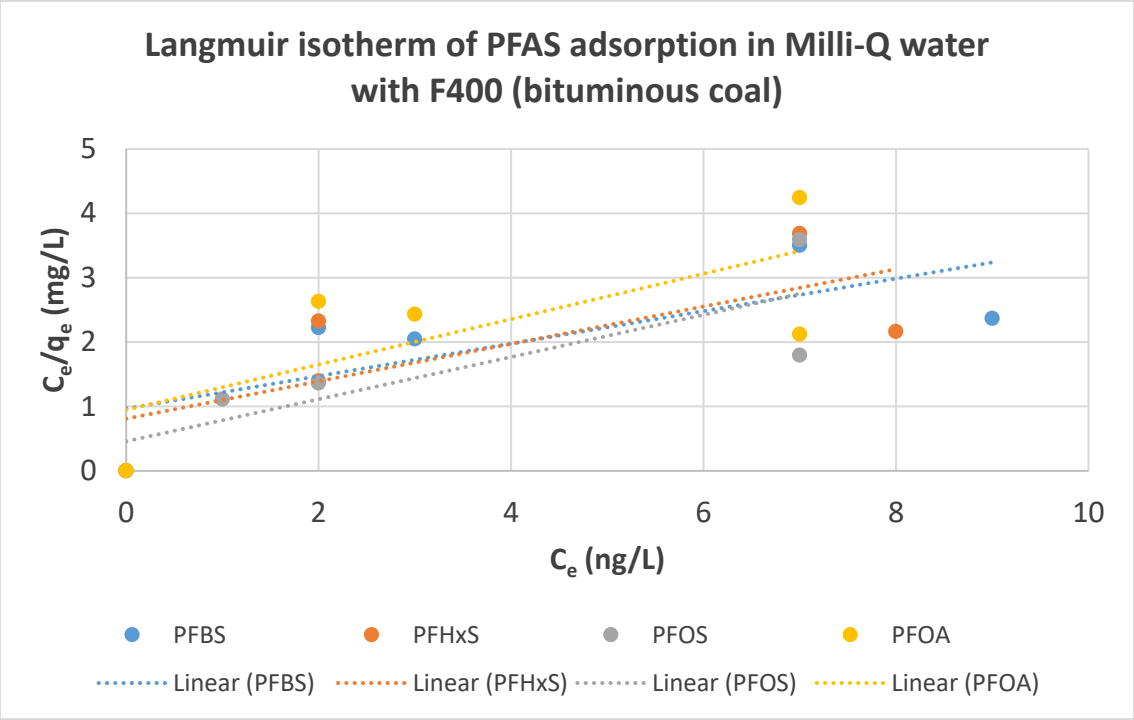

Figure 4.11 Langmuir isotherms of PFAS adsorption in Milli-Q water with F400 (bituminous coal).

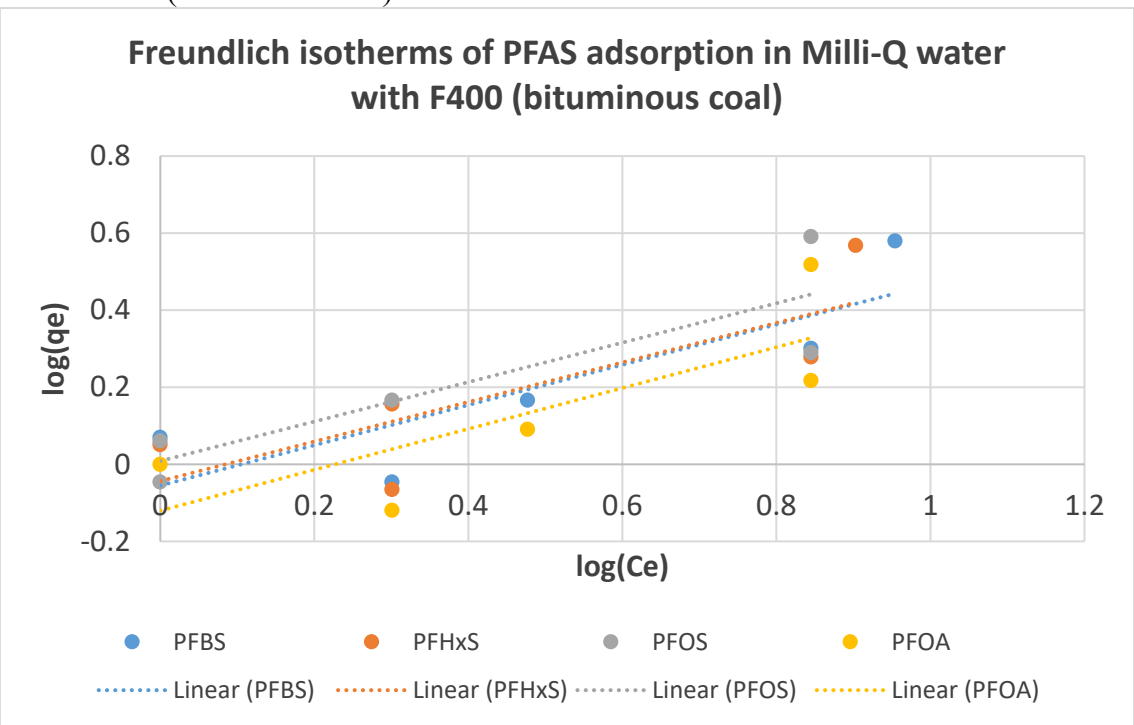

Figure 4.12 Freundlich isotherms of PFAS adsorption in Milli-Q water with F400 (bituminous coal).

doi:10.6342/NTU202503155

Table 4.9 The parameters of the Langmuir isotherm model and the Freundlich isotherm model. (The adsorbent is F400.)

Langmuir isotherm model			
	q_{max} (ng/mg)	**K_L (L/ng)**	**R^2**
PFBS	3.963	0.261	0.5421
PFHxS	3.444	0.359	0.5641
PFOS	3.053	0.715	0.7085
PFOA	2.836	0.373	0.5231
Freundlich isotherm model			
	1/n	**K_F [(ng/mg)(L/ng)$^{1/n}$]**	**R^2**
PFBS	0.5224	0.881	0.7231
PFHxS	0.5133	0.905	0.6760
PFOS	0.5118	1.020	0.7886
PFOA	0.5304	0.758	0.6231

doi:10.6342/NTU202503155

These results imply that the adsorption of PFOS onto F400 is better described by the Freundlich isotherm model, likely due to the heterogeneous nature of the activated carbon surface. While PFOA exhibited relatively lower adsorption capacity, its moderate K_L value suggests it can still be effectively adsorbed under dilute conditions. PFHxS and PFBS demonstrated balanced adsorption behavior across both models. Overall, both isotherm models offer valuable insights, but the Freundlich model provides a more accurate description of PFAS adsorption onto F400, particularly for PFOS.

4.4.3 A comprehensive discussion of the adsorption isotherms in Milli-Q water

According to the results of the adsorption isotherm experiments conducted in Milli-Q water, using high doses of activated carbon can create a similar equilibrium situation. The concentration levels of the samples taken at various doses after 72 hours are notably low, and in some cases, even non-detectable. Consequently, the adsorption isotherm models derived from the existing experimental data may have limitations. Nevertheless, a straightforward discussion can still be made based on the parameters obtained from the experimental results. Therefore, the doses of activated carbon in the later experiments were adjusted to compare the different water matrices.

doi:10.6342/NTU202503155

4.5 Rapid Small Scale Column Tests

The first phase of the Rapid Small Scale Column Test (RSSCT) evaluated the capability of granular activated carbon (GAC) to adsorb target PFAS in Milli-Q water, which was used as the matrix for testing. After that, RSSCT was conducted using field rapid filtered water as the matrix. An initial PFAS concentration of 100 ng/L was spiked into the water samples before RSSCT began.

For the RSSCT, the bed volume of GAC was 0.62832 cm^3, the water flow rate was 1 mL/min, and the empty bed contact time (EBCT) was 1.6 min. The conducting time of RSSCT for this phase was approximately two weeks, equivalent to the RSSCT operation of 30,000 filter bed volumes under these experimental conditions. TAC-C (coconut shell), F400 (bituminous coal), and TAC-Q (coal-based) were used as adsorbents, and all experiments were performed in duplicate.

In the following sections, C/C_0 would be used as the breakthrough indicators of RSSCT, where C is the concentration of PFAS in the effluent water samples collected every day. C_0 is the average result of the influent water directly collected every 5 days (day 1, 5, 10, and 14), from the 20 L pre-cleaned plastic water storage buckets. The following figures show the breakthrough curves of RSSCT with PFBS, PFHxS, PFOS, and PFOA.

4.5.1 Removal of PFAS in Milli-Q water with coconut shell GAC

The breakthrough curves with TAC-C (coconut shell GAC) for PFAS in Milli-Q water are presented in Figure 4.13. Initial breakthrough, indicated by a C/C_0 ratio beginning to rise above baseline, generally occurs around 2,000 to 4,000 bed volumes for most tested PFAS compounds. Specifically, PFBS and PFHxS show initial breakthroughs

doi:10.6342/NTU202503155

of around 2,000 to 3,000 bed volumes, while PFOS and PFOA appear to begin breakthroughs slightly later, closer to 3,000 to 4,000 bed volumes.

At approximately 15,000 bed volumes, the C/C_0 values vary among the compounds: PFBS shows a breakthrough of about 40 to 45% of the initial concentration, PFHxS is around 30 to 35%, PFOA is approximately 30%, and PFOS exhibits the lowest breakthrough, at roughly 20% of the initial concentration. As the operation continues to 25,000 bed volumes, the breakthrough generally increases further: PFBS reaches about 45 to 50%, PFHxS is around 35 to 40%, PFOA is about 30 to 35%, and PFOS remains the lowest, at approximately 25 to 30% C/C_0. Beyond 25,000 bed volumes, particularly nearing 28,000 bed volumes, a notable increase in breakthrough is observed for PFBS and PFOA, with their C/C_0 ratios exceeding 50% and approaching 60% respectively, indicating more rapid saturation of the GAC for these compounds.

The varying breakthrough behaviors observed for different PFAS compounds underscore the dynamic equilibrium in activated carbon adsorption. Compounds like PFOS consistently exhibit lower breakthroughs, suggesting a stronger adsorption affinity to the coconut shell GAC than PFBS, PFHxS, and PFOA. The more pronounced and earlier breakthrough of compounds like PFBS and PFOA, especially the sharp increase for PFBS after approximately 8,000 bed volumes and the significant rise for PFOA after 10,000 bed volumes, indicates a faster saturation of the adsorbent capacity for these specific substances. This phenomenon can be attributed to differences in the physicochemical properties of the PFAS molecules (e.g., chain length, functional group, and branching) affecting their interactions with the activated carbon surface and their susceptibility to competitive adsorption or displacement as the GAC filter bed becomes increasingly saturated over time.

doi:10.6342/NTU202503155

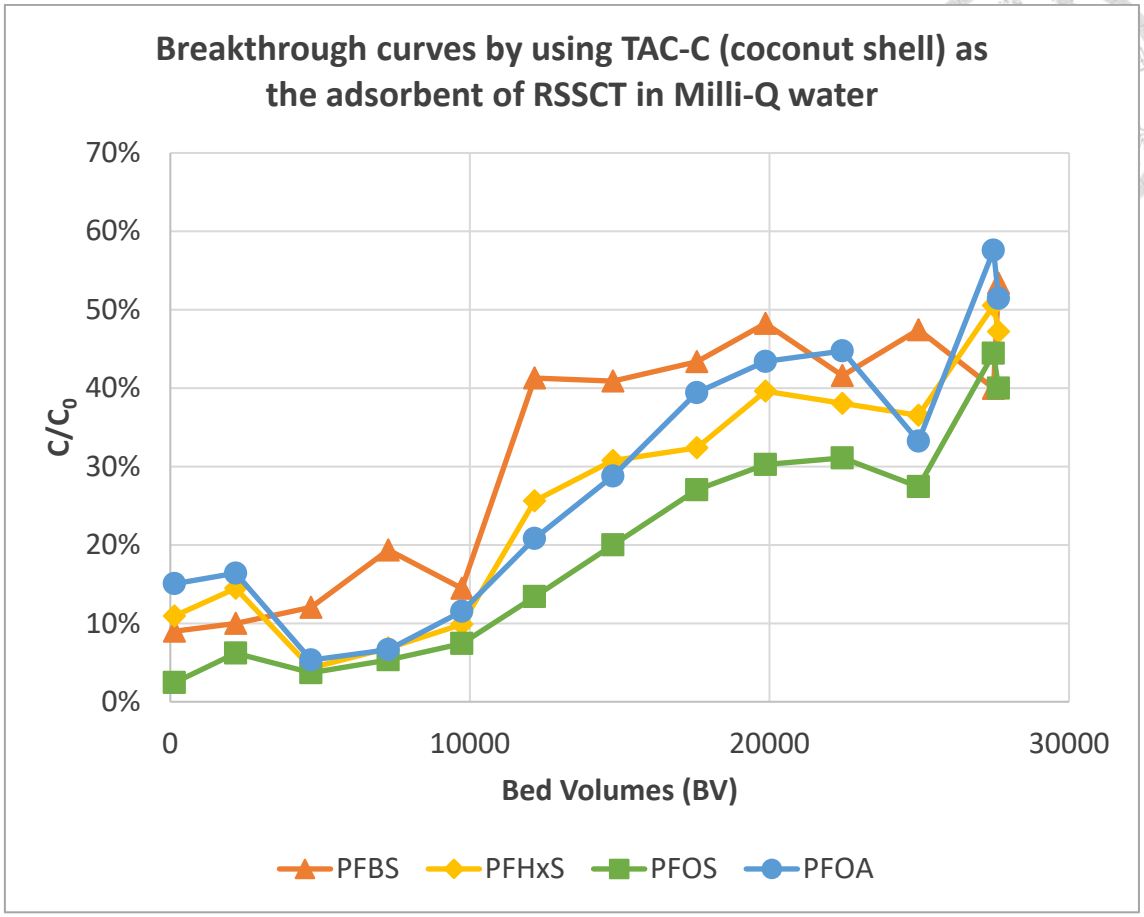

Figure 4.13 Breakthrough curves by using TAC-C (coconut shell) as the adsorbent from 2 weeks of RSSCT simulating the removal of PFBS, PFHxS , PFOS , and PFOA in Milli-Q water.

The result shows that using TAC-C as an adsorbent for various PFAS compounds demonstrates the selective affinity of the material, which is influenced by both the inherent properties of the coconut shell GAC and the unique characteristics of each PFAS molecule.

Coconut shell GAC is primarily characterized by its high microporosity, which has a large volume of tiny pores. This pore structure, combined with a relatively hydrophobic carbonaceous surface, makes it effective for adsorbing organic contaminants from water.

doi:10.6342/NTU202503155

4.5.2 Removal of PFAS in Milli-Q water with bituminous coal GAC

The breakthrough curves with F400 (bituminous coal GAC) for PFAS in Milli-Q water are presented in Figure 4.14. Compared to the coconut shell GAC tested previously, this coal-based GAC demonstrates significantly superior adsorption performance for PFAS, with breakthrough concentrations (C/C_0) maintained at remarkably lower levels throughout the experimental duration.

In the initial phase of the experiment, spanning up to approximately 10,000 bed volumes, the breakthrough concentration for all PFAS compounds remained exceptionally low, mostly below 2%. This indicates that the bituminous coal GAC exhibits very high adsorption capacity during the early stages of the column tests, effectively removing PFAS from the water.

At approximately 15,000 bed volumes, the C/C_0 values for all compounds were still maintained below 5%, mostly around 2-3%, signifying substantial remaining adsorption capacity. As the operation progressed, breakthrough concentrations gradually increased at around 25,000 bed volumes. The breakthrough for PFBS was approximately 7.5%. Both PFHxS and PFOS showed a breakthrough of about 7%. PFOA (blue circle) exhibited a slightly higher breakthrough, around 10%.

Towards the end of the experiment (approximately 29,000 bed volumes), the breakthrough concentrations for the different compounds diverged: PFOA showed the highest breakthrough, reaching approximately 15%, PFOS followed with a breakthrough of about 12%, and the breakthrough of PFHxS was around 8%. PFBS displayed an interesting phenomenon, with its breakthrough slightly decreasing towards the end of the experiment, settling at approximately 6%. This could suggest the influence of other adsorption mechanisms or dynamic equilibrium shifts in this specific stage.

doi:10.6342/NTU202503155

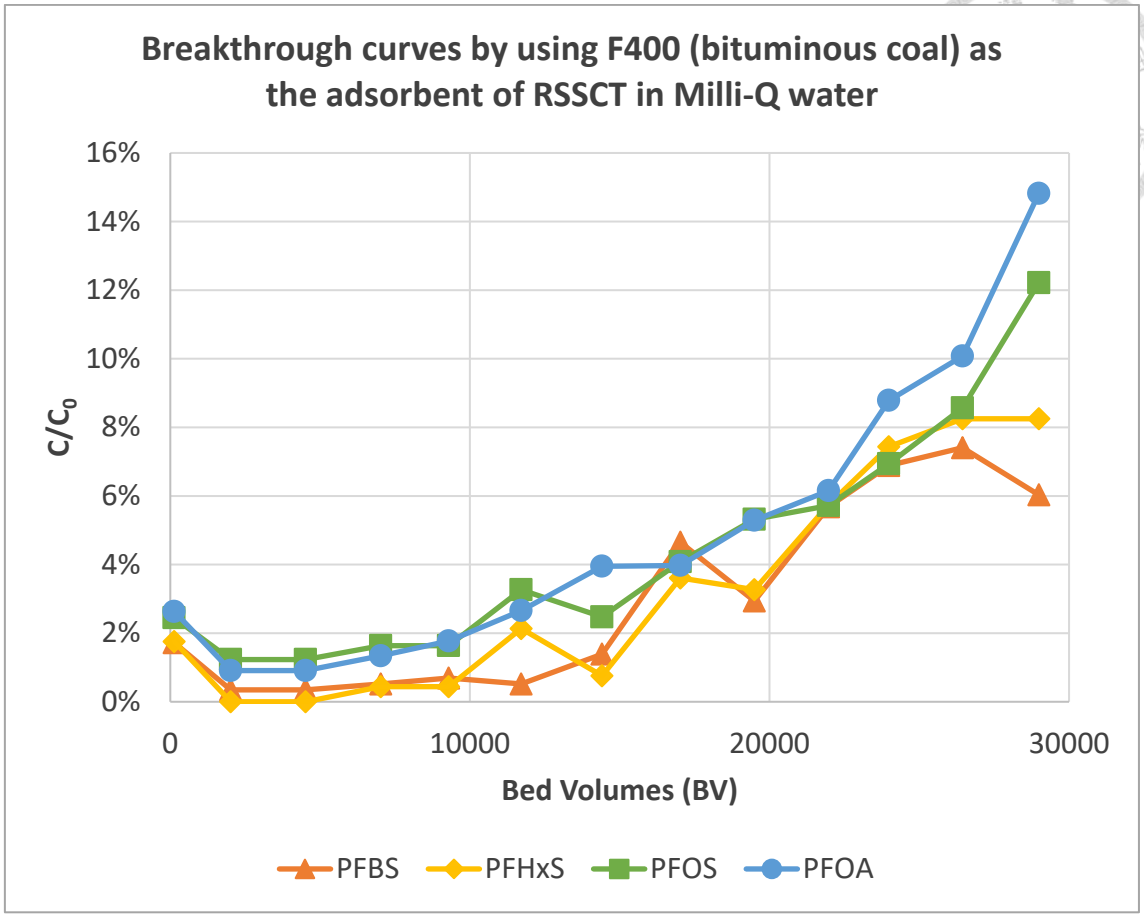

Figure 4.14 Breakthrough curves by using F400 (bituminous coal) as the adsorbent from 2 weeks of RSSCT simulating the removal of PFBS, PFHxS, PFOS, and PFOA in Milli-Q water.

The results in Figure 4.14 indicate that, under identical experimental conditions, bituminous coal GAC generally exhibits superior adsorption performance for PFBS, PFHxS, PFOS, and PFOA compared to coconut shell GAC. F400 maintained lower PFAS breakthrough concentrations for a significantly extended operational period (more bed volumes). Specifically, PFBS and PFHxS showed relatively stable and lower breakthrough concentrations on F400, while PFOA exhibited the highest breakthrough in the later stages, followed by PFOS. This superior performance is likely attributable to the unique pore size distribution (e.g., a higher proportion of mesopores or a different micropore distribution) and surface chemistry characteristic of bituminous coal GAC,

doi:10.6342/NTU202503155

which may be more favorable for the adsorption of these specific PFAS molecules.

4.5.3 Removal of PFAS in field rapid filtered water sample with coconut shell GAC

The breakthrough curves in Figure 4.15 illustrate the adsorption performance of TAC-C (coconut shell GAC) for various spiked PFAS in field rapid filtered water. Unlike previous tests conducted in Milli-Q water, the results in field rapid filtered water demonstrate significantly more rapid and higher breakthrough levels for all target PFAS. From the beginning of the RSSCT, a considerable breakthrough of PFAS was observed. Within the first few hundred bed volumes, PFBS, PFHxS, and PFOA already showed C/C_0 values ranging from approximately 5% to 30%. This indicates that the installed RSSCT column could not effectively adsorb PFAS from the field rapid filtered water at the beginning stage of the RSSCT.

As the operation progressed to approximately 5,000 bed volumes, PFBS, PFHxS, and PFOA had rapidly reached high breakthrough concentrations, effluent C/C_0 ranging from 70% to 75% of their initial concentrations. PFOS, while showing a comparatively better initial performance, still reached over 40% breakthrough at this point. By 15,000 bed volumes, breakthrough of PFBS was consistently at around 85%, PFOA around 70-80%, while PFHxS and PFOS showed more fluctuating behavior, with C/C_0 values around 50% and 25-30% respectively, suggesting complex adsorption dynamics.

Beyond 15,000 bed volumes, most PFAS compounds continued to show increasing breakthrough, often reaching relatively high C/C_0 values. By 25,000 bed volumes, PFHxS reached approximately 95% breakthrough, with PFBS and PFOA exceeding 90%. While PFOS maintained a relatively lower breakthrough initially, it also reached nearly 70% of

doi:10.6342/NTU202503155

influent concentration at 25,000 bed volumes, before fluctuating. By the end of the experiment (approaching 29,000 bed volumes), most compounds demonstrated near-complete breakthrough, often exceeding 80% to 90% of the initial concentration. The noticeable oscillations observed for PFHxS, PFOS, and PFOA throughout the tests suggest a complex interplay of adsorption, competition, and potentially desorption phenomena.

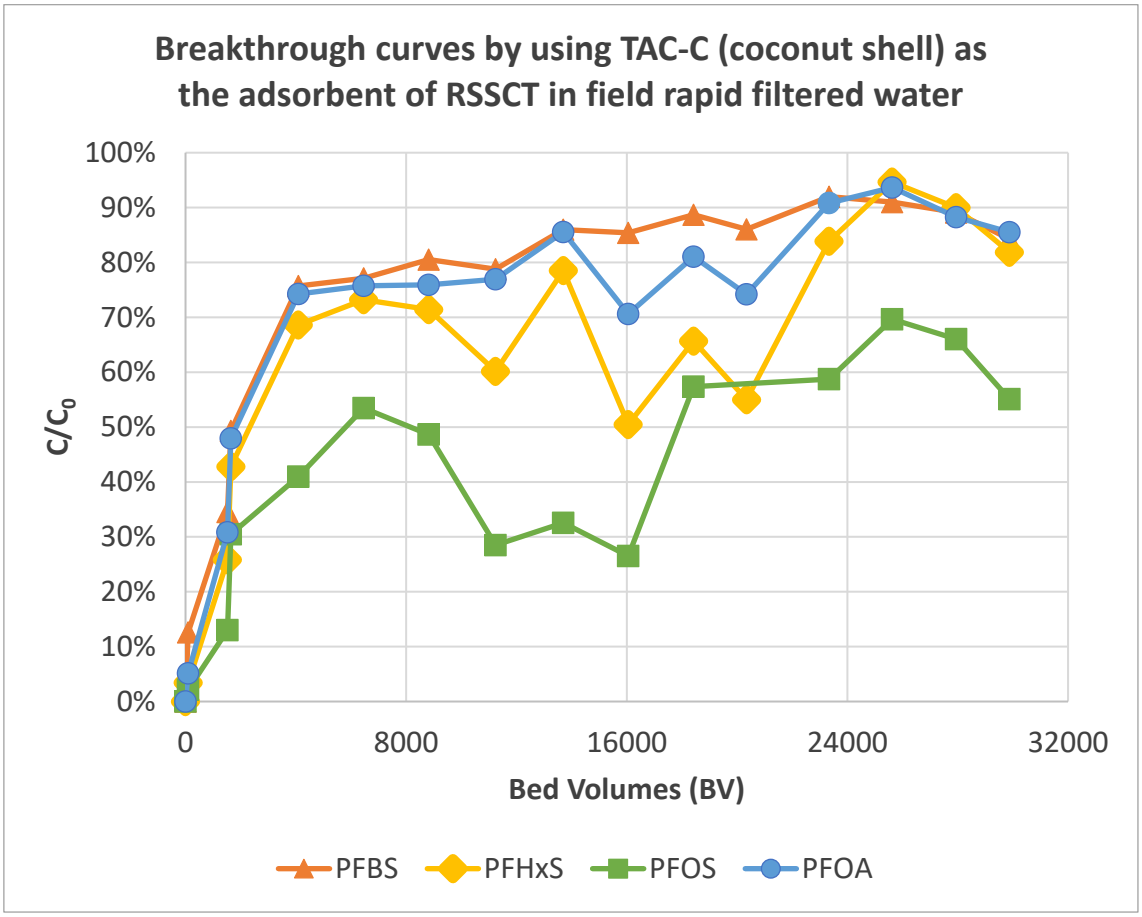

Figure 4.15 Breakthrough curves by using TAC-C (coconut shell) as the adsorbent from 2 weeks of RSSCT simulating the removal of PFBS, PFHxS, PFOS, and PFOA in field rapid filtered water

The rapid and high breakthrough observed in these RSSCT experiments with field rapid filtered water, particularly when compared to the results in Milli-Q water, strongly suggests the presence of significant matrix effects and competitive adsorption. Activated

doi:10.6342/NTU202503155

carbon adsorption of contaminants is a dynamic equilibrium process. In complex water matrices, such as field rapid filtered water taken from treatment plants, various naturally occurring organic matter (NOM) or other background contaminants are present, often at much higher concentrations than the target PFAS. These matrix constituents compete with PFAS for the limited adsorption sites on the GAC.

The elevated breakthrough from the initial stages indicates that the TAC-C could not effectively adsorb PFAS due to intense competitive adsorption with background constituents in the field rapid filtered water. This observation aligns with findings from Gagliano et al. (2020), who reported that the presence of natural organic matter (NOM) significantly suppressed PFAS adsorption by occupying active sites on GAC, resulting in early and elevated breakthrough levels even at low PFAS concentrations (E. Gagliano et al., 2020).

Furthermore, the observed fluctuations and high breakthrough in later stages suggest that the active adsorption sites of GAC were rapidly saturated by the cumulative load of co-existing PFAS and competing matrix components. This behavior is consistent with the results that mixed PFAS systems and organic co-contaminants can accelerate carbon exhaustion and reduce the adsorptive lifetime of GAC (Zhang et al., 2023).

It is also plausible that, as the carbon becomes saturated, some previously adsorbed PFAS may undergo displacement or desorption by more strongly adsorbing constituents. This potential for competitive desorption has been highlighted in previous studies, which found that high-affinity PFAS or NOM can displace earlier adsorbed species during breakthrough, leading to elevated effluent concentrations (C/C_0) and oscillatory trends in breakthrough curves (Nakazawa et al., 2024).

The accelerated breakthrough behavior observed indicates that when coconut shell granular activated carbon is used in real-world water matrices, such as field rapid filtered

doi:10.6342/NTU202503155

water taken from treatment plants, its effectiveness in removing PFAS is significantly reduced due to competitive adsorption from other components present in the water. Future applications must carefully consider the selection of activated carbon, which may involve implementing shorter operational cycles, such as more frequent regeneration or replacement, or exploring alternative treatment strategies to achieve the desired efficiency in PFAS removal.

4.5.4 Removal of PFAS in field rapid filtered water sample through bituminous coal GAC

Figure 4.16 displays the breakthrough curves for various PFAS with F400 (bituminous coal) as the adsorbent. Overall, F400 demonstrates an improved adsorption performance for PFAS in this complex matrix compared to the TAC-C (coconut shell) tested under similar conditions.

In the early stages of the experiment, even within only a few thousand bed volumes of water passing through the bed of GAC, all PFAS substances had apparent breakthrough, with C/C_0 ranging from 5% to 30%. Among them, PFBS had the fastest breakthrough, reaching about 30% before 5,000 BV, and PFOA showed a similar trend. In contrast, PFHxS and PFOS broke through more slowly, with initial C/C_0 less than 25%.

As the bed volume accumulated, the C/C_0 of all compounds continued to rise. PFBS showed the fastest breakthrough trend throughout the period, breaking through 50% at 16000 BV and eventually approaching 65%. PFOA rose steadily, reaching about 60% at the end of the experiment. PFHxS and PFOS showed more fluctuations. Although they sometimes broke through and rose, they still remained at a relatively low level, around 40% and 50% respectively, indicating that their adsorption behavior was affected by

doi:10.6342/NTU202503155

multiple factors.

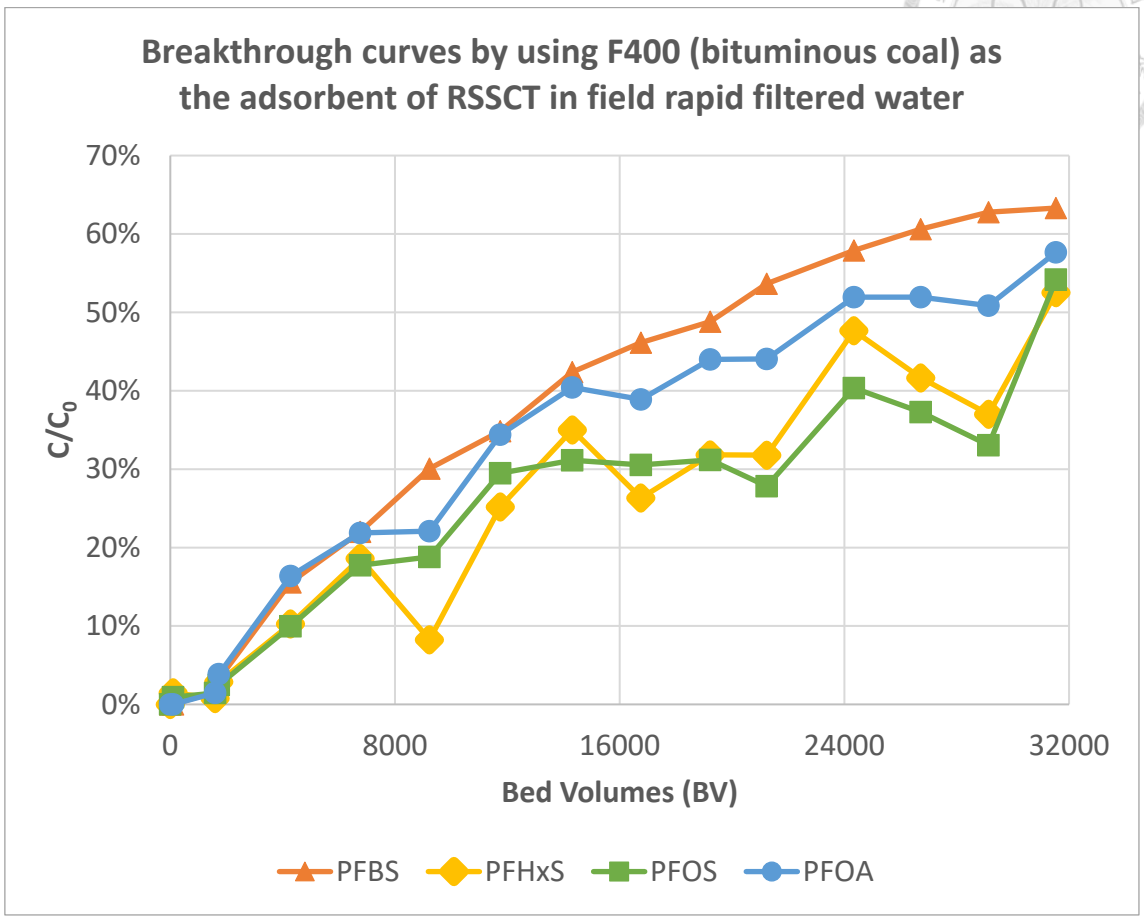

Figure 4.16 Breakthrough curves by using F400 (bituminous coal) as the adsorbent from 2 weeks of RSSCT simulating the removal of PFBS, PFHxS, PFOS, and PFOA in field rapid filtered water.

Overall, the adsorption effect of F400 activated carbon on PFBS and PFOA is relatively weak, and its breakthrough is observed at an early stage of the RSCCT experiment, and the rise rate is fast, indicating that its removal efficiency in real water samples is limited. PFHxS and PFOS performed relatively well but still showed a breakthrough rise under high bed volume conditions, indicating that the adsorption capacity is gradually saturated. The above results also reflect that in real water matrix (such as field rapid filtration water), the adsorption capacity of activated carbon for PFAS will be significantly reduced due to the competitive adsorption of natural organic matter

doi:10.6342/NTU202503155

and other background pollutants. These phenomena may also cause desorption or displacement behavior after adsorption saturation, further causing the C/C_0 value to fluctuate and increase.

It can be seen that, in practical applications of treating complex water quality, the selection and operating conditions of activated carbon should be carefully evaluated, such as shortening the operating cycle or combining with other treatment technologies to ensure the effective removal of PFAS.

4.5.5 Removal of PFAS in field rapid filtered water with coal-based GAC

In order to compare with the adsorption performance of GAC made with different raw materials, a coal-based GAC manufactured by the same manufacturer as TAC-C (coconut shell) was tested. The breakthrough curves in Figure 4.17 illustrate the adsorption performance of PFAS by TAC-Q (coal-based) with field rapid filtered water.

From the very onset of the RSSCT, a gradual breakthrough of PFAS was observed. Within the first few hundred bed volumes (around 1,000-2,000 BV), PFBS, PFHxS, PFOS, and PFOA exhibited C/C_0 values generally ranging from approximately 0% to 2%. This indicates that the RSSCT column using TAC-Q began to show initial signs of breakthrough for some PFAS, though at very low levels, from the start of the experiment.

As the operation progressed to approximately 5,000 bed volumes, PFBS had reached a breakthrough of approximately 10%. For comparison, PFOA was around 10%, while PFHxS and PFOS maintained lower breakthroughs, around 5%. At 10,000 bed volumes, the breakthrough of PFBS had rapidly increased to approximately 50% breakthrough, PFOA reached around 30%, PFHxS was at about 20%, and PFOS was at approximately 25%.

Beyond 15,000 bed volumes, most PFAS compounds showed increasing

doi:10.6342/NTU202503155

breakthroughs, often reaching high C/C_0 values. By 15,000 bed volumes, the breakthrough of PFBS had dramatically increased to approximately 90%. PFOA was around 45%, PFHxS dipped to around 20%, and PFOS was at approximately 30%. After 20,000 bed volumes of operation, PFBS had reached nearly 100% breakthrough, PFOA was around 55%, PFHxS fluctuated up to about 35%, and PFOS was near 40%. At 24,000 bed volumes, which marked the end of the RSSCT, the breakthrough of PFBS continued to increase to approximately 140%. This indicates a significant breakthrough and possible desorption. Alternatively, it could also mean that the instrument detected an error, leading to breakthrough readings above the initial concentration. PFHxS breakthrough reached around 65%, PFOA was near 65%, and PFOS was at approximately 45%, before showing a slight decrease. The noticeable oscillations observed for PFHxS, and to a lesser extent for PFOS and PFOA, throughout the test suggest a complex interplay of adsorption, competition, and potentially desorption phenomena in this real-world water matrix.

doi:10.6342/NTU202503155

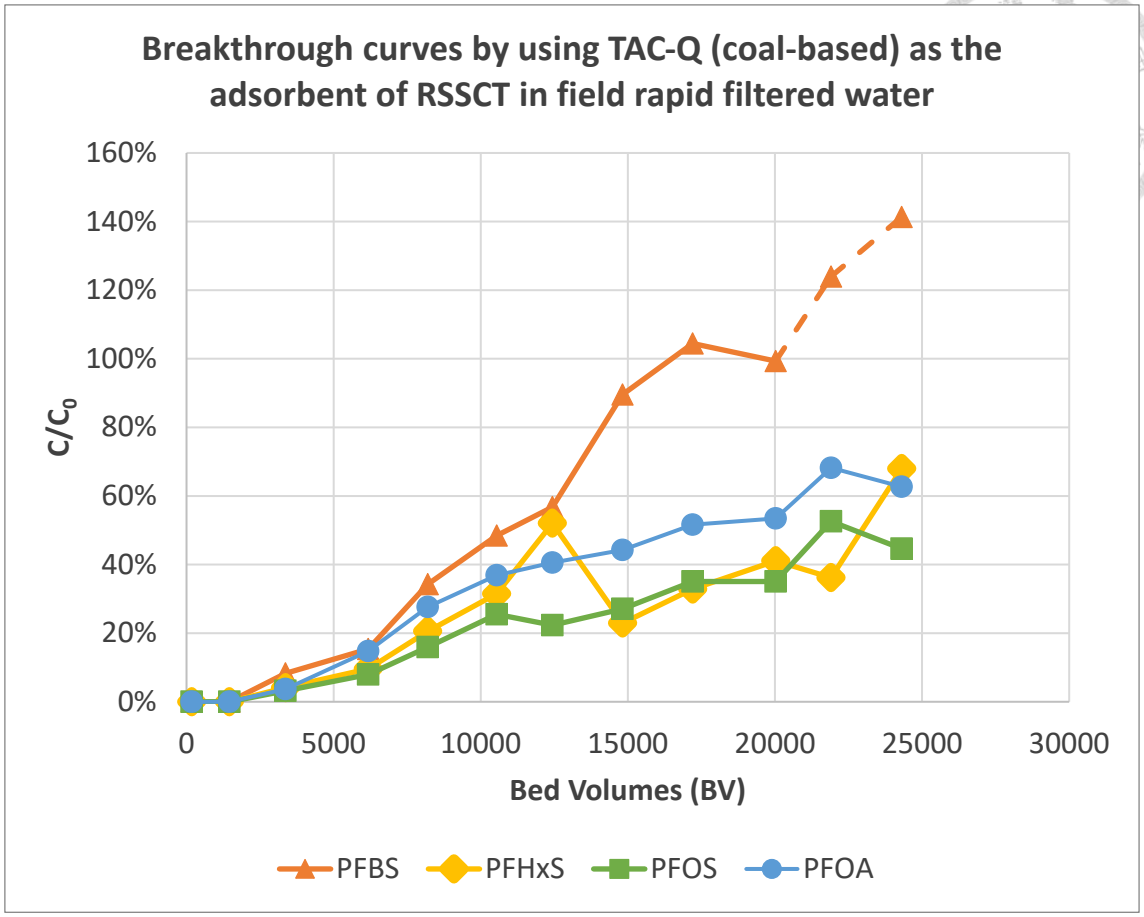

Figure 4.17 Breakthrough curves by using TAC-Q (coal-based) as the adsorbent from 2 weeks of RSSCT simulating the removal of PFBS, PFHxS, PFOS, and PFOA in field rapid filtered water.

While coal-based GAC (TAC-Q) generally performed better than the coconut shell GAC (TAC-C), the elevated breakthrough from the initial to later stages indicates that even this coal-based GAC was eventually challenged in effectively adsorbing all PFAS due to the intense competition from the water matrix. Furthermore, the observed fluctuations and high breakthrough in later stages, particularly for PFBS, suggest that the active adsorption sites of GAC were rapidly saturated by the collective load of PFAS and competing matrix components. It is also plausible that, as the carbon becomes saturated, some previously adsorbed PFAS might undergo displacement or desorption by more strongly adsorbing matrix constituents, contributing to the high C/C$_0$ values, especially

doi:10.6342/NTU202503155

for PFBS exceeding 100%.

The accelerated breakthrough behavior observed, particularly for PFBS, indicates that when coal-based GAC (TAC-Q) is used in real-world water matrices, such as when it serves as a post-contactor in a treatment plant, its effectiveness in removing all PFAS is still impacted by competitive adsorption from other contaminants present in water. Future applications should carefully consider the selection of activated carbon, which may involve implementing shorter operational cycles, such as more frequent regeneration or replacement, or exploring alternative treatment strategies to achieve the desired efficiency for PFAS removal, especially for more recalcitrant compounds like PFBS.

4.6 Research strengths and limitations

4.6.1 A comprehensive discussion of the adsorption kinetics, adsorption isotherms, and RSSCT

In this study, the effectiveness of different activated carbons in removing PFAS from water was systematically evaluated through a series of experiments. The adsorption behavior of activated carbon toward PFAS was comprehensively investigated through various experimental methods, including adsorption kinetics, adsorption isotherms, and RSSCT.

Based on the experimental results, in Milli-Q water, coconut shell activated carbon (TAC-C) exhibited adsorption behavior for all four PFAS compounds that conformed to the pseudo-second-order adsorption kinetics model, indicating that the adsorption process may involve chemical adsorption or stronger physical adsorption mechanisms. In contrast, the adsorption behavior of bituminous coal activated carbon (F400) conforms to the pseudo-first-order adsorption kinetic model, suggesting that its adsorption process is

doi:10.6342/NTU202503155

primarily controlled by physical adsorption or diffusion steps.

Recent studies on PFAS adsorption by activated carbon reveal complex kinetics and mechanisms. Adsorption rates increase with longer C-F chains and SO_3^- functional groups, following pseudo-second-order kinetics (Seo & Kim, 2025). However, at environmentally relevant concentrations (0.1-100 ng/L), adsorption capacities are lower than previously reported, with surface diffusion coefficients indicating slow PFAS mobility (Pranić et al., 2025). The results in this study provide insights into the rate-controlling steps and potential mechanism differences in PFAS adsorption by different activated carbon materials under specific experimental conditions. While batch kinetic models provide insights into adsorption rates, they cannot be directly applied to continuous-flow systems due to complex factors like fluid dynamics and mass transfer (Russo et al., 2017). These findings highlight the importance of considering specific experimental conditions and limitations when interpreting PFAS adsorption data and applying it to real-world treatment scenarios.

In Milli-Q water, the Freundlich isotherm model better describes the adsorption of PFAS by TAC-C and F400, reflecting the heterogeneity of adsorption sites on the activated carbon surface. However, the goodness of fit (R^2) of the isotherm model in this study was generally suboptimal. This may be primarily due to the range of activated carbon dosage used in the initial experimental design. The experimental design employed equidistant dosages (0, 10, 20, 30, 40, and 50 mg/L). This resulted in PFAS concentrations in many samples being too low, even near the detection limit, at equilibrium. This made it difficult to present a complete adsorption curve, thus affecting the accuracy of the R^2 value. Ideally, the activated carbon dosage should be adjusted to produce a wider distribution of equilibrium concentrations at equilibrium to obtain a more accurate fit.

Additionally, although four PFAS substances were added simultaneously to water

doi:10.6342/NTU202503155

during kinetic adsorption and isothermal adsorption experiments, a single-substance adsorption model formula was used for isothermal adsorption calculations. This is a significant limitation because, in a multi-component system, competitive adsorption effects exist between different PFAS substances and between PFAS and other background substances in water. These competing substances compete for adsorption sites on activated carbon, leading to differences (mostly reduction in adsorption capacities) in adsorption performance for a single PFAS substance compared to its performance in a competitive environment. Future studies should consider adopting competitive adsorption models to more accurately describe adsorption behavior in multi-component systems. Despite the aforementioned limitations, the results of dynamic adsorption, isothermal adsorption parameters, and RSSCT in this study exhibit consistency in certain aspects, confirming the selective adsorption capacity of activated carbon toward different PFAS.

For example, in all experiments, the adsorption efficiency of PFBS, the shortest-chain of PFSAs in this study, was generally poor, and it also exhibited earlier breakthrough in RSSCT. This is attributed to its higher water solubility and weaker hydrophobic interactions. Additionally, when comparing PFOA (carboxylic acid) and PFOS (sulfonic acid) with the same carbon chain, experimental results indicate that PFOA is less easily adsorbed, a trend also reflected in the breakthrough curves of RSSCT (e.g., in Milli-Q water, PFOA exhibits slightly higher breakthrough than PFOS). This may be related to the differences in the nature of their functional groups and their interactions with the functional groups on the activated carbon surface. Previous studies have also shown the same result: longer PFAS carbon chains and sulfonic acid functional groups generally exhibit higher adsorption rates and capacities due to increased hydrophobicity (Seo & Kim, 2025). Positively-charged and microporous activated carbons show better performance for hydrophilic and marginally hydrophobic PFAS, while mesoporous

doi:10.6342/NTU202503155

carbons are more effective for highly hydrophobic PFAS (Cantoni et al., 2021; Park et al., 2020).

RSSCT experimental results also clearly highlight the importance of the water matrix effect. Compared to performance in Milli-Q water, the adsorption capacity of activated carbon for PFAS is significantly reduced in the field rapid filtered water, with breakthrough occurring earlier and more severely. This demonstrates the competitive effect of background contaminants on PFAS adsorption, as they occupy activated carbon adsorption sites, accelerate activated carbon saturation, and reduce treatment efficiency.

4.6.2 Research strengths

This study has several advantages and can serve as a reference for future researchers involved in related studies.

1. Systematic evaluation:

   Using multiple experimental methods, including adsorption kinetics, adsorption isotherms, and rapid mini-column tests (RSSCT), the adsorption performance of activated carbon for PFAS was comprehensively and systematically evaluated.

2. Material comparison:

   The adsorption efficiency of activated carbon from two different raw material sources (coconut shell and coal) toward the treatment of PFAS was compared, providing a scientific basis for selecting activated carbon in practical applications.

3. Field water considerations:

   In addition to conducting idealized experiments in Milli-Q water, this study incorporated field rapid filtered water into the RSSCT experiments, accurately reflecting the influence of water matrix effects on PFAS adsorption and enhancing

doi:10.6342/NTU202503155

the practicality of the research.

4. Analytical method optimization:

   The SPE pretreatment method was optimized through testing, improving PFAS recovery rates and analytical accuracy, ensuring the reliability of the data. The revised analytical processes improved retention of short-chain PFAS with a higher initial solvent polarity while maintaining effective elution of long-chain compounds.

5. Practical application reference:

   The results from this study provide a concrete reference for water treatment plants in Taiwan to adopt activated carbon for PFAS treatment in the future and contribute to achieving SDG 6.

4.6.3 Research limitations

Although this study provides valuable insights into the adsorption behavior of PFAS on activated carbon, the following limitations still exist:

1. Lack of competitive adsorption modeling:

   Since the four PFAS are adsorbed simultaneously, their interactions may influence the adsorption performance of individual substances, making it impossible to fully explain the adsorption mechanisms of each PFAS independently. Although dynamic adsorption and isothermal adsorption experiments involve the simultaneous presence of multiple substances, model calculations still use single-substance formulas, failing to adequately account for competitive adsorption effects between PFAS, and between PFAS and NOM. This may result in an incomplete assessment of adsorption behavior in actual water bodies.

2. Differences between kinetic and dynamic systems:

   There are dynamic differences between batch adsorption kinetic experiment

doi:10.6342/NTU202503155

results and the continuous-flow RSSCT system. Batch experiments may not fully capture the complex mass transfer and fluid dynamics effects present in actual column operations.

3. Insufficient direct characterization of activated carbon surface functional groups:

   While this study discusses the influence of activated carbon surface chemical properties, it does not provide direct characterization data of activated carbon surface functional groups (e.g., infrared spectroscopy, X-ray photoelectron spectroscopy, etc.), limiting a more in-depth microscopic explanation of the adsorption mechanism.

4. Extrapolability limitations of the study results:

   This study only discusses four specific PFAS and specific initial concentrations. Whether the actual environmental concentrations are applicable to the experimental results of this study requires further discussion, but the results of this study can be used as a reference for future field operations.

doi:10.6342/NTU202503155

Chapter 5 Conclusions and Suggestions

This study assessed the treatment efficiencies with different types of GAC adsorption for removing PFAS in water. In order to revise the SPE method for optimization of the pretreatment for PFAS analysis, the results showed that, for Oasis WAX cartridges, the optimal PFAS recovery was achieved under acidified conditions ($pH \leq 3$) without a 0.1% formic acid rinse. Under these conditions, all four tested PFAS (PFBS, PFHxS, PFOS, and PFOA) showed over 75% of recoveries. The formic acid rinsing of the cartridge had negligible impacts on recovery in this study. These results underscore the critical role of sorbent selection and sample pH adjustment for optimizing low-concentration PFAS extraction from aqueous matrices.

This study analyzed the relative errors for each PFAS adsorption by TAC-C and F400 to determine the best-fitting adsorption kinetic model. For all four PFAS compounds, the model that uses TAC-C as the adsorbent corresponds with the pseudo-second-order kinetic model. In contrast, the results that use F400 as the adsorbent align with the pseudo-first-order kinetic model. In Milli-Q water, PFAS adsorption onto both TAC-C and F400 was better described by the Freundlich isotherm model.

The RSSCT experimental results showed that TAC-C exhibited earlier penetration for PFBS and PFOA in Milli-Q water. In contrast, F400 demonstrated the best overall adsorption capacity, maintaining breakthrough below 10% for most PFAS. However, when treating rapid filtered field water containing naturally occurring organic matter (NOM), the adsorption efficacy of GAC was significantly reduced due to competitive effects.

Further analysis revealed that TAC-C achieved a 90% breakthrough at 25,000 bed volumes, with the exception of PFOS. F400, on the other hand, showed a 30%

doi:10.6342/NTU202503155

breakthrough for the four types of PFAS at approximately 15,000 bed volumes. Notably, TAC-Q, which is the same brand of coal-based activated carbon as TAC-C, exhibited breakthrough curves, except for PFBS, which showed breakthrough beyond its initial concentration. However, the degree of breakthrough for other PFAS was lower than that observed with coconut shell activated carbon.

Based on the experimental findings and practical considerations for PFAS removal using activated carbon, the following recommendations are proposed for improving operational efficiency and treatment performance:

This study still has some limitations. One key limitation of PFAS adsorption using GAC is the uncertainty surrounding competitive effects. In real water matrices, various coexisting substances, particularly NOM, may compete with PFAS for adsorption sites on the carbon surface. This competition can significantly reduce the adsorption efficiency of target contaminants, particularly at low PFAS concentrations. Furthermore, the presence of diverse NOM species, which vary in molecular size, polarity, and structure, may hinder simultaneous adsorption. These substances may block or occupy active sites on the GAC, reducing its capacity and selectivity for PFAS. This issue is more pronounced in surface water, where NOM levels are typically higher. It is necessary to reduce the competitive adsorption from NOM by treating NOM before the adsorption unit.

Another important limitation is that, once saturated, the GAC system may release previously adsorbed compounds or fail to effectively remove new contaminants. This can result in a measurable increase in total organic carbon (TOC) in the treated water, which could compromise water quality and indicate the need for timely GAC replacement or regeneration.

The recommendations of this study are as follows: (1) Establish a comprehensive PFAS management system and conduct more thorough research and control measures

doi:10.6342/NTU202503155

targeting different exposure pathways. (2) Strengthen public participation and risk communication. The government should enhance public education and outreach to raise public awareness of PFAS pollution and prevention. (3) Assuming wastewater treatment plants adopt GAC control technology, regular monitoring of PFAS breakthrough levels is necessary to promptly adjust operational parameters and prevent PFAS from unknowingly passing through the system. (4) It is recommended to shorten the replacement cycle of activated carbon, especially under complex water quality conditions, to maintain sufficient adsorption capacity and reduce PFAS breakthrough. (5) For sustainability, whether the activated carbon used can be regenerated or whether bioactive carbon can be developed during the adsorption process is a topic worthy of further research.

doi:10.6342/NTU202503155

Reference

Agency for Toxic Substances and Disease Registry (ATSDR). (2021). *Toxicological Profile for Perfluoroalkyls*. https://www.atsdr.cdc.gov/toxprofiles/tp200.pdf

Ahrens, L., Gerwinski, W., Theobald, N., & Ebinghaus, R. (2010). Sources of polyfluoroalkyl compounds in the North Sea, Baltic Sea and Norwegian Sea: Evidence from their spatial distribution in surface water. *Marine Pollution Bulletin*, *60*(2), 255-260. https://doi.org/https://doi.org/10.1016/j.marpolbul.2009.09.013

Alameddine, M., Liu, Z., Sauvé, S., & Barbeau, B. (2025). Comparative Assessment of Powdered versus Granular Activated Carbon for PFAS Removal in Drinking Water Treatment Plants. *ACS ES&T Water*, *5*(2), 851-861. https://doi.org/10.1021/acsestwater.4c00901

Allen, S. J., McKay, G., & Porter, J. F. (2004). Adsorption isotherm models for basic dye adsorption by peat in single and binary component systems. *Journal of Colloid and Interface Science*, *280*(2), 322-333. https://doi.org/https://doi.org/10.1016/j.jcis.2004.08.078

Appleman, T. D., Higgins, C. P., Quiñones, O., Vanderford, B. J., Kolstad, C., Zeigler-Holady, J. C., & Dickenson, E. R. V. (2014). Treatment of poly- and perfluoroalkyl substances in U.S. full-scale water treatment systems. *Water Research*, *51*, 246-255. https://doi.org/https://doi.org/10.1016/j.watres.2013.10.067

Arvaniti, O. S., & Stasinakis, A. S. (2015). Review on the occurrence, fate and removal of perfluorinated compounds during wastewater treatment. *Science of The Total Environment*, *524-525*, 81-92. https://doi.org/https://doi.org/10.1016/j.scitotenv.2015.04.023

Babel, S., & Kurniawan, T. A. (2003). Low-cost adsorbents for heavy metals uptake from contaminated water: a review. *Journal of Hazardous Materials*, *97*(1), 219-243. https://doi.org/https://doi.org/10.1016/S0304-3894(02)00263-7

Baluyot, J. C., Reyes, E. M., & Velarde, M. C. (2021). Per- and polyfluoroalkyl substances (PFAS) as contaminants of emerging concern in Asia's freshwater resources. *Environmental Research*, *197*, 111122. https://doi.org/https://doi.org/10.1016/j.envres.2021.111122

Bansal, R. C. G., Meenakshi. (2005). *Activated Carbon Adsorption*. CRC Press. https://doi.org/10.1201/9781420028812

Benskin, J. P., Muir, D. C. G., Scott, B. F., Spencer, C., De Silva, A. O., Kylin, H., Martin, J. W., Morris, A., Lohmann, R., Tomy, G., Rosenberg, B., Taniyasu, S., & Yamashita, N. (2012). Perfluoroalkyl Acids in the Atlantic and Canadian Arctic Oceans. *Environmental Science & Technology*, *46*(11), 5815-5823. https://doi.org/10.1021/es300578x

Buck, R. C., Franklin, J., Berger, U., Conder, J. M., Cousins, I. T., de Voogt, P., Jensen, A. A., Kannan, K., Mabury, S. A., & van Leeuwen, S. P. (2011). Perfluoroalkyl and polyfluoroalkyl substances in the environment: Terminology, classification, and origins. *Integrated Environmental Assessment and Management*, *7*(4), 513-541. https://doi.org/https://doi.org/10.1002/ieam.258

Cai, Y., Wang, X., Wu, Y., Zhao, S., Li, Y., Ma, L., Chen, C., Huang, J., & Yu, G. (2018). Temporal trends and transport of perfluoroalkyl substances (PFASs) in a subtropical estuary: Jiulong River Estuary, Fujian, China. *Science of The Total Environment*, *639*, 263-270.

doi:10.6342/NTU202503155

https://doi.org/https://doi.org/10.1016/j.scitotenv.2018.05.042
Calafat, A. M., Kuklenyik, Z., Reidy, J. A., Caudill, S. P., Tully, J. S., & Needham, L. L. (2007). Serum concentrations of 11 polyfluoroalkyl compounds in the u.s. population: data from the national health and nutrition examination survey (NHANES). *Environ Sci Technol*, *41*(7), 2237-2242. https://doi.org/10.1021/es062686m
Cantoni, B., Turolla, A., Wellmitz, J., Ruhl, A. S., & Antonelli, M. (2021). Perfluoroalkyl substances (PFAS) adsorption in drinking water by granular activated carbon: Influence of activated carbon and PFAS characteristics. *Science of The Total Environment*, *795*, 148821. https://doi.org/https://doi.org/10.1016/j.scitotenv.2021.148821
Carlson, L. M., Angrish, M., Shirke, A. V., Radke, E. G., Schulz, B., Kraft, A., Judson, R., Patlewicz, G., Blain, R., Lin, C., Vetter, N., Lemeris, C., Hartman, P., Hubbard, H., Arzuaga, X., Davis, A., Dishaw, L. V., Druwe, I. L., Hollinger, H.,…Thayer, K. A. (2022). Systematic Evidence Map for Over One Hundred and Fifty Per- and Polyfluoroalkyl Substances (PFAS). *Environmental Health Perspectives*, *130*(5). https://doi.org/10.1289/ehp10343
CHEMICAL & ENGINEERING NEWS. *A guide to the PFAS found in our environment*. https://cen.acs.org/sections/pfas.html
Chemicals Administration Ministry of Environment (CAME). (2025). *毒性化學物質簡介*. https://www.cha.gov.tw/cp-92-313-9da3e-1.html
Chow, S. J., Croll, H. C., Ojeda, N., Klamerus, J., Capelle, R., Oppenheimer, J., Jacangelo, J. G., Schwab, K. J., & Prasse, C. (2022). Comparative investigation of PFAS adsorption onto activated carbon and anion exchange resins during long-term operation of a pilot treatment plant. *Water Research*, *226*, 119198. https://doi.org/https://doi.org/10.1016/j.watres.2022.119198
Corwin, C. J., & Summers, R. S. (2010). Scaling trace organic contaminant adsorption capacity by granular activated carbon. *Environ Sci Technol*, *44*(14), 5403-5408. https://doi.org/10.1021/es9037462
Cousins, I. T., DeWitt, J. C., Glüge, J., Goldenman, G., Herzke, D., Lohmann, R., Ng, C. A., Scheringer, M., & Wang, Z. (2020). The high persistence of PFAS is sufficient for their management as a chemical class. *Environ Sci Process Impacts*, *22*(12), 2307-2312. https://doi.org/10.1039/d0em00355g
Crittenden, J., Reddy, P., Arora, H., Trynoski, J., Hand, D., Perram, D., & Summers, R. (1991). Predicting GAC Performance with Rapid Small-Scale Test Columns. *Journal American Water Works Association - J AMER WATER WORK ASSN*, *83*, 77-87.
Crone, B. C., F., S. T., G., W. D., J., S. S., Gulizhaer, A., J., K. E., & and Pressman, J. G. (2019). Occurrence of per- and polyfluoroalkyl substances (PFAS) in source water and their treatment in drinking water. *Critical Reviews in Environmental Science and Technology*, *49*(24), 2359-2396. https://doi.org/10.1080/10643389.2019.1614848
Danish Environmental Protection Agency. (2024). *Agreement on a National Action Plan for PFAS*. https://mim.dk/media/hszhzysc/agreement-on-a-national-action-plan-for-pfas.pdf
Dauchy, X. (2019). Per- and polyfluoroalkyl substances (PFASs) in drinking water: Current state of the science. *Current Opinion in Environmental Science & Health*, *7*, 8-12. https://doi.org/https://doi.org/10.1016/j.coesh.2018.07.004
Delpla, I., Jung, A. V., Baures, E., Clement, M., & Thomas, O. (2009). Impacts of climate

doi:10.6342/NTU202503155

change on surface water quality in relation to drinking water production. *Environment International*, *35*(8), 1225-1233. https://doi.org/10.1016/j.envint.2009.07.001

Domingo, J. L., & Nadal, M. (2019). Human exposure to per- and polyfluoroalkyl substances (PFAS) through drinking water: A review of the recent scientific literature. *Environmental Research*, *177*, 108648. https://doi.org/https://doi.org/10.1016/j.envres.2019.108648

e-GOV Public Comment Portal (Japan). (2025). *「食品、添加物等の規格基準の一部を改正する告示（案）」（清涼飲料水（ＰＦＯＳ及びＰＦＯＡ）に係る改正）について（概要）*.

Ericson, I., Martí-Cid, R., Nadal, M., Van Bavel, B., Lindström, G., & Domingo, J. L. (2008). Human Exposure to Perfluorinated Chemicals through the Diet: Intake of Perfluorinated Compounds in Foods from the Catalan (Spain) Market. *Journal of Agricultural and Food Chemistry*, *56*(5), 1787-1794. https://doi.org/10.1021/jf0732408

Ersan, M. S., Wang, B., Wong, M. S., & Westerhoff, P. (2024). Advanced oxidation processes may transform unknown PFAS in groundwater into known products. *Chemosphere*, *349*, 140865. https://doi.org/https://doi.org/10.1016/j.chemosphere.2023.140865

Eun, H., Shimamura, K., Asano, T., Yamazaki, E., Taniyasu, S., & Yamashita, N. (2022). Removal of perfluoroalkyl substances from water by activated carbons: Adsorption of perfluorooctane sulfonate and perfluorooctanoic acid. *Environmental Monitoring and Contaminants Research*, *2*(0), 88-93. https://doi.org/10.5985/emcr.20220010

European Union. (2020). *Directive (EU) 2020/2184 of the European Parliament and of the Council of 16 December 2020 on the quality of water intended for human consumption (recast) (Text with EEA relevance)*.

Fenton, S. E., Ducatman, A., Boobis, A., DeWitt, J. C., Lau, C., Ng, C., Smith, J. S., & Roberts, S. M. (2021). Per- and Polyfluoroalkyl Substance Toxicity and Human Health Review: Current State of Knowledge and Strategies for Informing Future Research. *Environ Toxicol Chem*, *40*(3), 606-630. https://doi.org/10.1002/etc.4890

Fontanals, N., Cormack, P. A. G., & Sherrington, D. (2008). Hypercrosslinked polymer microspheres with weak anion-exchange character. Preparation of the microspheres and their applications in pH-tuneable, selective extractions of analytes from complex environmental samples. *Journal of chromatography. A*, *1215 1-2*, 21-29.

Fromme, H., Tittlemier, S. A., Völkel, W., Wilhelm, M., & Twardella, D. (2009). Perfluorinated compounds – Exposure assessment for the general population in western countries. *International Journal of Hygiene and Environmental Health*, *212*(3), 239-270. https://doi.org/https://doi.org/10.1016/j.ijheh.2008.04.007

Gagliano, E., Sgroi, M., Falciglia, P. P., Vagliasindi, F. G. A., & Roccaro, P. (2020). Removal of poly- and perfluoroalkyl substances (PFAS) from water by adsorption: Role of PFAS chain length, effect of organic matter and challenges in adsorbent regeneration. *Water Res*, *171*, 115381. https://doi.org/10.1016/j.watres.2019.115381

Gagliano, E., Sgroi, M., Falciglia, P. P., Vagliasindi, F. G. A., & Roccaro, P. (2020). Removal of poly- and perfluoroalkyl substances (PFAS) from water by adsorption: Role of PFAS chain length, effect of organic matter and challenges in adsorbent

doi:10.6342/NTU202503155

regeneration. *Water Research*, *171*, 115381. https://doi.org/https://doi.org/10.1016/j.watres.2019.115381

Garg, S., Kumar, P., Mishra, V., Guijt, R., Singh, P., Dumée, L. F., & Sharma, R. S. (2020). A review on the sources, occurrence and health risks of per-/poly-fluoroalkyl substances (PFAS) arising from the manufacture and disposal of electric and electronic products. *Journal of Water Process Engineering*, *38*, 101683. https://doi.org/https://doi.org/10.1016/j.jwpe.2020.101683

Gidstedt, S., Betsholtz, A., Falås, P., Cimbritz, M., Davidsson, Å., Micolucci, F., & Svahn, O. (2022). A comparison of adsorption of organic micropollutants onto activated carbon following chemically enhanced primary treatment with microsieving, direct membrane filtration and tertiary treatment of municipal wastewater. *Science of The Total Environment*, *811*, 152225. https://doi.org/https://doi.org/10.1016/j.scitotenv.2021.152225

Government of Canada. (2024). *Objective for Canadian drinking water quality- per- and polyfluoroalkyl substances*. https://www.canada.ca/en/health-canada/services/publications/healthy-living/objective-drinking-water-quality-per-polyfluoroalkyl-substances.html

Grandjean, P., Andersen, E. W., Budtz-Jørgensen, E., Nielsen, F., Mølbak, K., Weihe, P., & Heilmann, C. (2012). Serum Vaccine Antibody Concentrations in Children Exposed to Perfluorinated Compounds. *JAMA*, *307*(4). https://doi.org/10.1001/jama.2011.2034

Ho, Y. S., & McKay, G. (1999). Pseudo-second order model for sorption processes. *Process Biochemistry*, *34*(5), 451-465. https://doi.org/https://doi.org/10.1016/S0032-9592(98)00112-5

Hu, X. C., Andrews, D. Q., Lindstrom, A. B., Bruton, T. A., Schaider, L. A., Grandjean, P., Lohmann, R., Carignan, C. C., Blum, A., Balan, S. A., Higgins, C. P., & Sunderland, E. M. (2016). Detection of Poly- and Perfluoroalkyl Substances (PFASs) in U.S. Drinking Water Linked to Industrial Sites, Military Fire Training Areas, and Wastewater Treatment Plants. *Environmental Science & Technology Letters*, *3*(10), 344-350. https://doi.org/10.1021/acs.estlett.6b00260

Integrated Risk Information System (IRIS). (2025). *IRIS Toxicological Review of Perfluorohexanesulfonic Acid (PFHxS, CASRN 335-46-4) and Related Salts*. https://iris.epa.gov/static/pdfs/0705_summary.pdf

Interstate Technology & Regulatory Council. (2022). *Naming Conventions for Per- and Polyfluoroalkyl Substances (PFAS)*. https://pfas-1.itrcweb.org/wp-content/uploads/2022/09/NamingConventions_PFAS_Fact-Sheet_083122_508.pdf

Jiang, J.-J., Okvitasari, A. R., Huang, F.-Y., & Tsai, C.-S. (2021). Characteristics, pollution patterns and risks of Perfluoroalkyl substances in drinking water sources of Taiwan. *Chemosphere*, *264*, 128579. https://doi.org/https://doi.org/10.1016/j.chemosphere.2020.128579

Johnson, G. R., Brusseau, M. L., Carroll, K. C., Tick, G. R., & Duncan, C. M. (2022). Global distributions, source-type dependencies, and concentration ranges of per- and polyfluoroalkyl substances in groundwater. *Science of The Total Environment*, *841*, 156602. https://doi.org/https://doi.org/10.1016/j.scitotenv.2022.156602

Kalam, S., Abu-Khamsin, S. A., Kamal, M. S., & Patil, S. (2021). Surfactant Adsorption Isotherms: A Review. *ACS Omega*, *6*(48), 32342-32348. https://doi.org/10.1021/acsomega.1c04661

Kempisty, D. M., Arevalo, E., Spinelli, A. M., Edeback, V., Dickenson, E. R. V., Husted,

doi:10.6342/NTU202503155

C., Higgins, C. P., Summers, R. S., & Knappe, D. R. U. (2022). Granular activated carbon adsorption of perfluoroalkyl acids from ground and surface water. *AWWA Water Science*, *4*(1). https://doi.org/10.1002/aws2.1269

Kurwadkar, S., Dane, J., Kanel, S. R., Nadagouda, M. N., Cawdrey, R. W., Ambade, B., Struckhoff, G. C., & Wilkin, R. (2022). Per- and polyfluoroalkyl substances in water and wastewater: A critical review of their global occurrence and distribution. *Science of The Total Environment*, *809*, 151003. https://doi.org/https://doi.org/10.1016/j.scitotenv.2021.151003

Lee, C. H., Kim, D. H., Park, S. Y., Sim, K. T., & Seok, K. S. (2018). Analysis Characteristics of Perfluorinated Compounds Using Solid Phase Extraction. *Journal of Korean Society of Environmental Engineers*, *40*(11), 465-472. https://doi.org/10.4491/ksee.2018.40.11.465

Li, S., Oliva, P., Zhang, L., Goodrich, J. A., McConnell, R., Conti, D. V., Chatzi, L., & Aung, M. (2025). Associations between per-and polyfluoroalkyl substances (PFAS) and county-level cancer incidence between 2016 and 2021 and incident cancer burden attributable to PFAS in drinking water in the United States. *Journal of Exposure Science & Environmental Epidemiology*, *35*(3), 425-436. https://doi.org/10.1038/s41370-024-00742-2

Li, Z., Luo, Z.-M., Huang, Y., Wang, J.-W., & Ouyang, G. (2023). Recent trends in degradation strategies of PFOA/PFOS substitutes. *Chemosphere*, *315*, 137653. https://doi.org/https://doi.org/10.1016/j.chemosphere.2022.137653

Lin, A. Y.-C., Panchangam, S. C., & Lo, C.-C. (2009). The impact of semiconductor, electronics and optoelectronic industries on downstream perfluorinated chemical contamination in Taiwanese rivers. *Environmental Pollution*, *157*(4), 1365-1372. https://doi.org/https://doi.org/10.1016/j.envpol.2008.11.033

Lin, A. Y.-C., Panchangam, S. C., Tsai, Y.-T., & Yu, T.-H. (2014). Occurrence of perfluorinated compounds in the aquatic environment as found in science park effluent, river water, rainwater, sediments, and biotissues. *Environmental Monitoring and Assessment*, *186*(5), 3265-3275. https://doi.org/10.1007/s10661-014-3617-9

Lindstrom, A. B., Strynar, M. J., & Libelo, E. L. (2011). Polyfluorinated Compounds: Past, Present, and Future. *Environmental Science & Technology*, *45*(19), 7954-7961. https://doi.org/10.1021/es2011622

Lutze, H. V., Brekenfeld, J., Naumov, S., von Sonntag, C., & Schmidt, T. C. (2018). Degradation of perfluorinated compounds by sulfate radicals - New mechanistic aspects and economical considerations. *Water Res*, *129*, 509-519. https://doi.org/10.1016/j.watres.2017.10.067

Margot Lee, C. P. (2024). *Repeatability and Reproducibility of the Oasis™ GCB/WAX for PFAS Analysis Cartridges in Soil/Solid Samples for EPA Method 1633*. https://www.waters.com/content/dam/waters/en/app-notes/2024/720008494/720008494-en.pdf

McNamara, J. D., Franco, R., Mimna, R., & Zappa, L. (2018). Comparison of Activated Carbons for Removal of Perfluorinated Compounds From Drinking Water. *Journal AWWA*, *110*(1), E2-E14.

Miljøstyrelsen. (2024). *Grænseværdier for PFAS i miljøet*. https://mst.dk/media/x14n2bsd/graensevaerdier-ved-miljoestyrelsen_05-11-2024.pdf

Ministry of the Environment (Japan). (2024). *水道水における PFOS 及び PFOA の取扱いの改正方針等について（案）*.

doi:10.6342/NTU202503155

https://www.env.go.jp/content/000276966.pdf
Nakazawa, Y., Kosaka, K., Asami, M., & Matsui, Y. (2024). Maximum desorption of perfluoroalkyl substances adsorbed on granular activated carbon used in full-scale drinking water treatment plants. *Water Res*, *254*, 121396. https://doi.org/10.1016/j.watres.2024.121396
National Environmental Research Agency (NERA). (2024). *NIEA W542.52B：水中全氟與多氟烷基物質檢測方法－液相層析串聯式質譜儀法*. https://www.nera.gov.tw/zh-tw/Categoryquery/2302.html
National Research Council (US) Safe Drinking Water Committee. (1980). IV, An Evaluation of Activated Carbon for Drinking Water Treatment. In *Drinking Water and Health: Volume 2*. National Academies Press (US). https://www.ncbi.nlm.nih.gov/books/NBK234593/
Newcombe, G., Drikas, M., & Hayes, R. (1997). Influence of characterised natural organic material on activated carbon adsorption: II. Effect on pore volume distribution and adsorption of 2-methylisoborneol. *Water Research*, *31*(5), 1065-1073. https://doi.org/https://doi.org/10.1016/S0043-1354(96)00325-9
NHMRC. (2025). *Updated Australian Drinking Water Guidelines*. https://www.nhmrc.gov.au/about-us/news-centre/updated-australian-drinking-water-guidelines#:~:text=The%20Guidelines%20include%20revised%20health%2Dbased%20guideline%20values,acid%20(PFOS)%20%E2%80%93%208%20nanograms%20per%20litre
OECD Series on Risk Management of Chemicals. (2021). *Reconciling Terminology of the Universe of Per- and Polyfluoroalkyl Substances*. https://www.oecd.org/content/dam/oecd/en/publications/reports/2021/07/reconciling-terminology-of-the-universe-of-per-and-polyfluoroalkyl-substances_a7fbcba8/e458e796-en.pdf
Pan, C.-G., Liu, Y.-S., & Ying, G.-G. (2016). Perfluoroalkyl substances (PFASs) in wastewater treatment plants and drinking water treatment plants: Removal efficiency and exposure risk. *Water Research*, *106*, 562-570. https://doi.org/https://doi.org/10.1016/j.watres.2016.10.045
Park, M., Wu, S., Lopez, I. J., Chang, J. Y., Karanfil, T., & Snyder, S. A. (2020). Adsorption of perfluoroalkyl substances (PFAS) in groundwater by granular activated carbons: Roles of hydrophobicity of PFAS and carbon characteristics. *Water Research*, *170*, 115364. https://doi.org/https://doi.org/10.1016/j.watres.2019.115364
Poddar, M. (2013). A Review on the Use of Rapid Small Scale Column Test (RSSCT) on Predicting Adsorption of Various Contaminants. *IOSR Journal of Environmental Science, Toxicology and Food Technology*, *3*, 77-85. https://doi.org/10.9790/2402-0317785
Post, G. B., Cohn, P. D., & Cooper, K. R. (2012). Perfluorooctanoic acid (PFOA), an emerging drinking water contaminant: A critical review of recent literature. *Environmental Research*, *116*, 93-117. https://doi.org/https://doi.org/10.1016/j.envres.2012.03.007
Pranić, M., Carlucci, L., van der Wal, A., & Dykstra, J. E. (2025). Kinetic and isotherm study for the adsorption of per- and polyfluoroalkyl substances (PFAS) on activated carbon in the low ng/L range. *Chemosphere*, *370*, 143889. https://doi.org/10.1016/j.chemosphere.2024.143889
Rahman, M. F., Peldszus, S., & Anderson, W. B. (2014). Behaviour and fate of

doi:10.6342/NTU202503155

perfluoroalkyl and polyfluoroalkyl substances (PFASs) in drinking water treatment: A review. *Water Research*, *50*, 318-340. https://doi.org/https://doi.org/10.1016/j.watres.2013.10.045

Robertson, M., Lamb, B. G., Griffin, A., He, L., Ma, B., & Qiang, Z. (2025). Critical role of pore size on perfluorooctanoic acid adsorption behaviors in carbonaceous sorbents. *Materials horizons*.

Ross, I., McDonough, J., Miles, J., Storch, P., Thelakkat Kochunarayanan, P., Kalve, E., Hurst, J., S. Dasgupta, S., & Burdick, J. (2018). A review of emerging technologies for remediation of PFASs. *Remediation Journal*, *28*(2), 101-126. https://doi.org/10.1002/rem.21553

Rt Hon Dame Helen Winkelmann, A. o. t. G. (2022). *Water Services (Drinking Water Standards for New Zealand) Regulations 2022*. https://www.legislation.govt.nz/regulation/public/2022/0168/latest/whole.html#whole

Russo, V., Trifuoggi, M., Serio, M., & Tesser, R. (2017). Fluid-Solid Adsorption in Batch and Continuous Processing: A Review and Insights into Modeling. *Chemical Engineering & Technology*, *40*, 799-820.

Saeidi, N., Lai, A., Harnisch, F., & Sigmund, G. (2024). A FAIR comparison of activated carbon, biochar, cyclodextrins, polymers, resins, and metal organic frameworks for the adsorption of per- and polyfluorinated substances. *Chemical Engineering Journal*, *498*, 155456. https://doi.org/https://doi.org/10.1016/j.cej.2024.155456

Sanzana, S., Fenti, A., Iovino, P., & Panico, A. (2025). "A review of PFAS remediation: Separation and degradation technologies for water and wastewater treatment". *Journal of Water Process Engineering*, *74*, 107793. https://doi.org/https://doi.org/10.1016/j.jwpe.2025.107793

Seo, S., & Kim, M. (2025). Kinetics and Thermodynamics of Per - and Polyfluoroalkyl Substances (PFASs) Adsorption by Activated Carbon in Aqueous Systems. *Journal of Environmental Analysis, Health and Toxicology*, *28*(1), 1-10. https://doi.org/10.36278/jeaht.28.1.1

Smalling, K. L., Romanok, K. M., Bradley, P. M., Morriss, M. C., Gray, J. L., Kanagy, L. K., Gordon, S. E., Williams, B. M., Breitmeyer, S. E., Jones, D. K., DeCicco, L. A., Eagles-Smith, C. A., & Wagner, T. (2023). Per- and polyfluoroalkyl substances (PFAS) in United States tapwater: Comparison of underserved private-well and public-supply exposures and associated health implications. *Environment International*, *178*, 108033. https://doi.org/https://doi.org/10.1016/j.envint.2023.108033

Smith, S. J., Lauria, M., Ahrens, L., McCleaf, P., Hollman, P., Bjälkefur Seroka, S., Hamers, T., Arp, H. P. H., & Wiberg, K. (2023). Electrochemical Oxidation for Treatment of PFAS in Contaminated Water and Fractionated Foam—A Pilot-Scale Study. *ACS ES&T Water*, *3*(4), 1201-1211. https://doi.org/10.1021/acsestwater.2c00660

Smith, S. J., Wiberg, K., McCleaf, P., & Ahrens, L. (2022). Pilot-Scale Continuous Foam Fractionation for the Removal of Per- and Polyfluoroalkyl Substances (PFAS) from Landfill Leachate. *ACS ES&T Water*, *2*(5), 841-851. https://doi.org/10.1021/acsestwater.2c00032

Standardization Administration of China (SAC). (2022). *Standards for drinking water quality (GB 5749-2022)*.

Steenland, K., Fletcher, T., & Savitz, D. A. (2010). Epidemiologic evidence on the health effects of perfluorooctanoic acid (PFOA). *Environ Health Perspect*, *118*(8), 1100-

doi:10.6342/NTU202503155

1108. https://doi.org/10.1289/ehp.0901827
Sunderland, E. M., Hu, X. C., Dassuncao, C., Tokranov, A. K., Wagner, C. C., & Allen, J. G. (2019). A review of the pathways of human exposure to poly- and perfluoroalkyl substances (PFASs) and present understanding of health effects. *J Expo Sci Environ Epidemiol*, *29*(2), 131-147. https://doi.org/10.1038/s41370-018-0094-1
Tan, H.-M., Pan, C.-G., Yin, C., & Yu, K. (2023). Toward systematic understanding of adsorptive removal of legacy and emerging per-and polyfluoroalkyl substances (PFASs) by various activated carbons (ACs). *Environmental Research*, *233*, 116495. https://doi.org/https://doi.org/10.1016/j.envres.2023.116495
The International Agency for Research on Cancer (IARC). (2025). *Perfluorooctanoic Acid (PFOA) and Perfluorooctanesulfonic Acid (PFOS)*.
Tisler, S., Mrkajic, N. S., Reinhardt, L. M., Jensen, C. M., Clausen, L., Thomsen, A. H., Albrechtsen, H.-J., & Christensen, J. H. (2025). A non-target evaluation of drinking water contaminants in pilot scale activated carbon and anion exchange resin treatments. *Water Research*, *271*, 122871. https://doi.org/https://doi.org/10.1016/j.watres.2024.122871
U.S. EPA. (2017). *Technical Fact Sheet – Perfluorooctane Sulfonate (PFOS) and Perfluorooctanoic Acid (PFOA)*. https://19january2021snapshot.epa.gov/sites/static/files/2017-12/documents/ffrrofactsheet_contaminants_pfos_pfoa_11-20-17_508_0.pdf
U.S. EPA. (2024). *Our Current Understanding of the Human Health and Environmental Risks of PFAS*. Retrieved December 26 from https://www.epa.gov/pfas/our-current-understanding-human-health-and-environmental-risks-pfas
U.S. EPA. (2025a). *Drinking Water Treatability Database (TDB)*. Retrieved May 22, 2025 from https://www.epa.gov/water-research/drinking-water-treatability-database-tdb
U.S. EPA. (2025b). *EPA Announces It Will Keep Maximum Contaminant Levels for PFOA, PFOS*. https://www.epa.gov/newsreleases/epa-announces-it-will-keep-maximum-contaminant-levels-pfoa-pfos
U.S. EPA. (2025c). *Overview of Drinking Water Treatment Technologies*. https://www.epa.gov/sdwa/overview-drinking-water-treatment-technologies
U.S. EPA. (2025d). *Per- and Polyfluoroalkyl Substances (PFAS) Final PFAS National Primary Drinking Water Regulation*. https://www.epa.gov/sdwa/and-polyfluoroalkyl-substances-pfas
Wang, Z., Buser, A. M., Cousins, I. T., Demattio, S., Drost, W., Johansson, O., Ohno, K., Patlewicz, G., Richard, A. M., Walker, G. W., White, G. S., & Leinala, E. (2021). A New OECD Definition for Per- and Polyfluoroalkyl Substances. *Environmental Science & Technology*, *55*(23), 15575-15578. https://doi.org/10.1021/acs.est.1c06896
Wang, Z., DeWitt, J. C., Higgins, C. P., & Cousins, I. T. (2017). A Never-Ending Story of Per- and Polyfluoroalkyl Substances (PFASs)? *Environmental Science & Technology*, *51*(5), 2508-2518. https://doi.org/10.1021/acs.est.6b04806
Wang, Z., DeWitt, J. C., Higgins, C. P., & Cousins, I. T. (2017). A Never-Ending Story of Per- and Polyfluoroalkyl Substances (PFASs)? *Environ Sci Technol*, *51*(5), 2508-2518. https://doi.org/10.1021/acs.est.6b04806
Waters. (2025). *Oasis WAX for PFAS Analysis*. https://www.waters.com/waters/global/Oasis-WAX-SPE-for-PFAS-Analysis/nav.htm?cid=135045957

doi:10.6342/NTU202503155

We, A. C. E., Zamyadi, A., Stickland, A. D., Clarke, B. O., & Freguia, S. (2024). A review of foam fractionation for the removal of per- and polyfluoroalkyl substances (PFAS) from aqueous matrices. *Journal of Hazardous Materials*, *465*, 133182. https://doi.org/https://doi.org/10.1016/j.jhazmat.2023.133182

Whitehead, P. G., Wilby, R. L., Battarbee, R. W., Kernan, M., & Wade, A. J. (2009). A review of the potential impacts of climate change on surface water quality. *Hydrological Sciences Journal*, *54*(1), 101-123. https://doi.org/10.1623/hysj.54.1.101

Winchell, L. J., Ross, J. J., Wells, M. J. M., Fonoll, X., Norton, J. W., & Bell, K. Y. (2021). Per- and polyfluoroalkyl substances thermal destruction at water resource recovery facilities: A state of the science review. *Water Environment Research*, *93*(6), 826-843. https://doi.org/10.1002/wer.1483

Wu, C., Klemes, M. J., Trang, B., Dichtel, W. R., & Helbling, D. E. (2020). Exploring the factors that influence the adsorption of anionic PFAS on conventional and emerging adsorbents in aquatic matrices. *Water Research*, *182*, 115950. https://doi.org/https://doi.org/10.1016/j.watres.2020.115950

Xu, B., Liu, S., Zhou, J. L., Zheng, C., Weifeng, J., Chen, B., Zhang, T., & Qiu, W. (2021). PFAS and their substitutes in groundwater: Occurrence, transformation and remediation. *Journal of Hazardous Materials*, *412*, 125159. https://doi.org/https://doi.org/10.1016/j.jhazmat.2021.125159

Yadav, S., Ibrar, I., Al-Juboori, R. A., Singh, L., Ganbat, N., Kazwini, T., Karbassiyazdi, E., Samal, A. K., Subbiah, S., & Altaee, A. (2022). Updated review on emerging technologies for PFAS contaminated water treatment. *Chemical Engineering Research and Design*, *182*, 667-700. https://doi.org/https://doi.org/10.1016/j.cherd.2022.04.009

Young, C. J., Furdui, V. I., Franklin, J., Koerner, R. M., Muir, D. C. G., & Mabury, S. A. (2007). Perfluorinated Acids in Arctic Snow: New Evidence for Atmospheric Formation. *Environmental Science & Technology*, *41*(10), 3455-3461. https://doi.org/10.1021/es0626234

Yu, Q., Zhang, R., Deng, S., Huang, J., & Yu, G. (2009). Sorption of perfluorooctane sulfonate and perfluorooctanoate on activated carbons and resin: Kinetic and isotherm study. *Water Research*, *43*(4), 1150-1158. https://doi.org/https://doi.org/10.1016/j.watres.2008.12.001

Zahm, S., Bonde, J. P., Chiu, W. A., Hoppin, J., Kanno, J., Abdallah, M., Blystone, C. R., Calkins, M. M., Dong, G. H., Dorman, D. C., Fry, R., Guo, H., Haug, L. S., Hofmann, J. N., Iwasaki, M., Machala, M., Mancini, F. R., Maria-Engler, S. S., Møller, P.,…Schubauer-Berigan, M. K. (2024). Carcinogenicity of perfluorooctanoic acid and perfluorooctanesulfonic acid. *Lancet Oncol*, *25*(1), 16-17. https://doi.org/10.1016/s1470-2045(23)00622-8

Zhang, Y., Thomas, A., Apul, O., & Venkatesan, A. K. (2023). Coexisting ions and long-chain per- and polyfluoroalkyl substances (PFAS) inhibit the adsorption of short-chain PFAS by granular activated carbon. *Journal of Hazardous Materials*, *460*, 132378. https://doi.org/https://doi.org/10.1016/j.jhazmat.2023.132378

台灣自來水股份有限公司. https://www.water.gov.tw/ch/Subject/Detail/1396?nodeId=776

行政院. (2024). *全氟及多氟烷基物質(PFAS)管理行動計畫*.

環境部. (2023). *Investigation of Compounds of Emerging Concern in Drinking Water and Management of Water Quality 2023*. https://www.grb.gov.tw/search/planDetail?id=16327559

doi:10.6342/NTU202503155

環境部水質保護司. (2024). *環境部因應全氟化合物(PFAS)管制趨勢，預告修正飲用水水質標準，確保飲用水安全及品質*. https://enews.moenv.gov.tw/Page/3B3C62C78849F32F/c9fdf632-b0d3-4a13-ba10-52e9602dc3b2

doi:10.6342/NTU202503155

Appendixes

A.1 The analysis results by UPLC-MS/MS

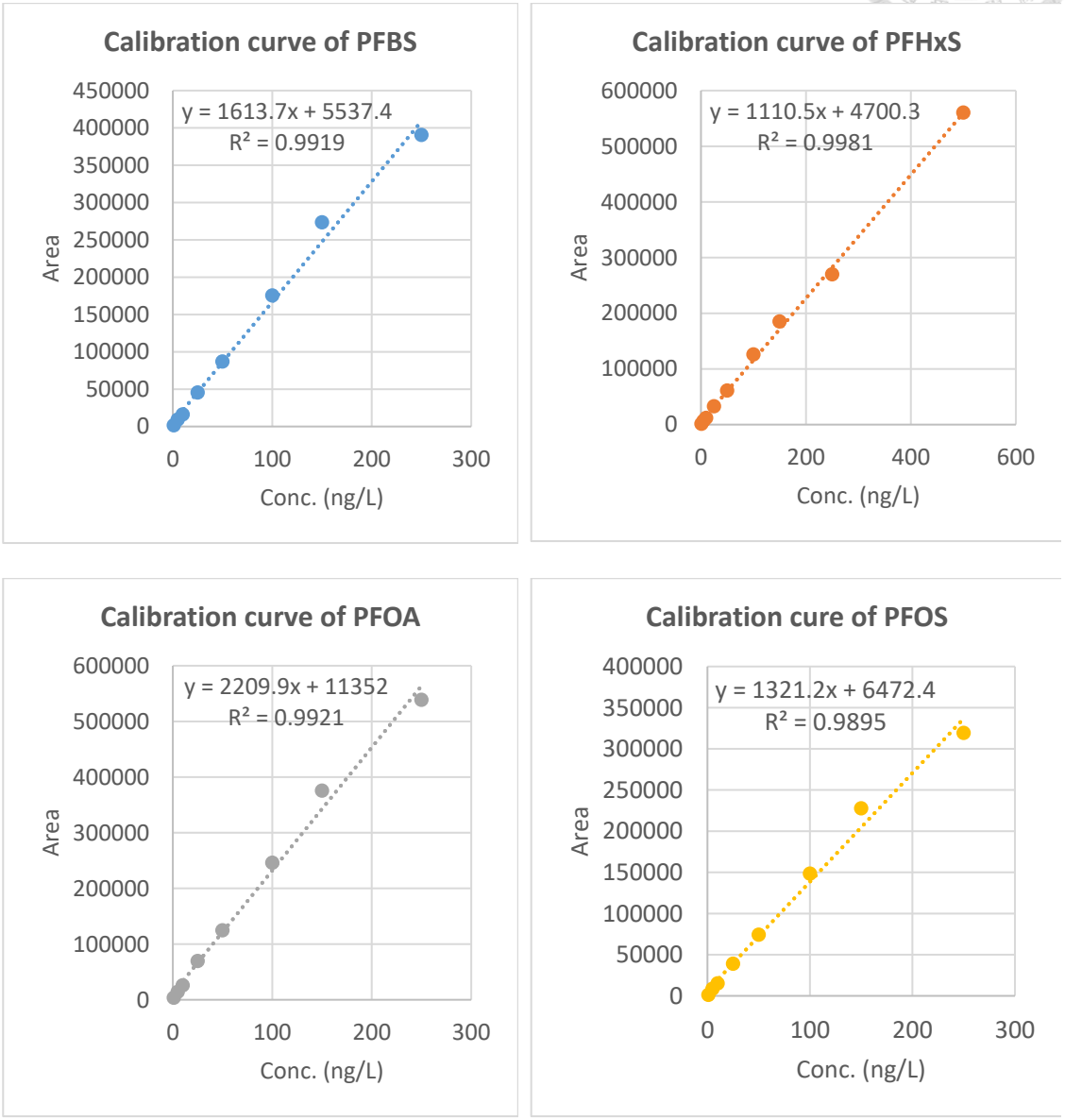

Figure A.1 Calibration curves of four compounds

doi:10.6342/NTU202503155

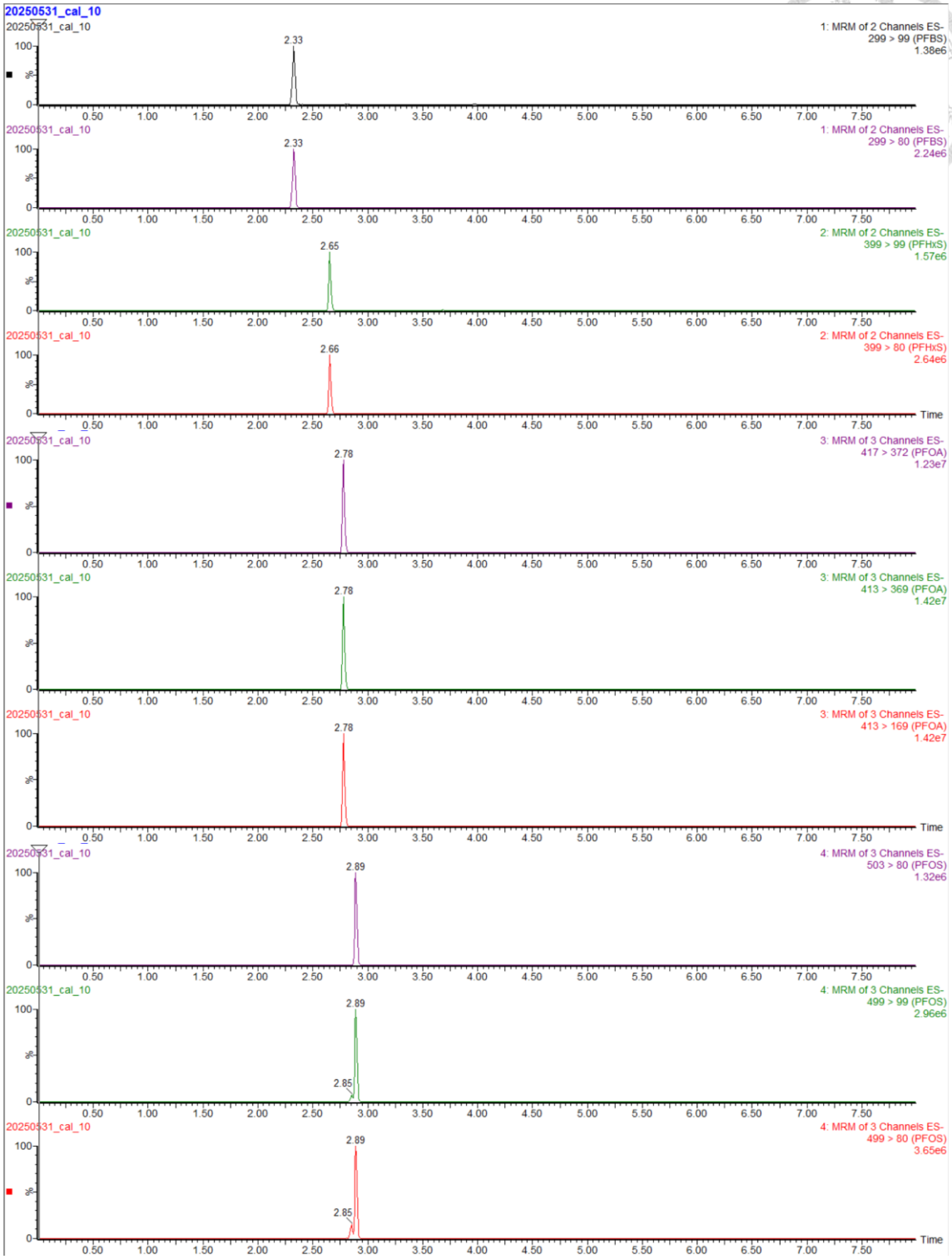

Figure A.2 The UPLC-MS/MS MRM chromatogram for the analyzed PFAS standard and internal standard in ESI negative mode

doi:10.6342/NTU202503155